# Electrolyte pH Conditioning of Regenesys®

by

Ian Michael Shropshire

A Master's Thesis

Submitted in partial fulfilment of the requirements
for the award of

Degree of Master of Philosophy of Loughborough University

30/9/01



# CONTENTS

## Abstract

Regenesys® is a regenerative fuel cell based on the sulphur and sodium bromide redox couple. On charging the system sulphur (polysulphide) is reduced to the sulphide and bromide oxidised to bromine. During discharge or power delivery the sulphide is oxidised back to sulphur (polysulphide) and the bromine reduced back to the bromide

The bromide electrolyte pH decreases during operation. This is symptomatic of the chemical imbalance within the system. $HS^-$ is transported across the membrane where oxidisation by the bromine ultimately yields sulphuric acid. Back diffusion of protons will occur if low pH is maintained. The result is the neutralisation of the polysulphide electrolyte ($HS^-$ and $OH^-$) and consequently the inhibition of the hydroxyl dependent discharge process that decreases the discharge capacity.

The pH changes in either or both electrolytes will be compensated for by the addition of hydroxyl ions. As we are in an electrochemical system with electricity at our disposal, an innovative and practicable approach would be to use electrolysis. Sodium bromide solution was electrolysed; hydroxide was produced by the reduction of water, protons and oxygen. Bromine evolution was conveniently selected as the counter reaction to offset direct losses due to diffusion during the charged state. Two configurations of the electrolyser were investigated: a flow by cathode and a separate electrolysis cell utilising the gas diffusion electrode in a novel application. Carbon materials were also investigated as candidate cathodes.

# Acknowledgements

I would like to thank Dr Roger Mortimer, Dr Phil Mitchell, Dr Ray Barton, the project team and Professor Steve Fletcher for their help and advice; John Spray, Alan Stevens and Tony Newbold for their technical skills and knowledge; Andy Wallace, Mebs Virji, Marcus Potter, Philippa Gladding, Alex Orsillo, Ben Wegg and the electrochemistry group; National Power for providing funding for my research and, of course, my family for their love, understanding and encouragement.

# Abbreviations

(Alphabetic order)

| | |
|---|---|
| a | activity |
| $\alpha$ | transfer coefficient |
| AC | alternating current |
| C | concentration |
| CNS | coconut shell |
| D | diffusion coefficient |
| DC | direct current |
| DMFC | direct methanol fuel cell |
| E | electrode potential |
| F | Faraday |
| G | Gibb's free energy |
| GDE | gas diffusion electrode |
| $\eta$ | overpotential |
| HER | hydrogen evolution reaction |
| HRP | horse radish peroxidase |
| I | current |
| $I_d$ | diffusion current |
| $I_l$ | limiting current |
| $I_t$ | transient current |
| IR | infra-red |
| j | exchange current and diffusional flux |
| La | intraplanar microcrystallite size |
| Lc | interplanar microcrystallite size |
| MEA | membrane electrode assembly |
| *n* | number of electrons |
| NASA | National Association of Space Administration |
| NMR | nuclear magnetic resonance |
| PAFC | phosphoric acid fuel cell |
| PCS | power conversion system |
| PTFE | polytetrafluoroethylene |
| PVDF | polyvinylidene difluoride |

| | |
|---|---|
| R | resistance and universal gas constant |
| RDE | rotating disc electrode |
| R-S | Randle-Sevcik |
| RVC | reticulated vitreous carbon |
| SCE | standard calomel electrode |
| SEM | scanning electron microscope |
| SHE | standard hydrogen electrode |
| SPEFC | solid polymer electrolyte fuel cell |
| T | temperature |
| TEM | transmission electron microscope |
| UCNS | unactivated coconut shell |
| v | kinematic viscosity and scan rate |

# Chapter 1 Introduction

This introduction will give a description of present electrochemical power systems of battery and fuel cell technology. This will be followed by a brief introduction to National Power's new electricity storage technology, Regenesys®[1,2] and the need for electrolyte management, which is the aim of the thesis. This will set the scene for the literature chapter which will review Regenesys® in the context of fuel cell and battery technology using the common lead-acid battery and two classes of low temperature hydrogen-oxygen fuel cells (alkali and acid) as representative examples.

Batteries are already an integral part of modern life and with recent advances in portable electronics the demand for these power sources will increase significantly. Now National Power's Regenesys®, which operates like a giant rechargeable battery, will be powering our homes and industry.

Fuel cells and batteries[3,4,5,6,7] convert chemical energy released from spontaneous chemical reactions into electrical energy (galvanic). The chemical free energy associated with the chemical reaction can often be converted into electrical energy with high efficiency. The requirements for efficient energy conversion are that it must be possible to decouple the component oxidation and reduction reactions of the chemical reaction, so that they occur separately, rapidly and as chemically reversible as possible with electron transfer mediated by electrodes. This process involves the transfer of electrons from one set of reactants to the anode and the transfer of electrons from a cathode to the second set of reactants. The electron flow is via an external circuit from anode to cathode and the resultant electrical current can be used to power a device. The main difference between the battery and the fuel cell is that batteries are self contained devices, the electroreactants are often part of the electrode, and are classified as primary or secondary. The term battery is often used for single cells but actually refers to several cells in series. Conversely the term fuel cell is often used for several cells in series, more accurately termed a fuel cell stack. This discussion will use the popular terms for both single and multiple cells. Primary batteries cannot be electrically recharged because their discharge reaction is irreversible but can sometimes be chemically 'refuelled'. In contrast a primary fuel cell's electroreactants are supplied from outside and the products continuously removed. In theory, the cell can operate indefinitely. Secondary batteries can operate reversibly; electrical energy is consumed to drive non-spontaneous reactions

(electrolytic), thus converting electrical energy back into chemically stored energy. In addition 'refuelling' may be possible depending on the system and application. Electricity can be generated on demand and thus these batteries are often referred to as accumulators or storage cells. To explain the principles of the operation of the battery and fuel cell a description of the familiar lead-acid car battery and the hydrogen-oxygen fuel cell follow.

## 1.1 Regenesys® and utility power storage

Regenesys® is a secondary battery-fuel cell hybrid and represents a separate class of electrochemical device called the regenerative fuel cell. Regenesys® can operate reversibly, like a secondary battery, and can supply and store the electroreactants externally, like the fuel cell. Electrochemical power storage has many advantages over conventional utility electricity. Mechanical technologies[8] such as pumped hydroelectric and compressed air have considerable, operational, economical and environmental problems:

- Delay in response time
- Delay in switching from charge to discharge
- Impact on the environment
- Sites limited by geology and geography
- Costly

Delay in response time and switching from charge to discharge are inherent problems with mechanical technologies. The very scale of these technologies is costly to the environment and in terms of the engineering involved. Siting of a reservoir relies on a suitable valley being located and the associated problems of destroying local ecology and communities. Finding suitable rock morphology such as caverns or porous rock for compressed air technology is also problematic. In contrast electrochemical energy storage[8] can provide:

- Fast response time
- Switch easily from charge to discharge
- Environmentally friendly
- Energy plants can be situated virtually anywhere
- Economic

The speed to react to energy requirements is very fast which is advantageous for load levelling. The system is closed so there is no discharge of chemicals or effluent. Due to their modular design, plants can be any size and therefore located to suit community needs. The biggest investment advantage is that the system gives lower lifetime costs than conventional technologies.

## 1.2 Aims of project

To prevent loss of redox species in Regenesys® by acidification of the electrolyte, pH changes in either or both sides of the cell will be compensated for by the addition of hydroxyl ions or discharge of protons. Bromine losses by diffusion will be countered directly by the addition of aqueous bromine. A sodium bromide solution will be electrolysed; hydroxide will be produced by the reduction of water or oxygen and bromine evolution can be conveniently selected as the counter reaction to offset direct losses due to diffusion during the charged state of Regenesys®. The hydroxyl delivery or proton discharge system will ultimately have two embodiments; as a free standing electrolyser integrated in the electrolyte circuit of Regenesys® or a flow through porous carbon electrode system inserted into the process stream.

It is expected that under operational conditions an incoming flux of protons through the electrolyser membrane will be reduced to hydrogen or water (oxygen reduction control). If local pH does increase and basic conditions are attained then the proton flux will be neutralised by the hydroxyl species present at the Nafion®-electrode interface. The rebalancing reaction will only run to meet the level of acid in the bulk electrolyte in what is essentially a titration. Thus excessive hydroxide concentrations will not be a problem. However, during this study excessive hydroxide generation and extreme pH depression of bulk electrolyte will be investigated. Investigations under these extreme operating conditions will provide insight into the efficiency of mass transfer of protons and hydroxyl ions.

**Summary of aims**

**1(a)** Electrochemically rebalance system chemistry applying fuel cell gas diffusion electrode technology in a novel way.

- Generate bromine to offset losses
- Generate hydroxide to neutralise acid or direct discharge of protons
- Study of capability to deliver hydroxyl to either bromine or polysulphide electrolyte circuits

- Use hydrogen evolution as the cathodic reaction
- Use oxygen reduction as the cathodic reaction

1(b) Investigate delivery system configurations

- Separate flow cell electrolyser
- Porous carbon cathode probe

2 Carbon materials

- Identify suitable electrode materials
- Understand electrochemistry involved
- Study the effect of porosity on current density

## 1.3 An overview of Regenesys® and electrolyte management

Most conventional secondary batteries, such as the lead-acid battery, use electrodes to store products and reactants often by solid state reactions.[2,9] In contrast regenerative fuel cell technology keeps the products and reactants as liquid electrolytes and the electrodes as inert electron transfer surfaces. The electrolytes are stored externally enabling the power system to have a greater energy storage capacity than that dictated by cell geometry. In addition, quick re-fuelling or chemical charging is possible by exchanging electrolytes. The electrolytes are circulated continuously during operation and are separated by an ion exchange membrane. The whole process is carried out under ambient temperature and low pressure. There are a limited choice of compounds or elements that meet the ideal requirements of complete solubility at two oxidation states and can give a suitable electrochemical couple. The various oxidation states of vanadium, iron and chromium have been investigated with limited success. Two examples of redox systems are the hydrogen-bromine[10] and the aluminium-sulphur couples[11]. Flow cells based on the aluminium-sulphur couple are still restricted in energy capacity due to the area of the aluminium anode whilst the hydrogen-bromine cell is only limited by the size of the external electrolyte storage tanks. The Regenesys® system uses the couple between elemental bromine and sulphide ions and is described in the following section.

### 1.3.1 The energy storage and power delivery system

The energy storage and power delivery system is based on the sulphur/sodium bromide redox couple. On charging the system zero valent sulphur in the polysulphide anion is reduced to

the sulphide and bromide oxidised to bromine. During discharge or power delivery the sulphide is oxidised back to sulphur (polysulphide) and the bromine reduced back to bromide. Although the regenerative fuel cell modules are the heart of the energy storage system it represents only part of the system. The interaction of the components of the system is illustrated in Figure 1.1.

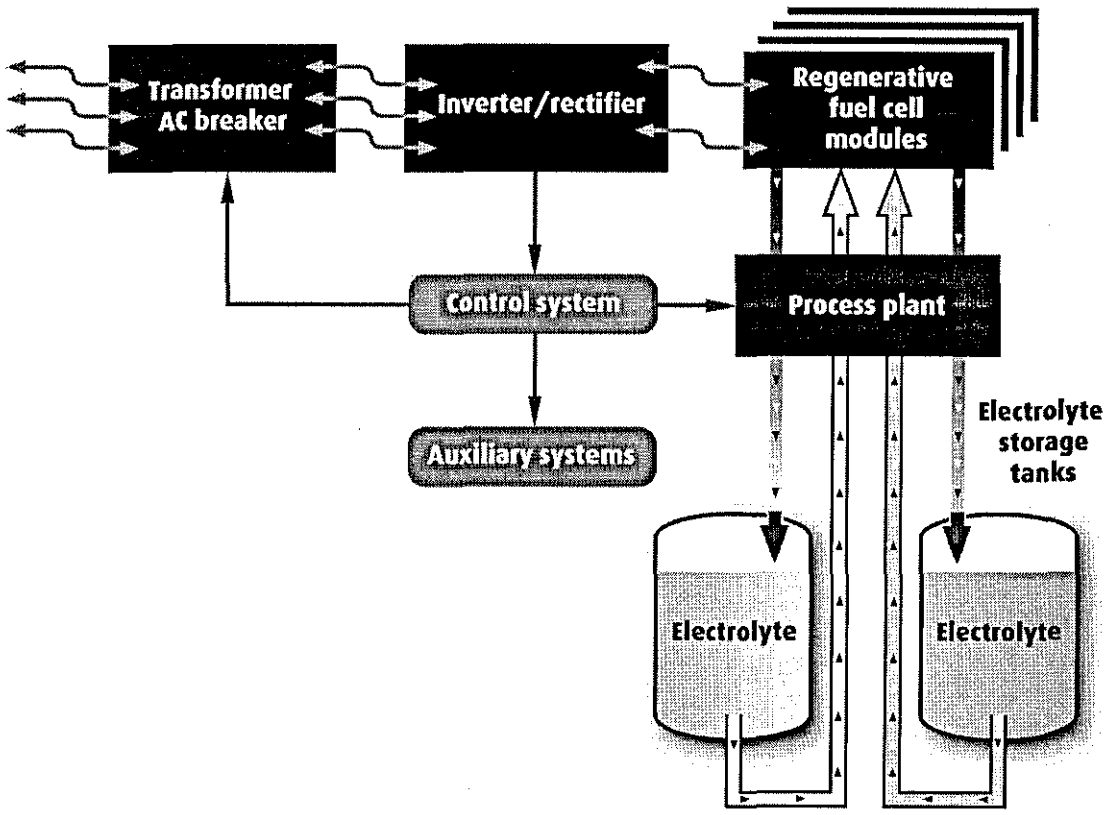


Figure 1.1 Block diagram showing relationship of the components of the utility energy storage system[8]

To give the required DC voltage, tens or hundreds of fuel cell modules are connected electrically in series forming a string. These strings are added in parallel until the required power rating is acheived. The electrolyte is supplied in parallel and stored in tanks of the required volume for the energy rating of the system. The energy rating of the system is therefore only limited by the size and number of tanks. The system can operate under a daily charge and discharge regime due to the available storage times of up to 12 hours and longer. A process plant is required to monitor operation, remove waste heat, optimise flow rates and condition the electrolyte due to changes in composition to ensure electrochemical efficiency.

The integrated operation of the plant is secured by a control system. The interface between the AC network and Regenesys® is provided by the power conversion system (PCS).

The PCS (inverter/rectifier) consists of two operationally independent converter systems, the DC/AC converter or chopper unit linking to the variable voltage of the fuel cell modules and the DC/AC inverter unit. The two converter units are connected by a DC link with a fixed DC voltage level. To maintain the required energy exchange between the energy storage system and the grid a control system adjusts the incoming and outgoing voltages and currents in real time.

As stated in the beginning of this section the sulphide is oxidised to sulphur (polysulphide) during power delivery and reduced back to sulphide during energy storage by bromine and bromide respectively. Equations (1.1), (1.2) and (1.3) describe the reactions during energy storage or the charge cycle. Reverse reactions represent discharge or power delivery.

$$2Br^- \Rightarrow Br_2 + 2e^- \qquad (1.1)$$
$$E^\theta = 1.09V$$

$$S + 2e^- \Rightarrow S^{2-} \qquad (1.2)$$
$$E^\theta = 0.50V$$

and overall

$$S^{2-} + Br_2 \Rightarrow S + 2Br^- \qquad (1.3)$$
$$E^\theta = 1.59V$$

The reagents are circulated through the cell many times during operation at ambient temperature and separated by a Nafion® 117 membrane[2,12] to prevent electrolyte mixing and undesirable electrode reactions. The system is almost ideal for energy storage applications with an efficiency in the region of 95%. It has been shown that the decrease in efficiency of the cell during prolonged operation is mainly due to sulphur and bromine loss. This is accompanied by a drop in system pH. The mechanism has been identified as acidification of the polysulphide side with subsequent $HS^-$ transportation[13] and reaction with the bromine electrolyte ultimately giving sulphuric acid. A disulphur dibromide intermediate has been proposed[13] . The mechanism for the hydrolysis of disulphur dihalogen compounds is very

complex, thus no simple equation can be given. In addition, aqueous bromine is lost due to diffusion and hydrolysis during the charged state. Diffusion of bromine[1] across the membrane to the polysulphide side and $HS^-$ transportation results in an electrolyte imbalance and a coloumbic loss. Therefore an electrolyte management strategy needs to be employed to improve the redox cell's performance by rebalancing the composition of the anolyte and the catholyte. The mechanism of electrolyte imbalance is represented by equations (1.4) and (1.5).

Polysulphide side

$$S + H_2O + 2e^- \Rightarrow HS^- + OH^- \qquad (1.4)$$

Membrane transport of $HS^-$

Bromide side

$$Br_2 + HS^- \Rightarrow [S_2Br_2] \Rightarrow\Rightarrow\Rightarrow \text{hydrolysis products including } H_2SO_4 \qquad (1.5)$$

The aim of this thesis is to counter these changes in electrolyte composition and is discussed in the following sections.

### 1.3.2 Balancing chemistry and process control

In the proposed rebalancing scheme, to prevent loss of redox species by acidification, pH changes in either or both sides of the cell will be compensated for by the addition of hydroxyl ions in the form of sodium hydroxide. Bromine losses by diffusion will be countered directly by the addition of aqueous bromine. As we are in an electrochemical system with electricity at our disposal, an innovative and practicable approach would be to use electrochemical technology. Sodium bromide solution could be electrolysed; hydroxide will be produced by the reduction of water or oxygen and bromine evolution can be conveniently selected as the counter reaction to offset direct losses due to diffusion during the charged state.

In neutral and basic media the main hydrogen evolution reaction (HER) for the cathodic reactions of the rebalancing cell are:

$$2H_2O + 2e^- \Rightarrow H_2 + 2OH^- \qquad (1.6)$$

$$E^\theta = -0.83V$$

and in acid conditions,

$$2H^+ + 2e^- \Rightarrow H_2 \qquad (1.7)$$
$$E^\theta = 0.00\ V$$

or oxygen reduction

$$O_2 + 2H_2O + 4e^- \Rightarrow 4OH^- \qquad (1.8)$$
$$E^\theta = 0.40\ V$$

Oxygen reduction will normally go via hydrogen peroxide[14]. This will be discussed in more detail in section 1.5.

The electrolyser rebalancing system can be integrated with the main cell in two different ways. One arrangement will have a separate flow cell membrane electrolyser with its cathode running to either hydrogen evolution or oxygen reduction and the other will involve a porous carbon open cathode running to the hydrogen evolution reaction with one or more separate anodes directly inserted into the process stream. Both approaches will be investigated.

# Chapter 2 Literature Review

The Regenesys® system is based on regenerative fuel cell or redox flow cell technology, as stated in chapter one, and will be discussed in this chapter in the context of the existing technology of specialised power storage and generation. Redox ( two fluids ) flow cells can be chemically refuelled and electrically recharged. Non-reversible primary battery systems can often be refuelled or chemically recharged of the electrochemical reagents. Both electrochemical systems rely on the ability to successfully de-couple the component oxidation and reduction reactions of the overall chemical reaction. The reduction and oxidation must occur separately to extract electrical energy from the chemical reaction. This chapter will discuss some of the electrochemical couples that have been investigated for power generation and storage and which have a direct relevance to the evolution of the Regenesys® system. This technology can often be applied to transportation in addition to utility power storage.

The three areas of energy storage technologies to be discussed are:

- Primary batteries
- Secondary batteries
- Redox fuel cell

A selection of electrochemical couples utilised in these technologies and their application will be described in the following sections.

## 2.1 Primary batteries

A number of practical primary or chemically rechargeable batteries have been developed for specialised purposes. These devices may be kept in continuous operation by maintaining a supply of fuel and oxidant and can therefore be thought of as a fuel cell. Depending on the electrochemical couple used these systems can operate under various regimes to suit many application requirements. The battery may be left for indefinitely long periods of time in fully or partially discharged until power is required without loss of storage capacity. An obvious application for this kind of system is emergency standby power sources. To simplify operation the electrochemical reagents need to be in a liquid form to facilitate removal and replacement. In addition the fluids must be relatively safe to handle and easily obtainable. Suitable redox agents would be aqueous solutions of compounds of sodium or potassium.

Dichromates, permanganates, sulphide, sulphites and thiosulphates have been investigated amongst others. A practical primary battery has been developed using sulphide and based partly on the following half cell reaction.

$$S^{2-} = S + 2e^- \qquad (1.2)$$
$$E^\theta = 0.50\ V$$

A variety of oxidising agents have been used including ferric chloride, hydrogen peroxide, sodium persulphate and sodium hypochloride. The sulphide/ferric couple (equation 2.1) has been developed into a low cost practical refuelable primary battery. The sulphide can be electrochemically regenerated while the ferric chloride is obtained readily

$$S^{2-} + 2Fe^{3+} = S + 2Fe^{2+} \qquad (2.1)$$
$$E^\theta = 1.20\ V$$

Another oxidising agent which has been utilised with suphide is hypochloride (equation 2.2). Hypochloride is easily replaced when expended.

$$S^{2-} + ClO^- + H_2O = S + Cl^- + 2OH^- \qquad (2.2)$$
$$E^\theta = 1.40\ V$$

These systems have in common the very important advantage of using abundant, cheap and relatively environmentally benign chemicals. In addition, these primary or fuel cell systems operate reliably and safely under ambient conditions.

## 2.2 Secondary batteries

Secondary batteries can operate reversibly; electrical energy is consumed to drive non-spontaneous reactions (electrolytic), thus converting electrical energy back into chemically stored energy. This section will start with a description of the familiar lead-acid car battery and then two electrochemical couples which have being developed into operable batteries based on zinc/bromine and iron/ferric redox systems. These will be discussed in the following sections.

### 2.2.1 The lead-acid battery

The net chemical reaction of the familiar lead-acid battery is

$$Pb + PbO_2 + 2H_2SO_4 = PbSO_4 + 2H_2O \qquad (2.3)$$

The standard free energy ($\Delta G^{\theta}$) for this reaction is -393.9 KJ $mol^{-1}$. The voltage produced by a cell with the above reaction, under standard conditions, can be represented by

$$E^{\theta} = -\Delta G^{\theta} / nF \qquad (2.4)$$

Where $n$ is the number of electrons involved in the reaction and F is the Faraday constant, a fundamental constant with the value of 96 458 C $mol^{-1}$. If reaction (2.3) is split into its constituent cathodic and anodic processes, two half cell equations can now describe the reaction, giving

$$Pb + H_2SO_4 = PbSO_4 + 2H^+ + 2e^- \qquad (2.5)$$

for the anodic reaction and

$$PbO_2 + H_2SO_4 + 2H^+ + 2e^- = PbSO_4 + 2H_2O \qquad (2.6)$$

for the cathodic process. The respective standard electrode potentials for the reactions are -0.36 and +1.69 V. Using equation (2.4) and substituting for $n$, the voltage developed under standard conditions is found to be 2.04 V. This value, as is expected, is also obtained from the difference of the individual half cell electrode potentials.

When current is drawn from a cell using the above electrode reactions, the voltage delivered is lower than the calculated or theoretical value. This is due to inherent sources of irreversibility of a working electrochemical cell. Electrochemical processes occur at a finite value with the rate increasing exponentially with increase in potential for an anodic process and a decrease in potential for a cathodic reaction relative to the standard electrode potenial. Another origin of irreversibility is the internal resistance of the cell. This is due to the resistance of the components of the cell, passivation of electrode surfaces and in particular electrolyte resistance. This manifests itself by part of the cell voltage being dropped within

the cell. Therefore, some potential is unavailable for external work. Internal resistance becomes increasingly dominant with increase in current.

### 2.2.2 The zinc-bromine battery

The secondary battery couple between elements zinc and bromine provide an attractive system on the basis of high energy and power density which is represented by the following reversible reaction (equation 2.7).

$$Zn + Br_2 = ZnBr_2 \qquad (2.7)$$
$$E^{\theta} = 1.80\ V$$

The electrochemical couple is well behaved and systems can be designed to function reliably under a long cycle life operation regime. Batteries based on this couple have the advantage of only one electrolyte which may be a full flow circulating system, a static liquid system or an immobilised (solid) electrolyte. Two main problems were maintaining zinc plating quality, i.e., control of dendrite shorting, and the storage of bromine. Adsorptive electrodes have been developed to store bromine in a reversible fashion at high levels of bromine. The storage of bromine within the electrode structure makes the system much safer and minimises material compatibility problems but restricts the energy capacity. The system is much simpler and less costly than systems which use bromine complexes and remote reservoir storage. This configuration as the additional advantage of the bromine being always immediately available for discharge. However, in utility power storage and transportation energy capacity of the system is of prime importance. External storage, and adsorptive electrode, can be applied together in these situations to avoid restrictions in energy capacity and speed of discharge response on the bromine side but limitations do occur due to the amount of zinc that can be plated on the carbon electrode.

### 2.2.3 The iron-redox battery

The iron redox or iron/ferric battery uses the reactions between the three oxidation states of iron (equations 2.8 and 2.9).

$$Fe + 2Fe^{3+} = 3Fe^{2+} \qquad (2.8)$$

$$Fe + 2FeBr_3 = 3FeBr_2 \qquad (2.9)$$

Although this couple is not very energetic and there has been severe problems with electrolyte stability of the cell, this system offers low cost, maintenance free long cycle life, safe production and disposal.

## 2.3 The redox fuel cell

This section will discuss the general principles of the two fluid redox fuel cell that the Regenesys® system is based upon describing the origin of Regenesys® system from the field of redox batteries and fuel cell technology. A description of present electrochemical power systems using the two classes of low temperature hydrogen-oxygen fuel cells (alkali and acid) as representive examples of current fuel cell technology.

### 2.3.1 The hydrogen-oxygen fuel cell

This discussion will be confined to the discussion of the alkaline hydrogen-oxygen fuel cell made famous by its adoption by NASA for the Apollo space programme and the solid polymer electrolyte hydrogen-oxygen fuel cell (SPEFC), each representing the old and new respectively These fuel cell technologies also have relevance to the present electrolyte management work.

For the direct conversion of the free energy from the oxidation of hydrogen to electrical power, in what can be seen as the equivalent to the combustion of hydrogen in air, the separation of the component redox reactions involved in equation (2.10) is required.

$$H_2 + ½\ O_2 = H_2O \qquad (2.10)$$

The resultant cathodic and anodic processes are determined by the electrolyte pH and discussed in the following sections.

### 2.3.2 The alkaline hydrogen-oxygen fuel cell

The alkaline fuel cell uses a potassium hydroxide electrolyte. The anodic and cathodic half cell reactions under basic conditions involve a hydroxyl conductance mechanism and are

$$H_2 + 2OH^- = 2H_2O + 2e^- \qquad (2.11)$$

at the anode and

$$\tfrac{1}{2}\,O_2 + H_2O + 2e^- = 2OH^- \qquad (2.12)$$

at the cathode with the respective standard electrode potentials of -0.83 and +0.40V. The alkaline fuel cell is the simplest low-temperature fuel cell and operates at around 70°C for maximum efficiency; a 50% drop in power is obtained at room temperature operation. In principle, the fuel cell offers a more energy efficient alternative to combustion technology with the additional advantage of being intrinsically 'green', but inevitably there are problems with all technologies. One of the main problems here is obtaining hydrogen easily enough to sustain a hydrogen economy sufficiently to drive the commercialisation of fuel cell technology. Complex engineering, high temperatures and expensive catalysts are required for the reforming of our present fuel sources such as oil and natural gas to generate hydrogen due to the stability of the carbon bond and carbon-hydrogen bond to electrochemical activation. This has generally only been most successful with the high temperature fuel cells. A recent renewal of interest in regenerative systems may provide a route to a sustainable hydrogen economy and a complete break from fossil fuels. In these systems, hydrogen and oxygen are generated by electrolysis of water using photovoltaics and used by a fuel cell. The water produced can then be electrolysed to regenerate the hydrogen and oxygen as and when required. There are problems also on the cathodic side of the hydrogen-oxygen fuel cell. The major problem is probably the limited rate of the cathode reaction, namely the reduction of oxygen. Now, with the oxygen reduction reaction an appreciable rate is often only obtained at the relatively high overpotential of ~0.3V. Fortunately, in alkaline electrolytes oxygen reduction is relatively facile and non-noble metal catalysts may be used. As current is increased ohmic losses become more important due to electrolyte resistivity. At extreme power loads the mass transport limitations of the oxygen and hydrogen in the electrolyte will cause the cell's performance to drop dramatically and eventually fail as the cell potential drops to zero due to fuel and oxidant starvation.

The electrode's construction is very important in addressing these inherent inefficiencies which are encountered in all low temperature fuel cells. The essential requirements for the electrode are:

- Good electronic conductivity
- Mechanical stability with an appropriate porosity

- Chemical stability
- Extensive catalyst lifetime

The electrodes, known as gas diffusion electrodes (GDE), are usually made from a carbon PTFE mixture. The PTFE functions to control porosity and hydrophobicity of the electrode, thus allowing gas to reach a catalysed layer on the electrolyte side without electrolyte loss and resultant flooding of electrode. The main cost in the construction of these electrodes is the catalyst. Prevailing research is devoted to making efficient use of the catalyst so low loadings can be used to obtain the desirable current densities. Much of the deposited catalyst does not take part in the electrochemical process. The requirements for efficient reaction is the so called three phase zone. The electrochemically active area , within a pore of the electrode, is where the catalyst meets the gas and electrolyte, giving the shortest and hence the most efficient diffusion path from the gas phase and through the electrolyte to the electrode surface.

The major problem of operating an alkali fuel cell is the fouling and poisoning of the electrodes and electrolyte dilution. Operation of the alkali fuel cell in air is preferred due to the weight considerations associated with an oxygen supply, but the presence of carbon dioxide, which is absorbed by the hydroxide electrolyte, giving the carbonate which fouls the cathode. Therefore air must be scrubbed to remove the carbon dioxide before being used as the oxidant. The anode may be poisoned by traces of carbon monoxide or sulphur containing compounds remaining after the fuel reforming process. Finally, the dilution of the electrolyte must be prevented by the efficient removal of water produced during operation. This can be achieved by removing excess water by passing the electrolyte through an evaporator and returning it to the cell at its normal concentration.

Even with all the progress made, fuel cell technology remains a specialist market as present fuel cell technology, compared to internal combustion engine technology, is rather expensive, thus prohibiting the development of the fuel cell family car. The technology has become accessible, suitable and economic for certain terrestrial applications. The low thermal signature of a fuel cell powered military vehicle hinders detection by the enemy and as environmental concerns grow, fuel cell buses are destined to take a greater role in the public service vehicle sector.

### 2.3.3 The acid electrolyte hydrogen-oxygen fuel cell

In acid electrolyte carbon dioxide is less of a problem and air can be used as the oxidant. This is essential in keeping the weight down of the fuel cell system for transport applications such as buses and cars.

In acid media the cell reactions for hydrogen oxidation and oxygen reduction now become

$$H_2 = 2H^+ + 2e^- \qquad (2.13)$$

at the anode and

$$2H^+ + ½\ O_2 + 2e^- = H_2O \qquad (2.14)$$

at the cathode giving a proton transfer mechanism.

The choice of acid for the electrolyte has been problematic. Adequate conductivities of many of the common oxy-acids are only obtained close to the decomposition temperatures and with catalysts present poisoning of the electrode is likely. In addition, the restriction on the working temperature precludes the compensation of poor kinetics of oxygen reduction at low temperature. Perchloric acid was found to be explosively unstable in the presence of hydrogen. Fluorosulphonic acid appeared to be a good candidate showing good conductivity and thermal stability but its high wettability on PTFE caused flooding of the porous electrode structure. The choice mineral acid became phosphoric acid. The phosphoric acid fuel cell has dominated the low temperature fuel cell market since its introduction in 1967. The performance of phosphoric acid at room temperature was initially not promising. Conductivities were low even at high concentrations and the oxygen reduction kinetics were extremely poor due to the competitive adsorption of phosphate ions. However, at elevated temperatures around 150°C the pure acid is mostly present as pyrophosphoric acid which shows high conductivity. Furthermore, the anions of this polymeric acid, as a consequence of their size, have a low charge density and chemisorption is disfavoured. In addition, other benefits of phosphoric acid include good fluidity, carbon dioxide tolerance, high oxygen solubility and a low rate of corrosion.

The operating temperature of the PAFC is in the range of 190-210°C and cooling systems are therefore essential for efficient heat management. The electrodes are attached to bipolar plates, i.e., they have a cathodic and anodic side, which are shared between adjacent cells.

The electrode consists of a ribbed porous carbon paper with a catalyst layer of high surface area carbon powder compacted with PTFE. The space between the cathode and anode of the cell is occupied by a porous PTFE-silicon composite which acts as a separator and reservoir for the aqueous electrolyte.

An alternative to using an aqueous acid electrolyte is to utilise a proton conducting solid polymer. This has been made possible by the success of Du Pont in developing perfluorinated sulphonic acid polymers. These materials consist of a PTFE backbone with pendant sulphonic acid moieties grouped together in a cluster structure like a reverse micelle. Clusters are connected by sulphonic acid channels and provide the means for cation conductance. These materials will be described in a later section. The anode and cathode are bound directly to the polymer electrolyte, which is in a membrane form, by hot pressing the layers together, resulting in a membrane electrode assembly. The current collectors are porous plates of carbon or graphite.

The performance of solid polymer fuel cell (SPEFC), using hydrogen at only a few bars pressure, is quite impressive with a high power/weight ratio but the fuel must be quite pure due to extreme sensitivity to contaminants. This is especially important if the source of hydrogen is from a reformed fuel such as methanol. Carbon monoxide levels as little as 10 ppm will cause deterioration of anode performance. This necessitates fuel processing adding complexity to the fuel cell system and extra weight, both of which have adverse consequences and in particular to transport applications were power/weight ratio is a major consideration. Also, hydrogen transport in its self greatly decreases the power/weight ratio because a significant proportion of the vehicle houses the compressed hydrogen cylinders. A choice solution would be to have a fuel cell system which combines the high power/weight ratio of the SPEFC with the utilisation of hydrogen directly from methanol. This is a convenient fuel to transport requiring no special technology and is comparable to petrol or diesel storage. This technology is currently being developed and is called the direct methanol fuel cell (DMFC). The hydrogen, generated at the anode, is in the proton form and is represented by the following reaction.

$$CH_3OH + H_2O = CO_2 + 6H^+ + 6e^- \qquad (2.15)$$

The accompanying cathode reaction is

$$3/2O_2 + 6H^+ + 6e^- = 3H_2O \qquad (2.16)$$

Some of the fundamental problems faced by the DMFC are poor anodic kinetics, requiring the discovery of better catalysts, the slow cathodic reduction of oxygen and the permeability of the presently available membrane materials to methanol. The latter problem is currently of major concern. Fuel crossover to the cathode, giving a mixed potential, results in a decline in cell performance. As with all fuel cell technology progress is good but applications currently remain in the specialist market. The following section will show the suitability of electrochemical energy technology, and in particular the Regenesys® system, in the specialist market of utility power storage.

## 2.4 The Regenesys® system in context

This system incorporates both fuel cell and secondary battery like performance. The two fluids, an oxidant and reductant are circulated through the reactor cell. When a load is applied electrical power is generated by the electrochemical reactions of the oxidant and reductant. The redox fuel cell battery offers the opportunity to be recharged by replacing the electrolytes or chemical reagents in addition to electrical recharging. The facile refuelling process can be a practical solution to range limitation of any battery powered vehicle, with the reagents being regenerated at depots for further use, and also offers greater flexibility for utility power storage applications. The reagents employed are aqueous solutions of alkali metal salts because solubility is maintained during electrical charge and discharge. In addition these compounds are not flammable, have very low vapour pressure, cheap and importantly compatible with the environment. The choice alkali metal salt in these systems has been sulphide which can be coupled with reagents such as ferric chloride or sodium hypochloride to give the primary or electrically irreversible two fluid systems described in section 2.1. To obtain an electrically reversible battery system the bromide-bromine half cell reaction, used in the zinc-bromide secondary battery, can be combined with the sulphide half cell reaction giving the electrochemical system upon which the Regenesys® system is based. The system discussed above is compared with the zinc-bromide, iron redox and the lead acid battery in the following table (table 2.1)

| Battery | Theoretical energy density Wh/kg | Practical energy density Wh/kg |
|---|---|---|
| Lead-acid | 167 | 40 |
| Zinc/bromine | 400+ | 100+ |
| Iron-redox | 180 | 44 to 66 |
| Two fluid redox | 200 to 300 | 60 to 150 |

Table 2.1 Comparison of energy densities of the two fluid redox system with the zinc-bromide, iron redox and the lead acid battery

Practical energy densities are a function of design parameters and system power density trade-offs. It can be seen from the above table that the two fluid battery system displays attractive energy densities. The high energy densities obtained, combined with the ease and rapidity of chemical recharging offers a very practicable solution to the powering of electric vehicles, portable power tools and emergency power supply.

### 2.4.1 The Regenesys® system

Regenesys® stores and releases electrical energy by means of the reversible electrochemical reaction between the solutions of sodium bromide and sodium polysulphide electrolytes. Other couples were studied during the development stage, but were not found to be suitable due to factors of efficiency, safety and cost. The simplified chemical reaction is represented by the following equation:

$$2Na_2S_2 + NaBr_3 = Na_2S_4 + 3NaBr \qquad (2.17)$$

The electrolytes circulate through the cell in two separate circuits and are stored in separate containers. The circulation of the electrolytes allows on-line electrolyte management such as filtration and routine reconstitution. Within the cell the cation selective membrane prevents the direct reaction between sulphide anions and the bromine. Electrical balance is achieved by sodium ion transport across the membrane.

On charging, the bromide ions are oxidised to bromine and complexed to bromide as tribromide or pentabromide ion. Free bromine is not very soluble in water but is very soluble in the bromide solutions due to the formation of polybromide ions. The sodium ions are transported through the cation selective membrane from the positive to the negative side of

the cell. The zero valent sulphur, present in the polysulphide anion, is converted to monosulphide as the charging process proceeds (equations (1.1) and (1.2)).

$$2Br^- \Rightarrow Br_2 + 2e^- \qquad (1.1)$$
$$E^\theta = 1.09V$$

$$S + 2e^- \Rightarrow S^{2-} \qquad (1.2)$$
$$E^\theta = 0.50V$$

During power generation or discharging, the polarity of the cell and reactions (1.1) and (1.2) reverse. Bromine is reduced to bromide while sulphide is oxidised to sulphur producing the electrons that form the current through a load. The energy density of the bromine/sulphide couple is limited only by the concentration of the bromine and not the concentration of the highly soluble bromide and polysulphide ions. The reacting ions cycle between the elemental form during the redox process. The cation associated with $S^{2-}$ and $Br^-$, in this case sodium, functions only to maintain electrical balance. Sodium and potassium compounds are preferred due to their high solubilities and low cost.

The membrane, in addition to preventing bulk mixing, impedes the migration of $S^{2-}$ ions from the cathodic to the anodic chamber. Migration of $S^{2-}$ results in coulombic loss and a sulphur suspension or precipitation due to its insolubility in the sodium bromide solution. Bromine produced during the charging process will be reduced by any sulphide present. During extended cycling sulphur may accumulate in the bromine/bromide electrolyte. The sulphur suspension can be trapped by an in-line filter and returned to the sulphide side and re-solubilised.

Another problem associated with the bromide side is the tendency of the molecular bromine, generated during the charging process, to react with water to form acids. The presence of activated carbon, if used in the anode, will catalyse the formation of acid. A mixture of silicon dioxide and activated carbon may be used to counter this effect but may cause the pH to rise on the bromine side as protons are transported across the membrane to the sulphide side. In addition, if the electrode becomes partially starved or the charging potential is too high oxygen will be generated forming more acid and further decreasing the efficiency of the system. The aim of this thesis is to address this inefficiency by employing electrolyte management strategies.

## 2.5 Perfluorinated membranes

Nafion® perfluorinated membranes are prepared from a precursor copolymer of tetrafluoroethylene and a sulphonyl vinyl ether. The sulphonic acid group, which is the site of ion exchange in Nafion® materials, is easily formed by the hydrolysis of the sulphonyl fluoride group. Nafion® materials have great thermal, chemical and mechanical stability and have therefore been utilised as a separator-ion conductor in electrochemistry and as an acid catalyst in synthetic chemistry. These materials are available in a variety of equivalent weights and as laminates of different equivalent weights and thickness for custom applications. Equivalent weight can be defined as the mass, in grams, of the dry polymer in the acid form that would neutralise one equivalent of base. The general chemical formula of the copolymer is represented in figure 2.1.

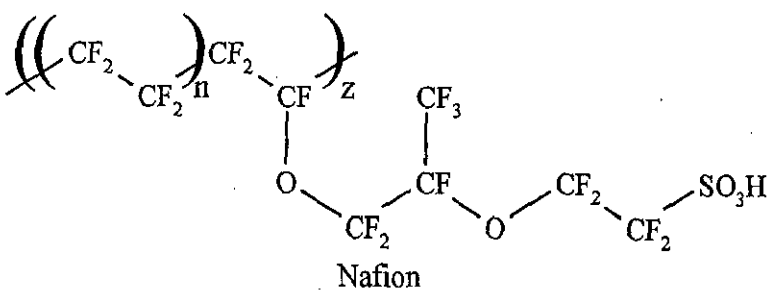

Nafion

Figure 2.1 Structural formula of Du Pont's Nafion® precursor copolymer where n varies between 6 and 13

The main commercial use of Nafion® is as a membrane separator in chlor-alkali cells. This application has direct relevance to the present work. In a typical chlor-alkali cell, chloride in brine is oxidised at the anode to chlorine, and water is decomposed into hydrogen and hydroxyl ions to produce sodium hydroxide at the cathode. This is represented by equations (2.18) and (1.6).

$$2Cl^- \Rightarrow Cl_2 + 2e^- \qquad (2.18)$$

$$2H_2O + 2e^- \Rightarrow H_2 + 2OH^- \qquad (1.6)$$

The role of the membrane is to allow the transport of sodium ions and to restrict the transport of hydroxyl ions. In an idealised Donnan membrane the homogeneous ion exchange sites and

the concentration of fixed ions must be greater than the corresponding free ion, i.e., the sulphonic acid group and the hydroxyl respectively.[16,17] In Nafion® membranes this condition is not usually met and the hydroxyl rejecting properties of Nafion® must be due to their unusual heterogeneous morphology.

### 2.5.1 Ion clustering

A cluster-network model has been proposed for Nafion® membranes and is consistent with the results of experimental measurements. The techniques which have been used to investigate the structure of Nafion® include scanning electron microscopy (SEM), nuclear magnetic resonance (NMR), infrared spectroscopy (IR), X-ray and transport studies. X-ray experiments have provided considerable evidence of ion clustering in Nafion® materials. A variety of cluster morphologies could give rise to the diffraction peaks observed in these experiments. Possible structures would include spherical, cylindrical and lamella arrangements of the ion exchange sites. Evidence to support a spherical morphology has come from transmission electron microscopy (TEM) of stained ultra-microtomed Nafion® sections. The micrographs showed approximately circular stained areas and are unlikely to be an artefact of electron microscopy. Working on the assumption that the clusters are spherical Gierke and co-worker [17] developed the cluster-network model for the arrangement of the ion exchange sites in Nafion.® (figure 2.2)

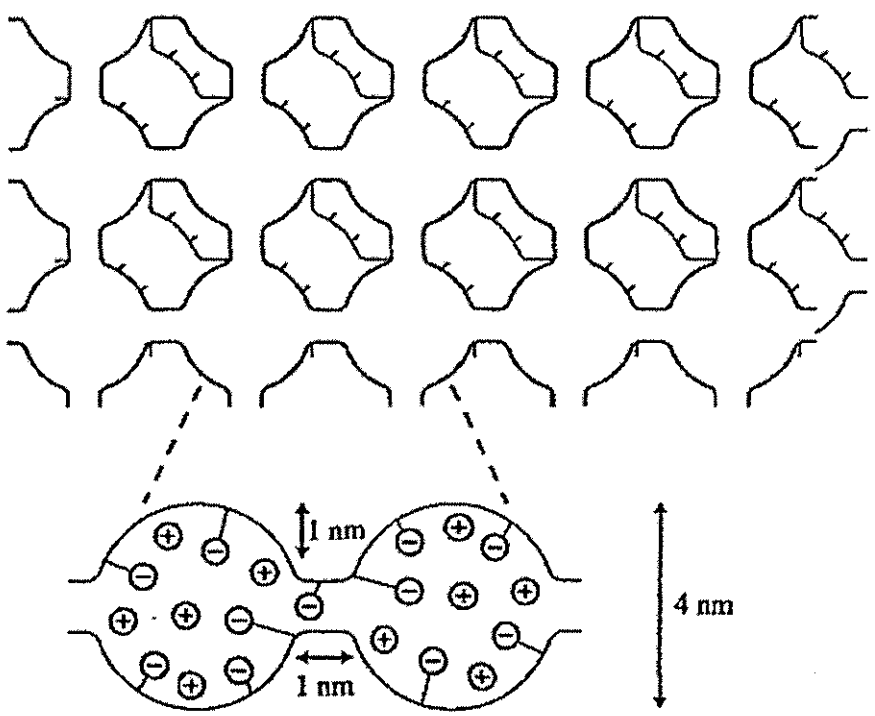


Figure 2.2 Diagram representing the cluster-network model of Nafion®[12]

In their model the polymeric ions and absorbed water separate from the fluorocarbon matrix into approximately spherical domains connected by short narrow channels. The polymeric charges are probably very near the water/fluorocarbon interface so as to minimise both the hydrophobic interaction of the water with the fluorocarbon phase and the electrostatic repulsion of neighbouring sulphonate groups. The resultant structure resembles that of an inverted micelle with communicating polymeric channels and is represented by figure 2.2.

### 2.5.2 Transport Properties

The physical model of Nafion® is very different to an idealised Donnan membrane model. In a Donnan system the ion exchange sites and the associated aqueous phase are uniformly distributed throughout the entire membrane. In contrast the cluster-network model of Nafion® represents a heterogeneous system with conductive ion-clusters randomly distributed in an insulating fluorocarbon matrix. Ion transport is best described by a percolation mechanism as proposed by Gierke and co-worker[17]. If the clusters are linked sufficiently, i.e., they are connected to form an extended network or pathway in three dimensions, a transition from ionic-insulator to conductor occurs at a threshold electrolyte loading of the membrane. Evidence for the percolative cluster-network model is provided by the very high ion selectivity of the Nafion® membrane (i.e., preferential sodium transport), and current efficiency of the cell, in spite of high membrane hydroxyl concentration. This behaviour cannot be explained by simple Donnan exclusion. In the percolative cluster-network model the negatively charged sulphonic acid groups electrostatically exclude hydroxyl ions from the cluster surface and the connecting channels. The concentration of hydoxyl ions in the clusters may be similar to external concentrations due to the shielding from the sulphonic acid groups by free water. However for an hydroxyl ion to traverse a channel to a neighbouring cluster a relatively high electrostatic potential has to be overcome. The associated double layer region with the cluster structure extends over the inner surface of the micelle with a thickness of ~0.5 nm but occupies the whole of the channel as its width is 1nm, i.e., a two double layer thickness, thus excluding free anions electrostatically from the channel.

The potential a hydroxyl ion will experience as it attempts to traverse the membrane in a Chlor-alkali cell can be envisaged as a descending potential ramp or voltage drop with an oscillating potential component superimposed. This relates to the electrostatic potential barrier (peaks) and a potential minimum (troughs) corresponding to the channel and cluster regions respectively.

At high sodium hydroxide concentrations the concentration gradient is sufficiently great to drive the back diffusion of the hydroxyl ions. The decreased water content of the membrane at high electrolyte concentration should disfavour transport. Mauritz and co-worker[18] suggested a tunnelling process that would enhance hydroxide ion transport at the decreasingly low water content of the membrane[19] due to the increased polarisation of the O-H bond. It is envisaged that the hydroxyl ions 'hop' through the channels by a mechanism analogous to the 'Grothuss' transport for protons.[20]

$$OH^- + H\text{-}OH + (H_2O)n + H_2O \Rightarrow \Rightarrow \ldots\ldots \Rightarrow \Rightarrow H_2O + H_2O + (H_2O)n + OH^- \qquad (2.19)$$

This tunnelling mechanism provides a path of lower energy that minimises repulsion by charge delocalisation of the negative charge on the hydroxide onto the water molecule. Mauritz and co-worker proposed that a tunnelling process involving the polarisation of the O-H bond in water molecules by the $Na^+$ ion would enhance hydroxide ion transport in environments of decreasing water content. This was due to the increasing population of $Na^+$-$OH^-$ ion pairs and the decreasing population of the $H_3O_2^-$ moiety. Polarisation induces an antisymmetrisation of the double energy well corresponding to the proton in the water experiencing a repulsion away from the $Na^+$ ion and an attraction to the $OH^-$ ion. This process would be enhanced by the electric field during electrolysis, thus giving the efficient movement of hydroxide in the anodic direction to the bulk electrolyte. Eventually the increasing antisymmetrisation will inhibit the tunnelling process, that is the energy gap will be too great, and hydroxide transport across the membrane will be disfavoured.

This mechanism will be important in the delivery of hydroxide to the circulating bulk sodium bromide electrolyte. Due to the cell's two phase electrolyte system the site of hydroxide generation is at the Nafion®-cathode interface. The local hydroxide concentration will become extremely high rapidly. The hydroxide will either drain-off out of the cathodic side aided by the osmotic flow of the water and the inhibition of the tunnelling process or diffuse across the membrane to the free aqueous electrolyte until antisymmetrisation of the double energy well is too great. Inhibition of back diffusion can also be achieved by the use of weak acid membranes and have been employed in combination with the strong acid membrane by the chlor-alkali industry. These composite or bilayer membranes combine the advantageous properties of the individual membranes whilst minimising any inherent disadvantages. Strong acid membranes have good sodium conductivity but allow the passage of sodium hydroxide when concentrations are greater than 15% by weight. In contrast, weak acid membranes have

poorer sodium conductivity but act as a better barrier to sodium hydroxide; due to lower water content. The weak acid layer is thin (10 μm) to compensate for its poorer inherent sodium conductivity. The resultant composite membrane has improved hydroxyl ion rejection properties whilst having acceptable conductivity.

## 2.6 Electrode reactions, process considerations and carbon materials

This section will discuss the cathodic reactions, the mechanisms involved and their relevance to the process considerations for electrolyte management. Finally, a brief description will be given of the carbon materials available to effect these reactions and processes. All reaction potentials quoted were measured versus the standard hydrogen electrode ( SHE ) unless otherwise stated.

### 2.6.1 Electrode Reactions

As was stated previously there is a choice of cathodic reactions; reduce water or oxygen. It is convenient to reduce water in the electrolyte because nothing additionally has to be supplied to the cathode. In addition, the hydrogen produced may be used in short term energy storage applications. The cell could operate galvanically consuming hydrogen and generating power when rebalancing is not required. The hydrogen gas would be stored within the cell, possibly in a highly porous electrode, and discharged as and when required. The hydrogen produced could offset electrolysis costs; a factor often overlooked when selecting a counter electrode reaction. Alternatively, oxygen reduction can be used as the cathodic reaction to give a lower cell potential but the relative slowness of the electrode reaction and mass transfer limitations pose technical problems. These problems could offset the advantages gained by the saving of volts.

There are several possible pathways for oxygen reduction[21] involving 2 or 4 electron transfer. The pathways can be classified as two or four electron reductions which occur in both acid and basic media. The four electron pathway corresponds to complete reduction to the hydroxide and is favoured thermodynamically but not kinetically. This can be explained by examining the necessary steps required for complete reduction. Multi-electron transfers with unstable intermediates accompanied by large increments of free energy must occur. Furthermore, ultimately the stable O-O bond must be cleaved to result in the hydroxide.

Consequently the two-electron process dominates, with the O-O bond intact and the net transfer of one or two protons corresponding to alkaline and acid conditions respectively.

In acid electrolyte - Direct 4-electron Pathway

$$O_2 + 4H^+ + 4e^- = 2H_2O \qquad (2.20)$$
$$E^\theta = 1.23\ V$$

In acid electrolyte - Peroxide Pathway

$$O_2 + 2H^+ + 2e^- = 2H_2O_2 \qquad (2.21)$$
$$E^\theta = 0.67\ V$$

followed by

$$H_2O_2 + 2H^+ + 2e^- = 2H_2O \qquad (2.22)$$
$$E^\theta = 1.77\ V$$

and/or

$$2H_2O_2 = 2H_2O + O_2 \qquad (2.23)$$

In alkaline electrolyte - Direct 4-electron Pathway

$$O_2 + 4H_2O + 4e^- = 4OH^- \qquad (1.8)$$
$$E^\theta = 0.40\ V$$

In alkaline electrolyte - Peroxide pathway

$$O_2 + H_2O + 2e^- = HO_2^- + OH^- \qquad (2.24)$$
$$E^\theta = -0.07\ V$$

followed by

$$HO_2^- + H_2O + 2e^- = 3OH^- \qquad (2.25)$$
$$E^\theta = 0.87\ V$$

and/or

$$2HO_2^- = 2OH^- + O_2 \qquad (2.26)$$

The 2-electron peroxide pathway is thought to be the main mechanism for both acid and basic media. In acidic electrolyte a further 2-electron reduction of the peroxide occurs readily. In addition the cathodic platinum catalyst layer decomposes the peroxide. In basic medium the first 2-electron step is relatively fast but the overpotential for the second 2-electron transfer is high. This results in a highly alkaline solution of peroxide.

Peroxide generation is not compatible with the operation of the main cell. If the reduction of the peroxide occurs in the main cell it will compete with the energy delivery/storage electrode reactions. In particular, oxygen from the decomposition of hydrogen peroxide will compete with bromine reduction during the discharge cycle. Therefore it is important to chemically or electrochemically consume the peroxide prior to delivery to the main cell.

It is fortunate for the rebalancing process that the peroxide is not very stable and is relatively easily decomposed. The further electroreduction proceeds readily on most cathodic surfaces and in addition the cathode material acts as a heterogeneous decomposition catalyst. However, in alkaline solution the overpotential for the further reduction to hydroxide is high (i.e., peroxide reduction potentials are negative of -0.7 V vs. SCE) and chemical decomposition is relatively low on uncatalysed or treated carbons. However, the paper bleaching industry coincidently requires alkaline peroxide solutions in the concentrations obtained by the cathodic reduction[22]. In addition the pulp and paper industry have decreased consumption of traditional chlorine based bleaching agents on environmental grounds increasing the demand for peroxide as a substitute. This has created a renewed interest in the electrolytic reduction of oxygen. H-D Tech. Inc. has developed a process for production of hydrogen peroxide in alkaline solution by the cathodic reduction of oxygen.[23]. The present work on the rebalancing cell will have relevance to industrial on site hydrogen peroxide electrosynthesis. As stated earlier for the rebalancing cell application oxygen reduction must be complete. This can be achieved by compensating for the high overpotential for reduction to the hydroxide by catalysing both oxygen reduction and peroxide decomposition. This is achieved by the heterogeneous catalytic properties of the platinum in the MEA and the homogeneous catalytic properties of bromide and hydroxide ions present in the electrolyte. The net result is an increase in the contribution of the 4-electron mechanism. The

thermodynamic instability of hydrogen peroxide[24] in aqueous solution can be represented by the following reaction scheme

$$2H_2O_2 = O_2 + 2H_2O \qquad (2.23)$$

$E^{\theta} = 1.07$ V (acid solution) and 0.79 V (basic solution)

Catalytic decomposition of hydrogen peroxide by the halogens[23] is well known. If the standard electrode potential of peroxide decomposition ($E^{\theta} = 1.07$ V) is compared, especially under acid conditions, to that for the bromine/bromide redox couple ($E^{\theta} = 1.09$ V) it is evident that the potentials match closely. This would explain the greater decomposition rate of hydrogen peroxide in the sodium bromide electrolyte. It is well known that a more favourably reducible system can act as an intermediate or electron carrier; nature abounds with such examples. Electrons are transferred between metal sites within proteins or a complex of proteins, i.e., the respiratory electron transport chain, comprising of four discrete redox complexes, which ultimately reduce oxygen to water[25] and the horse radish peroxidase (HRP), with its iron III active site, which decomposes hydrogen peroxide to water.[26] To maximise the efficiency from such a system, the reversible potential of the redox couple should be as close as possible and reaction of the hydrogen peroxide to the reduced form of the catalyst should be rapid. The reactions responsible for catalysis in the bromide-hydrogen peroxide system are probably,

$$H_2O_2 + 2Br^- + 2H^+ = Br_2 + 2H_2O \qquad (2.27)$$

$$Br_2 + H_2O_2 = 2Br^- + 2H^+ + O_2 \qquad (2.28)$$

The system will reach a steady state, in which the concentration of both forms of the catalyst will be constant and reactions (1.19) and (1.20) will proceed at equal rates giving the overall reaction (1.15). The mechanisms of these reactions may involve a two electron process with a hypobromite intermediate or a 1 electron mechanism involving $OH^{\cdot}$ and $HO_2^{\cdot}$ radicals in a chain reaction. These processes do not necessarily involve free electrons. An oxygen atom transfer is equivalent to a loss of two electrons while a hydroxyl radical transfer is equivalent to a transfer of an electron in the opposite direction. In alkaline solution hydroxyl ions may catalyse the decomposition of peroxide by the following mechanism.[24]

$$H_2O_2 + OH^- = HO_2^- + H_2O \qquad (2.29)$$

$$H_2O_2 + HO_2^- \Rightarrow H_2O + O_2 + OH^- \qquad (2.30)$$

The resultant oxygen can then be reduced.

In addition a redox-dismutation mechanism is available for the decomposition of peroxide. This process utilises the reverse half cell reaction for the first step of the peroxide pathway (1.16), which is of an intermediate thermodynamic value close to zero, coupled with the forward reaction of the second step of the peroxide pathway.

$$HO_2^- + OH^- = O_2 + 2H_2O + 2e^- \qquad (2.24)$$
$$E^\theta = -0.07\ V$$

$$HO_2^- + H_2O + 2e^- = 3OH^- \qquad (2.25)$$
$$E^\theta = 0.87\ V$$

The above treatment of the electrode reactions has only dealt with the equilibrium case when the cell current is zero. This situation can be represented as convention demands by the following equation:

$$E^e_{CELL} = E^e_C - E^e_A \qquad (2.31)$$

When the cell current is none zero the cell potential shifts considerably from the equilibrium value. In the case of an electrolytic cell, like the rebalancing cell, the potential is far more negative than the equilibrium value and represents an increase in energy input to the system, i.e., the free energy becomes more positive (equation 2.32).

$$\Delta G^\theta_{CELL} = -nF\,(E^e_C - E^e_A) \qquad (2.32)$$

The additional voltage drops are due to the sum of the overpotentials at the electrodes due to limitation of electron transfer and interfacial mass transfer, $\Sigma\,\eta$ , combined with the potential ohmic drops within the circuit, $\Sigma$ IR. The actual cell potential, $E_{CELL}$, can therefore be represented by the following equation,

$$E_{CELL} = E^e_{CELL} - \Sigma\eta - \Sigma\,IR \qquad (2.33)$$

Where the overpotential, $\eta$ , can be defined as

$$\eta = E - E_e \qquad (2.34)$$

The overpotentials can be discussed in terms of the effect on the net current density, j, of the system:

$$j = -j + j \qquad (2.35)$$

The measured current density is the algebraic sum of the component cathodic and anodic currents (1.22). Where -j is the cathodic current and j the anodic current according to convention.

At the equilibrium potential the current density is zero:

$$j = -j + j = 0 \qquad (2.36)$$

This represents a dynamic equilibrium where the partial currents are of opposite sign and of equal magnitude. The magnitude of the partial current is an important kinetic parameter as it measures the extent of charge transfer activity at the equilibrium potential and is termed the exchange current density, $j_o$, which is defined by:

$$j_o = - (-j ) = j \qquad (2.37)$$

The equilibrium electrode potential is given by the Nernst equation:

$$E_e = E^\theta + RT / nF \ln(a_O / a_R) \qquad (2.38)$$

where $a_O$ and $a_R$ are the activities of the oxidant and reductant respectively. $E^\theta$ is the standard electrode potential as used in the discussion of the electrode reactions of the rebalancing cell. It is more convenient to work with concentrations and so the relationship can be expressed in terms of concentration as follows,

$$E_e = E_e^{'} + RT / nF \ln (c_O / c_R) \qquad (2.39)$$

and alternatively:

$$E_e = E_e' + 2.3\ RT / nF \log (c_O / c_R) \quad (2.40)$$

where the formal potential, $E_e'$, is the equilibrium potential when concentrations are equivalent. The Nernst equation represents the special case of dynamic equilibrium, i.e., no net current flows according to equation 2.36

$$j = -j + j = 0 \quad (2.36)$$

The Nernst equation is therefore fundamentally a thermodynamic description of the system and gives no information on the rate of reaction. In practise, as in the electrolyser, significant overpotentials and ohmic losses inherent in the system develop as current flows thus driving the system far from equilibrium. Therefore, this situation can be best described in terms of electron transfer and potential. The Butler-Volmer equation relates the measured current density to the overpotential and exchange current density of non-equilibrium systems. Equation (1.28) represents one of the limiting forms of the Butler-Volmer relationship.

$$j = j_0 \left\{ \left[ \exp \frac{\alpha_a nF\eta}{RT} \right] - \left[ \exp \frac{\alpha_c nF\eta}{RT} \right] \right\} \quad (2.41)$$

The two exponential terms describe the contribution from the backward and forward reactions. The observed current and overpotential relationship depends on the exchange current density, $j_o$, and the transfer coefficients, $\alpha$, for the opposing anodic and cathodic processes. The transfer coefficients are related, i.e., $\alpha_a = \alpha_c = 0.5$, and can therefore be regarded as the fraction change in overpotential which gives a change in the electron transfer rate constant. The observed current density increases when the exchange current density and the overpotential increases. If the exchange current density is sufficiently high current density may be obtained at low overpotentials. The exchange current density may vary depending on electrode material and its surface condition. The modification of electrode surfaces and reactions to increase the exchange current density and consequentially lower overpotential is the principle of electrocatalysis. This has relevance to this study and the continuing development of the sulphide reaction of the Regenesys® system.

### 2.6.2 Process considerations

The relatively low rates of oxygen reduction and mass transport limitations can be compensated further by using high surface area cathodes in a variety of configurations. High

porosity carbon materials may be used to compensate for the small oxygen reduction current using a packed particle bed and mass transport increased by configuring the high porosity cathode in a fuel cell-type arrangement as in one of the present embodiments of the rebalancing cell. The fuel cell MEA arrangement reduces the mass transfer problem by keeping the gas feed side dry. This gives a reaction zone at the gas-liquid interfacial region with only a thin layer of liquid over the active area of the electrode, thus enhancing gaseous transport of oxygen to the electrode or the efficient venting of hydrogen. These electrodes show good short-term performance but after prolonged operation sodium peroxide and hydroxide may precipitate in the pores due to the solubility product of these species being exceeded.[27] This effect has caused a problem in obtaining adequate electrode lifetimes for the electrosynthesis of hydrogen peroxide. This is not perceived as a problem in the present application. The rebalancing cell only needs to operate sufficiently to neutralise excess protons in Regenesys®'s electrolyte process stream or streams. Therefore, the electrolyser will not stray excessively into the alkaline region of operation and concentrations will not build-up to critical levels.

The alternative approach using a packed bed electrode avoids precipitation problems, as the pores are relatively large, but the thin layer of liquid giving the shortest diffusion path is now lost. In addition, operation is complicated by the need to control fluid flow rates and oxygen pressure. The fuel cell electrode is the most suitable for the present application. Having established the most suitable configuration of the cathode the choices of available carbon materials for the electrode will be discussed. A review of $sp^2$ hybridised carbon materials and the voltammetric techniques used to assess them follows.

### 2.6.3 Carbon materials

Many types of $sp^2$ hybridised carbon have been studied and utilised in electrochemistry.[28] They all share similar bonding with a bulk bond length of 1.42 Angstroms (one Angstrom unit is equal to $10^{-10}$ metre). Changes in bond length would be expected near the edges of the $sp^2$ carbon planes but as yet have not been measured. The bulk behaviour of these materials is very different and is determined by the graphitic crystallite orientation (interplanar microcrystallite size, Lc) and graphitic crystallite size (intraplanar microcrystallite size, La). For example carbon black is highly disordered. Here the order is only short ranged and may involve only a few graphitic layers. On heating carbon to above 2000°C crystallite stacking increases, i.e., larger Lc, and interplanar bonding through weak van der Waal's forces becomes increasingly important. This is reflected in the familiar property of softness due to

planar slip. The intraplanar microcrystallite size, La, is the mean size of the graphitic unit through the plane of the $sp^2$ hybrids, i.e., in the plane of the lattice. Crystallites can vary from 2 or 3 to millions of aromatic rings in one $sp^2$ carbon sample and are thus considered to be a collection of molecules with varying properties. Therefore it is likely that the behaviour of carbon samples will vary dramatically. A brief profile of the various carbons used in this study will be described in the following sections.

**Glassy carbon**

Glassy carbon is widely used in electroanalysis[28,29] The key properties making it the choice material in electroanalytical chemistry are its impermeability to water or organic solvents and its ability to work at more negative potentials than platinum. Glassy carbon, having a small La and Lc, is relatively disordered giving it vitreous or glass like properties.

**Reticulated Vitreous Carbon (RVC)**

RVC is essentially a high surface area glassy carbon due to its high volume voidage. An RVC electrode can posses as much as 96% void volume. This clearly gives many hydrodynamic advantages including efficient mass-transfer within a rotating disc electrode (RDE) for analytical purposes and efficient drainage of products in an electrolyser.

**Carbon composites and porous carbons**

These materials are composed of powdered graphite dispersed in an insulating binder. The non-porous materials consist of varying ratios of polyvinylidene difluoride (PVDF) to carbon. The porous carbon materials provided had been prepared from a mixture of carbon (90% w/w) and polyethylene (10% w/w) passed under 200 tons at 200 to 240°C with a variety of chemical treatments. The treatments were air and sulphuric acid to enhance activation of carbon surfaces. Materials derived from the heating of coconut shell were treated with hydrogen and nitric acid. Chemically untreated materials were also received.

Non-porous carbon composites, being only partially carbon, exhibit low background currents due to a low active area. This is a great advantage for electroanalytical applications but may not be for the rebalancing cell. Here we require the highest active area possible. These materials do, however, offer the advantage of modifying the electrode by incorporating species into the matrix such as redox mediators or catalysts. To effectively assess the suitability of the materials the well-characterised hexacyanoferrate (II) and hexacyanoferrate (III) redox couple was selected to characterise the carbon materials using voltammetry.

## 2.7 Carbon based electrodes

Several electrolyte management strategies have been explored[1]. As stated above, a first step in preventing the over acidification of the bromide electrolyte is the coating of the electrode with silicon dioxide. To prevent the pH rising too much an optimum mixture of silicon dioxide and activated carbon can be selected to give only a slow decrease in pH. The slow decrease in pH can easily be compensated for by the delivery of hydroxyl ions from the rebalancing cell utilising the electrolysis of the sodium bromide electrolyte. In previous embodiments of the rebalancing cell the hydrogen generated is either vented from a tank or if the cell is separated by a microporous membrane the gas maybe vented directly from the cathodic compartment. As was discussed, in the introduction to electrolyte management section, the present work discussed in this thesis utilises a novel application of membrane electrode assembly technology. The following chapters describe this work.

### 2.7.1 Introduction to present electrolyte management

Electrolyte management can be approached in two different ways. One arrangement of the rebalancing system comprised of a separate flow cell electrolyser and the other a porous carbon cathode which can be directly inserted into the process stream of the Regenesys® system. Both approaches will be discussed in the following sections.

### 2.7.2 Porous carbon open cathode

The rebalancing cell based on a porous carbon cathode (figure 2.3) will comprise of a cylindrical cathode with one or more anodes in a flowing or static electrolyte when integrated into the Regenesys® system. The porous carbon structure acts as a gas conduit. The cathode has a large internal void structure which provides a gas path for the electrolytically generated hydrogen, thus avoiding hydrogen permeation into the electrolyte.

It is preferable to coat the cathode with an ion exchange membrane to prevent chemical reaction of bromine with the hydrogen. Also, the ion exchange material maintains a continuous water flux from the electrolyte to the reaction sites on the cathode. The hydroxyl ions, generated at the reaction sites, are either driven out through the membrane due to the large concentration gradient and neutralise hydroxonium ions in the bulk electrolyte, or are neutralised by an incoming proton flux. The latter process helps in maintaining the water balance of the membrane. The advantage of this hydroxyl delivery system is that minimal disruption of the process stream is required. The aim of this work was to demonstrate the

feasibility of hydrogen venting away from the process stream of the electrolyte. Hydrogen generated on the electrode surface will be retained in the carbon matrix aided by the application of negative pressure prior to venting. Thus preventing the mixing and chemical reaction between the hydrogen and bromine.

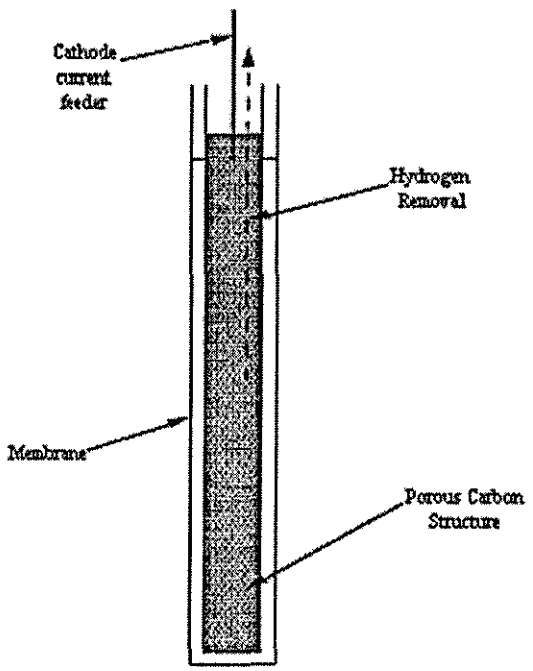


Figure 2.3 Porous carbon cathode with membrane coating

### 2.7.3 A novel solid polymer electrolyte - aqueous electrolyte hybrid cell

The second proposed approach to electrolyte rebalancing used fuel cell gas diffusion electrode (GDE) technology applied in a novel way (figure 2.4). In the cell the anolyte (5 M NaBr) chamber and a cathode (gas) chamber are separated by a membrane (Nafion®) electrode assembly (MEA) giving a cell with an innovative two phase (solid-liquid) electrolyte. In addition to the membrane conducting the current to and from the electrode, neutral species such as hydrogen and bromine are prevented from mixing. This would result in inefficiency due to chemical combination and reduction of bromine at the cathode. Reticulated vitreous carbon (RVC)[14], a glassy carbon foam, ensured good electrical contact between the back of gas diffusion electrode and cathode current collector. In addition, the RVC provides a path of low fluid flow resistance to hydrogen and other process fluids including sodium hydroxide. This is due to its very high voidage (96%) and glassy surface.

The cathode current collector and anode were 50% EG10/50% PVDF an electrolytic graphite polyvinylidene difluoride composite. The GDE was an E-TEK electrode. All areas were 55

$cm^2$ . The volume of the sodium bromide electrolyte was 200 $cm^3$ and the maximum volume of the flow cell system, including headspace, was 350 $cm^3$.

The hydroxide generated will be drained off through the RVC to rebalance the polysulphide electrolyte. Some hydroxide will traverse the membrane if concentrations are greater than wt 15% due to the high local concentration gradient and the non Donnan properties of the membrane which was explained in section 2.5. This hydroxide will neutralise protons in the bromide electrolyte. If hydroxide delivery to the bromide side is not required back diffusion can be prevented by the use of composite weak and strong acid bilayer membranes as used in the chloralkali industry. Alternatively, the cathodic gas chamber can be flushed with water to prevent sodium hydroxide building up.

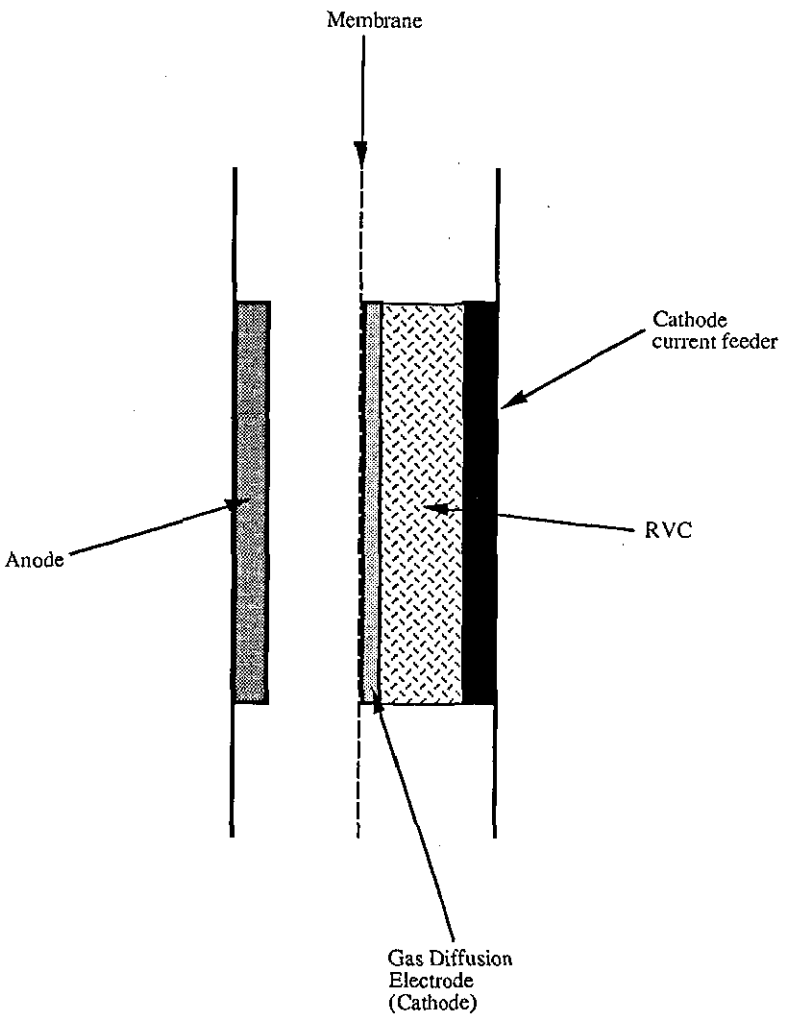


Figure 2.4 Schematic representation of the rebalancing cell

## 2.8 Voltammetry

Voltammetry[30,31,32] is a broad term which refers to techniques where the electrode potential is controlled and the resultant current is measured. The action occurs at the electrode-solution interface. Here, the chemical and electrochemical reactions take place. The potential of the electrode determines what processes occur here and may result in the solution near the electrode being very different from the bulk. If the potential is sufficiently positive or negative a redox reaction will occur changing the concentration of the electroactive species. The region affected by the electrode is called the diffusion layer and extends only a few microns. Faraday's law links the current produced to the concentration of the electroactive species, i.e., the quantity of charge passed corresponds to the quantity of electroactive species oxidised or reduced at the electrode. At sufficient potentials the current is only limited by how fast the electroactive species reaches the electrode surface. In still electrolytes the species must do this by traversing the diffusion layer from the bulk solution. The driving force for this is provided by the concentration gradient set up when species are consumed at the electrode. The greater the concentration gradient the faster the diffusion process. This is described mathematically by Fick in his First Law of Diffusion (equation1.18) . It states that the diffusional flux ( j ) is directly proportional to the concentration gradient multiplied by the constant of proportionality known as the diffusion coefficient ( D ) which is characteristic of the diffusing species.

$$j = -D\, dC / dx \qquad (2.42)$$

Now, if Faraday's Law is combined with Fick's First Law of Diffusion a general expression for the diffusion limited current, $I_d$, is obtained,

$$I_d = n\, F\, A\, D\, (dC / dx) \qquad (2.43)$$

Where n is the number of electrons involved, F is Faraday's constant, A is electrode area. This expression clearly shows the proportional relationship between current and concentration in voltammetry. Furthermore, it can be seen that any differences in voltammetric techniques are only due to the way the concentration gradient, and hence how the diffusion layer, is created and maintained as the distance the analyte molecule travel in unit time is always related to $t^{-1/2}$. Voltammetric techniques can be placed into three general

groups: sweep, hydrodynamic and pulse techniques. The following discussion will survey examples of the trinity of techniques.

### 2.8.1 Potential Sweep methods

The simplest potential sweep method is linear sweep voltammetry. The potential is swept from an initial potential to a final potential. The potentials are chosen to enclose the formal potential of the electroactive species. Initially, no current flows but as the potential passes the formal potential a current begins to flow. The current peaks and decays gradually giving the signature asymmetric current transient. The decay in current is due to the depletion of species causing an extension of the diffusion layer further out from the electrode surface. The peak current, $I_p$, is given by the Randle-Sevcik equation,

$$I_p = 0.4463\ n\ F\ A\ C\ (n\ F\ v\ D\ /\ R\ T)^{½} \qquad (2.44)$$

where n is the number of electrons in the electrode reaction, F is the Faraday constant (96485 C $mol^{-1}$), A is the electrode area ($cm^2$), C is the concentration (mol $cm^{-3}$), v is the scan rate (V $s^{-1}$), D is the diffusion coefficient ($cm^2$ $s^{-1}$), R is the universal gas constant (8.314 J $mol^{-1}$ $K^{-1}$) and T is the absolute temperature (K). The temperature is assumed to be 298.15 K.

The Randle-Sevcik equation can be written more concisely as

$$I_p = (\text{constant})\ n^{3/2}\ v^{1/2}\ D^{1/2}\ A\ C \qquad (2.45)$$

where the constant = 2.687 x $10^5$ C $mol^{-1}$ $V^{-1/2}$. This equation only applies to the equilibrium situation, i.e., when electrode kinetics are fast and or if the potential sweep rate is sufficiently slow enough to match the kinetics.

A variation of the previous technique involves cycling between the initial and final potentials and is known as cyclic voltammetry.[33] This enables the fate of electrogenerated species to be probed. For example a species may be reduced on the forward sweep and then oxidised on the return scan. This results in a voltammogram showing two peaks of equal size but have opposite sign. Alternatively, the reduced species may be unstable or diffuse away on the time-scale of the experiment and the oxidation peak could be smaller than the reduction peak or in the extreme case absent.

### 2.8.2 Rotating disc electrode voltammetry [30,32]

The previous methods keep the solution still so that mass transfer is only by simple diffusion. So, at first it seems strange to agitate the electrolyte by rotating the electrode. If the solution is stirred in a controlled way, i.e., by the rotation of the electrode itself, a laminar flow of electrolyte is directed to the disc electrode. The electrolyte must stop when it reaches the electrode and in fact a 'skin' of electrolyte clings to the electrode surface and they rotate together. Here mass transport is solely simple diffusion even though the transport in the bulk is by convection (forced). This has consequences for the current response to the potential scan. A very compact diffusion layer is maintained by the convection of the bulk electrolyte during the experiment giving a constant steep concentration gradient with respect to time and hence a diffusion limited or steady state current.

The limiting current is given by the Levich equation

$$I_L = 0.620\, n\, F\, A\, D^{2/3}\, \omega^{1/2}\, v^{-1/6}\, C \qquad (2.46)$$

Where $\omega = 2\pi$ (revolutions per second) and v is the kinematic viscosity ($cm^2\ s^{-1}$)

### 2.8.3 Chronoamperometry [34,35]

The simplest chronoamperometric method is a single potential step procedure. Unlike the sweep methods, where the potential is changed gradually, chronoamperometry involves a 'jump' in potential or a pulse. This involves stepping the electrode potential from an initial potential to a final potential. The potential window is chosen to cover the formal potential for the analyte and the second potential is sufficiently oxidising or reducing. No significant current flows at the first potential but once the potential is stepped to the final potential the analyte begins to be consumed by either an oxidation or reduction process. The concentration at the electrode-electrolyte is rapidly driven to zero. The resultant high concentration gradient gives a very large current directly after the step. After a while the concentration gradient relaxes and the diffusion layer extends further from the electrode surface, thus giving decay in current with time.

The Cottrell equation describes the current transient $I_t$ and its relationship with time,

$$I_t = nFAC(D/\pi)^{1/2}\, t^{-1/2} \qquad (2.47)$$

where n is the number of electrons in the electrode reaction, F is Faradays constant (96485 C $mol^{-1}$), A is the electrode area ($cm^2$), C is the concentration (mol $cm^{-3}$) and D is the diffusion coefficient ($cm^2$ $s^{-1}$). The experimental data is usually plotted as I versus $t^{-1/2}$. The result is a straight line graph or Cottrell plot. The slope of the plot can yield either the concentration of the analyte or the diffusion coefficient. This will be discussed in more detail in Chapter 4.

### 2.8.4 The hexacyanoferrate(III) - hexacyanoferrate(II) redox couple

The electrochemistry of hexacyanoferrate(III) and hexacyanoferrate(II) redox couple has been widely studied.[29,30] The candidate carbon cathode materials will be assessed with this well characterised system using cyclic voltammetry. The iron complexes are classed as outer sphere because electron transfer is not complicated by ligand reorganisation and coupled chemical reactions. Therefore the redox system is reversible with the current only dependent on mass transfer when the potential is sufficiently reducing or oxidising. The half reaction for the redox couple is

$$Fe(CN)_6^{3-} + e^- \Leftrightarrow Fe(CN)_6^{4-} \qquad (2.48)$$

hexacyanoferrate(III) + e- <=> hexacyanoferrate(II)

The formal potential of the half reaction is around +400 mV vs. the standard hydrogen electrode. If the potential is more negative than +400 mV then the hexacyanoferrate(III) complex is reduced to the hexacyanoferrate(II) complex. Conversely if the potential is made more positive the hexacyanoferrate(II) complex is oxidised back to the hexacyanoferrate(III) complex. This results in a voltammogram showing two peaks of equal size but of opposite sign. The system can be cycled between the two states indefinitely.

# Chapter 3 Experimental Details

## 3.1 Porous carbon open cathode

The porous carbon cathode comprises a cylindrical carbon rod with dimensions of 1 cm diameter and 13 cm length coated by spraying with a 50% (by volume) aqueous Nafion® solution. Dipping with a neat solution was also employed. The top of the rod was encased in a PTFE collar of 4 cm in length. Electrical connection was made by attachment of copper wire with silver epoxy resin. This was housed in a glass cell with a platinum loop counter electrode positioned around the central cathode (figure 3.1).

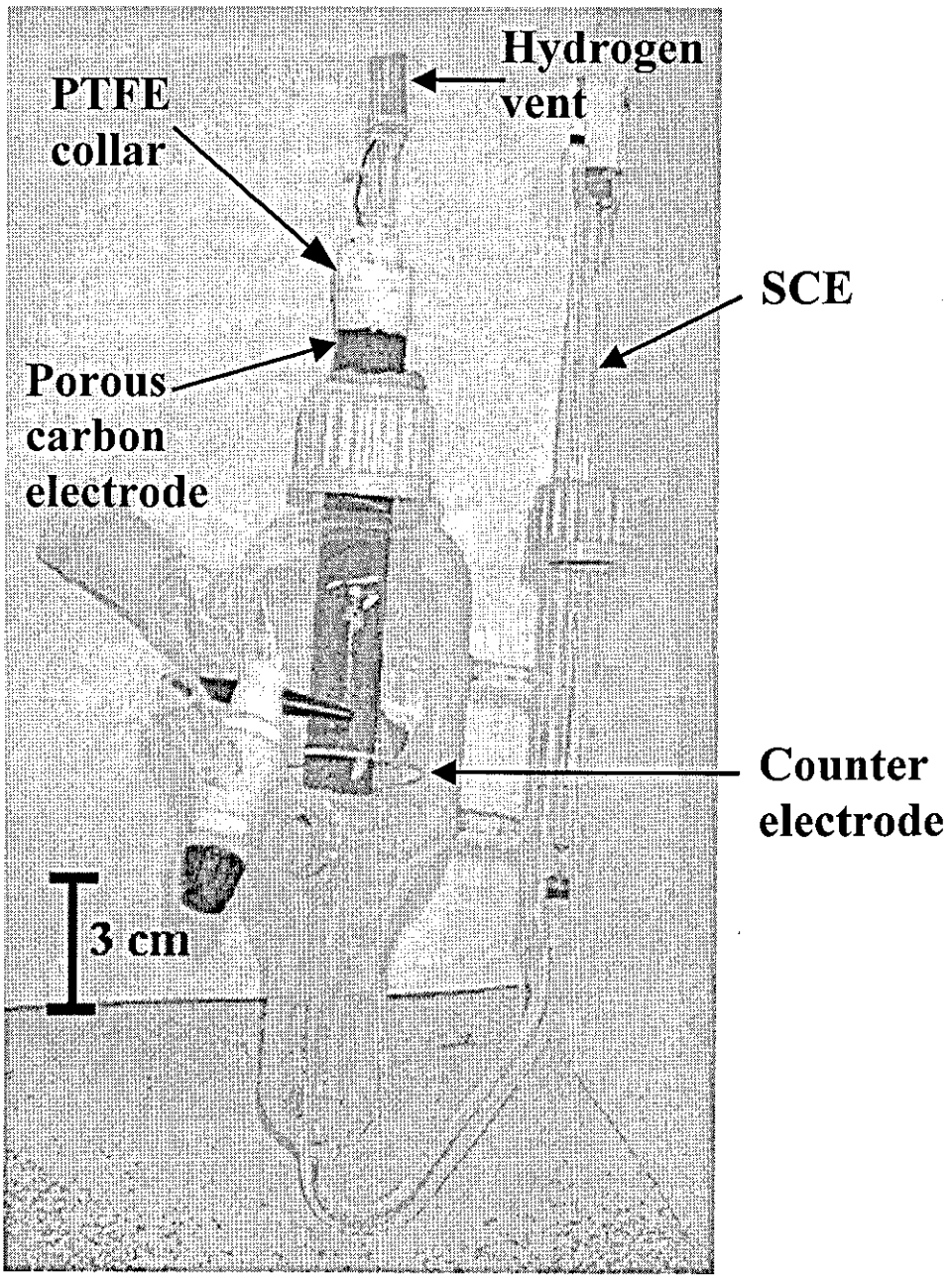


Figure 3.1 Photograph of the electrochemical cell for testing the porous carbon cathode

The cathode has a large internal void structure which provides a gas conduit for the electrolytically generated hydrogen. The aim of this work was to demonstrate the feasibility of hydrogen venting away from the process stream of the electrolyte. Hydrogen generated on the electrode surface will be retained in the carbon matrix aided by the application of negative pressure prior to venting.

### 3.1.1 *Electrochemical measurements*

A current was demanded from the system and allowed to equilibrate. The responding potential was measured when the reading became stable versus a standard calomel reference electrode. The current was applied incrementally in 5 mA steps to a 50 mA limit.

### 3.1.2 Instrumentation

Ministat Precision Potentiostat, Thompson Electrochemistry Ltd. Beckman Tech-310 multimeter.

## 3.2 The novel solid polymer electrolyte - aqueous electrolyte hybrid cell

The rebalancing cell comprised of a PVDF (polyvinylidene difluoride)/graphite composite electrode of area 55 $cm^2$ for bromine generation (anode) with a turbulence promoter. This is backed onto the membrane side of the MEA (membrane electrode assembly). The MEA was constructed by hot pressing an E-TEK gas diffusion electrode (cathode)[36-39] onto a Nafion® 117 membrane so as the catalyst layer was intimately bonded to the membrane. This is helped by spraying a solution of Nafion® ionomer onto the platinum side of the electrode. The press was heated to 100°C and the membrane and cathode were put under pressure (10 kg $cm^{-2}$) between two steel sheets. The temperature was set to 140°C maintaining the pressure. When the temperature reached 120°C the pressure was increased to 3-4000 kg $cm^{-2}$ for one minute. Then the heater was turned off and pressure released. The MEA was installed into the cell by backing it onto a reticulated vitreous carbon (RVC) sheet which made electrical contact to a PVDF/graphite current collector. The anode was exposed to a 5 M sodium bromide electrolyte loop. The RVC provides a path of low resistance for process fluids due to its high voidage (96%) and glassy surface. The volume of the flow cell system, including headspace, was 350 $cm^3$ (figure 3.2).

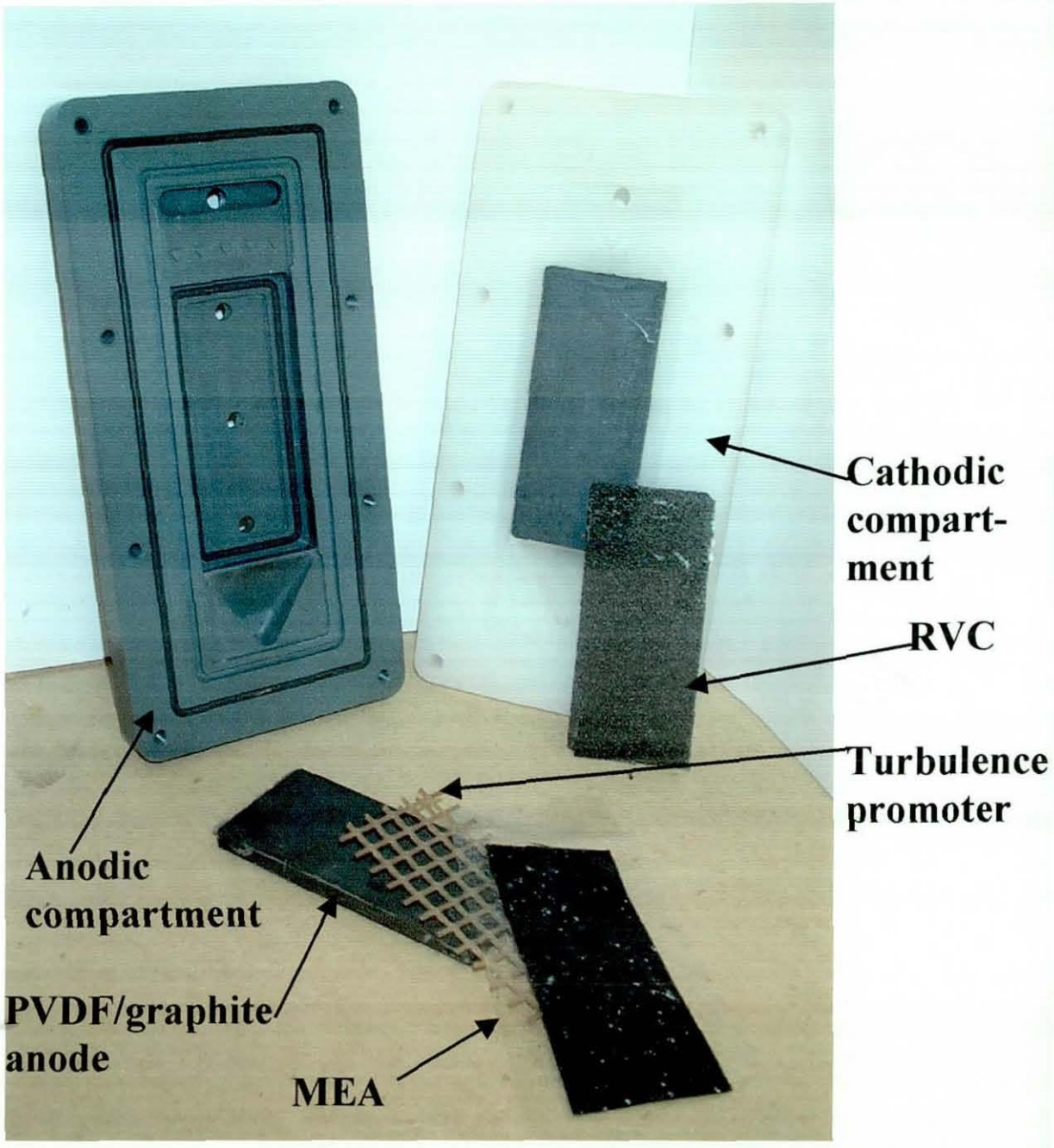


Figure 3.3 Photograph of rebalancing cell components (scale: electrode 55 $cm^2$)

The hydroxide generated was drained off through the RVC and out of the cell. Some hydroxide will traverse the membrane due to the large concentration gradient. This hydroxide neutralised protons in the bromide electrolyte and membrane. If hydroxide delivery to the bromide side was not required back diffusion can be prevented by the use of hydroxyl repelling membranes as used in the chloralkali industry. Alternatively, the cathodic gas chamber can be flushed with water to prevent sodium hydroxide building up.

### 3.2.1 Electrochemical and pH measurements

The operating cell potential-current density data was obtained up to 70 mA $cm^{-2}$. Potential and pH measurements of the electrolyte were taken when the potential was stable, usually within 5 minutes. No reference electrode was used as the operating cell voltage was measured.

Potential and pH data were acquired over a period of over 4 hours, thus enabling the electrolyser to be tested under bromine concentrations encountered during normal operation of the main cell.

Potential and pH measurements were obtained when the electrolyte was adjusted to pH 1 and 4 with 1 M sulphuric acid, to simulate part of the charge cycle. During the experiments the cathodic gas chamber was purged with nitrogen, oxygen and air.

### 3.2.2 Instrumentation

Thurlby 14 V- 4A power supply. Russell pH probe; combination type with epoxy body and gel filled. WPA pH meter CD7400. Beckman Tech-310 multimeter.

## 3.3 Carbon materials for the cathode

Cyclic voltammetry was performed on activated and unactivated carbon materials in an aqueous potassium chloride (0.5 M) supporting electrolyte with a hexacyanoferrate (III) analyte (5 mM). Experiments were also performed in 5 M sodium bromide to investigate the electrochemistry of the electrolyte and dissolved oxygen. Electrode discs of 7 mm diameter were slightly abraded and mounted on PVDF:EG10 composite disc of same diameter. Some electrodes were mounted without abrasion.

### 3.3.1 Instrumentation

AutoLab GPES (general purpose electrochemical system). RDE motor, Oxford Electrodes.

### 3.3.2 Hexacyanoferrate-potassium chloride system at the glassy carbon electrode using the three voltammetric techniques

Good experimental set up was confirmed using this well characterised reversible system. Reproducible hexacyanoferrate signature cyclic voltammetric behaviour was observed in the potential window 1 to 0 V vs. a silver/silver chloride reference electrode and a glassy carbon working electrode. Scan initiated in the cathodic direction. Cyclic voltammograms (CVs)

were obtained at the following scan rates: 5, 10, 20, 50 and 100 mV $s^{-1}$ in still electrolyte to check linearity of the variation of peak current with the square root of voltage scan rate. Reversible systems must show this response. Current-voltage plots were obtained to characterise the system with convection in addition to diffusion. This involved measuring scans at 5 mV $s^{-1}$ with rotation of the electrode at 5, 10, 15 and 20 Hz. The mass transport-limited current must vary linearly with rotation rate and have an intercept at zero. Chronoamperometry was also performed.

These techniques enable the experimental set-up to be checked. This will be described fully in the results section. The diffusion coefficient was calculated from the chronoamperometry results.

### 3.3.3 Hexacyanoferrate-potassium chloride system at graphitic electrodes

Having characterised the standard hexacyanoferrate its electrochemistry was studied at a variety of graphitic materials and compared to its behaviour at glassy carbon.

Cyclic voltammetry was performed using a variety of carbon electrodes: unactivated coconut shell (UCN), reticulated vitreous carbon (RVC), a PVDF/graphite composite material and activated carbon composites. A silver/silver bromide reference electrode was used. Rotation of the electrode was employed with a range of frequencies, i.e., 1, 1.5, 2, 2.5, 5, 10, 15 and 20 Hz

### 3.3.4 Electrochemical behaviour of glassy carbon in 5 M NaBr and NaCl

The cyclic voltammetric behaviour of glassy carbon, under basic conditions, in 5 M NaBr, 5 M NaCl and with Sodium hydroxide (2 M) was studied. Bromine generation was avoided by working in a potential window of 0.2 to -0.2 V. To overcome the low current in this potential window the potential range was extended anodically and held for several seconds to generate oxygen at the electrode. The two-step reduction of oxygen to the hydroxide was observed.

### 3.3.5 Electrochemistry of the activated carbon materials in sodium bromide electrolyte

Having characterised oxygen reduction at the glassy carbon electrode, where electrochemistry is relatively uncomplicated, the behaviour of the porous activated carbon materials was investigated and compared to unactivated materials. The aim of this work was

to investigate the behaviour of these materials in the sodium bromide (5 M) electrolyte and identify the most suitable carbon for the cathode.
The materials that performed well in the hexacyanoferrate work were selected for further investigation were the activated carbons; air treated and coconut shell carbons. In addition, numerous activated and unactivated carbon materials were screened.

The potential was scanned from +0.2 to -0.2 V vs. Ag/AgBr, until reproducible CVs were obtained. Reproducible results were obtained after around 20 runs, comprising 40 scans for the system to stabilise. Polarisation characteristics changed on each scan due to distributed IR drop within the pores, ingress of electrolyte solution and the build-up of peroxide. Eventually, reproducible data were obtained indicated by the superimposition of the plots. RDE experiments were also performed at 16.67 Hz (1000rpm).

Physical characterisation of the unactivated coconut shell, activated coconut shell and the chemically surface treated materials was carried out by SEM and nitrogen porosimetry.

SEM work was conducted by Mr. John Bates in IPTME, Loughborough University and the nitrogen porosimetry measurements (Prof. Walsh and Dr.Gavin Read) Portsmouth University.

Carbons supplied by Sutcliffe carbons.

# Chapter 4 Evaluation of novel electrochemical electrolyte management strategies

It was stated in the introduction how Regenesys® relies on process control to ensure operation is optimal. Process control is essential for efficient management of the supply chain between producer and consumer. An important aspect of process control is electrolyte pH management. The bromide electrolyte pH can drop to around pH 1 or less. This is symptomatic of the chemical imbalance within the system. It has been shown that $HS^-$ is transported across the membrane where it is oxidised by the bromine to ultimately yield sulphuric acid. If low pH is maintained back diffusion of protons will occur. The polysulphide electrolyte is neutralised ($HS^-$ and $OH^-$) and consequently the hydroxyl dependent discharge process is inhibited and decreases the discharge capacity of the system (equation 4.1)

$$HS^- + OH^- \Rightarrow S + H_2O + 2e^- \qquad (4.1)$$

Sodium hydroxide can be delivered into the polysulphide electrolyte to recover some of this lost capacity and directly into the bromide electrolyte to neutralise the protons at source.

The aim of this present work was to evaluate an electrochemical electrolyte management strategy with a variable configuration which can restore the pH. This chapter describes the work on the porous cylinder carbon cathode and the flow cell electrolyser to improve the efficiency of the redox power cell by rebalancing the chemical composition of the electrolyte.

## 4.1 Porous carbon cathode

It has been stated that the decrease in efficiency of the cell during normal operation is due to sulphur and bromine loss. To prevent loss of redox species, pH changes in either or both sides of the cell were compensated for by the electrogeneration of hydroxyl ions and bromine, to offset bromine losses directly. The porous carbon cathode achieved this by direct delivery of hydroxide into the bromide electrolyte stream along with the bromine generating electrode in a flow by configuration. The cathode must be coated in ion exchange resin or membrane for proton transport and as a barrier for neutral species such as bromine and hydrogen when integrated in the Regenesys® system. The aim of this work was to electrolyse

a sulphuric acid solution to generate hydrogen and to see if the hydrogen was retained in the porous structure.

## 4.2 Results and discussion

A preliminary investigation into a porous carbon open cathode was carried out. Hydrogen generation at the cathode was signalled by the onset of oxygen evolution at the counter electrode and soon after hydrogen bubbles were observed, initially on the bottom edge of the cylindrical carbon electrode, the site of greatest current density, and then the side surface.

Characterisation of the uncoated electrode proved to be impossible due to the constant change and uncertainty of active electrode area. Build-up of hydrogen in the carbon matrix continually blinds off electrode area. Therefore working current densities were very uncertain. Electrical resistance was also a problem due to the thickness of electrode material enhancing resistivity[40]. This is especially important with the hydrogen evolution reaction because the current is carried through the thickness of the electrode to the surface where proton discharge occurs. In addition, pore resistance will cause preferential proton discharge on electrode surface, rather than internally. Surface bubble formation was probably increased by the hydrodynamic resistance of the electrolyte. Electrolyte flooding of the body of the electrode impedes hydrogen transport from the reactive sites on the surface to the internal structure prior to venting. This is probably more pronounced at the bottom of the electrode due to the volume of electrolyte and hence the hydrostatic pressure to overcome. Bubble formation remained a problem even when the electrode was coated in Nafion® ionomer resin. The macroscopic roughness of the surface and porosity prevented the ion exchange material coating the electrode evenly. Penetration of the film, known as holidays, will provide areas of low electrical resistance and high current density which will favour reduction and thus bubble formation.

## 4.3 Conclusions

The porous carbon cathode will be a viable method for rebalancing when The following modifications to the porous carbon cathode are required to ensure a viable method for electrolyte rebalancing.

- The cathode needs to be enveloped in an ion exchange membrane to prevent hydrogen permeation into the electrolyte

- The electrode needs to be hollowed to facilitate hydrogen removal or oxygen feed

- Dual porosity to prevent flooding and aid gas venting or supply

## 4.4 A novel solid polymer electrolyte - aqueous electrolyte hybrid cell

The alternative approach to electrolyte rebalancing used solid polymer electrolyte (SPE) fuel cell technology applied in a novel way. The gas diffusion electrode functioned as either a gas generating (hydrogen evolution) or gas consuming (oxygen reduction) electrode. The Nafion® membrane acted as an electrolyte in addition to excluding the aqueous sodium bromide electrolyte, thus giving a cell with an innovative double phase (solid-liquid) electrolyte.

## 4.5 Results and discussion

Potential - current density data was obtained up to 70 mA $cm^{-2}$. The operating cell potential and pH measurements of the electrolyte were taken when the potential was stable, usually within minutes. Potential and pH data were acquired over a period of up to 5 hours to test the performance when bromine concentrations approach levels encountered during normal operation of the main cell. Potential and pH measurements were also obtained when the electrolyte was adjusted to pH 1 and 4 to simulate the electrolyte imbalance of the main cell.

## 4.6 Variation of potential with current density

Preliminary studies showed the system performed well. Potential - current density plots were linear and reproducible (figure 4.1). Current densities were generally stable, which indicated efficient hydrogen removal from active area of the cathode. Bromine generation was visible within a few seconds of electrolysis at all current densities. Delamination of the MEA occurred during electrolysis. This probably occurred when the rate of sodium hydroxide generation exceeded the hydroxyl back diffusion and the opposing water flux which remove sodium hydroxide from the site of generation. Osmotic pressure increases with the rising local concentration. Water is forced through the membrane to dilute the solution. Where the adherence of the MEA is weak the increase in water pressure blisters the membrane while spreading the area of delamination between the layers. These effects may be avoided by using hydroxyl repelling membranes and/or periodically flushing the cathodic gas chamber

prior to hydroxide delivery to the bromide or polysulphide side. Alternatively, the rate of hydroxyl generation can be decreased to match the rate of the incoming proton flux, thus avoiding sodium hydroxide build-up and delamination. This provides a novel way of delivering hydroxide directly into the bromine process stream, neutralising the excess acid by titration. This will be advantageous to Regenesys® as the bromine side is the site of acidification.

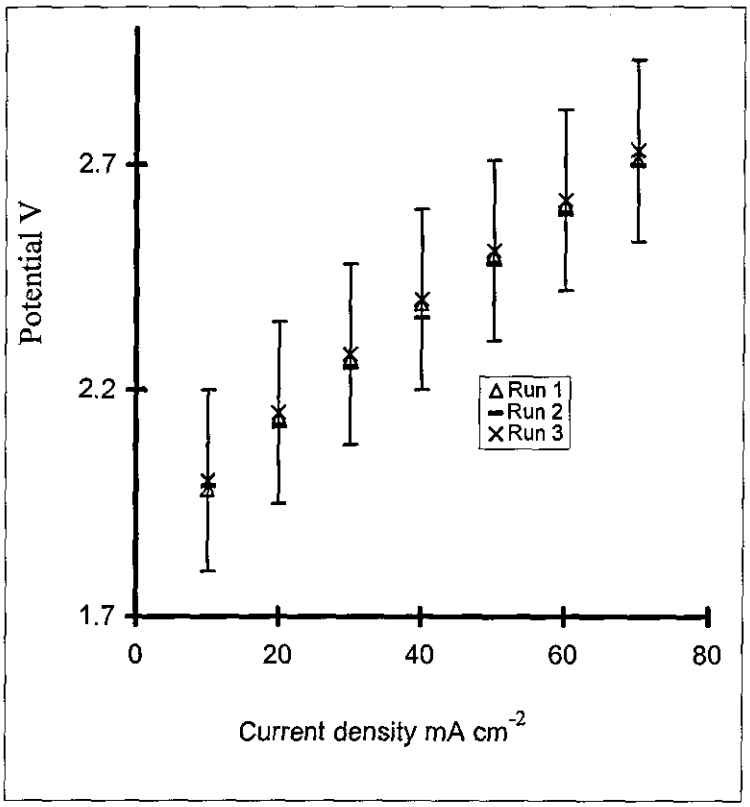


Figure 4.1 Operating cell potential ( no reference electrode) as a function of current density for the rebalancing cell without pH modification of electrolyte.

## 4.7 Potential and pH variation with time

In neutral and basic media the main HER cathodic reactions of the rebalancing cell are:

$$2H_2O + 2e^- \Rightarrow H_2 + 2OH^- \qquad (1.6)$$

$$E^\theta = -0.83\ V$$

and under acid conditions,

$$2H^+ + 2e^- \Rightarrow H_2 \qquad (1.7)$$

$$E^\theta = 0.00\ V$$

It was stated in the introduction that the Nafion® membrane is not an ideal Donnan system, i.e., the conductive ionic clusters are randomly distributed and connected by narrow channels in an insulating fluorocarbon matrix. Therefore hydroxyl back diffusion is expected due to a local high concentration of sodium hydroxide and the high water content of the membrane. Furthermore, the concentration of fixed ions in the membrane does not exceed the hydroxyl ion concentration. Free electrolyte in the ionic clusters shield the hydroxide from the sulphonic acid groups but the hydroxyl ion is expected to be electrostatically prevented from entering the channels which connect adjacent clusters. The width of these channels is that of approximately a two double layer thickness and therefore the hydroxyl species will feel a fairly high electrostatic potential barrier induced by the close proximity of the sulphonic acid groups. The hydroxyl ion as it traverses the membrane will see a potential consisting of two parts, an oscillating potential superimposed on the constant sloping portion originating from the voltage drop across the membrane. The peak and troughs of the oscillating component correspond physically to the channel and cluster regions respectively.

It is thought that the hydroxyl ions appear to 'hop' through the channels by a mechanism analogous to the Grothuss transport for protons.[20]

$$OH^- + H\text{-}OH + (H_2O)n + H_2O \Rightarrow H_2O + H_2O + (H_2O)n + OH^- \qquad (1.11)$$

This tunnelling mechanism provides a path of lower energy that minimises repulsion by charge delocalisation. It may be recalled from the introduction that Mauritz and co-worker proposed that a tunnelling process involving the polarisation of the O-H bond in water molecules by the $Na^+$ ion would enhance hydroxide ion transport in environments of decreasing water content. This was due to the increasing population of $Na^+$- $OH^-$ ion pairs and the decreasing population of the $H_3O_2^-$ moiety. Polarisation induces an antisymmetrisation of the double energy well corresponding to the proton in the water experiencing a repulsion away from the $Na^+$ ion and an attraction to the $OH^-$ ion. This process would be enhanced by the electric field during electrolysis. Thus giving the efficient movement of hydroxide in the anodic direction to the bulk electrolyte. Eventually the increasing antisymmetrisation will inhibit the tunnelling process, that is the energy gap will be to great, and hydroxide transport across the membrane will be disfavoured.

During normal operating conditions the rebalancing cell will only operate at low pH to neutralise the incoming proton flux. If the cell continues to run sufficiently above pH 7 the

basic conditions that may favour bromate electrosynthesis will occur. The following chemical and electrode reactions[41] may occur in the anolyte at high pH

$$2OH^- + 2Br_2 \Rightarrow 2HBrO + 2Br^- \qquad (4.2)$$

$$2HBrO + BrO^- \Rightarrow BrO_3^- + 2H^+ + Br^- \qquad (4.3)$$

$$4OH^- \Rightarrow 2H_2O + O_2 + 4e^- \qquad (4.4)$$

$$3Br_2 + 3H_2O \Rightarrow BrO^-_3 + 6H^+ + 5Br^- \qquad (4.5)$$

These equations contain hydroxyl and hydrogen ions and therefore the corresponding reactions are sensitive to pH changes in the electrolyte and may affect cell performance. For example the disproportionation of bromine (equation 4.5) only becomes thermodynamically possible at pH 9. Therefore it is important to monitor pH and potential over a sufficient period of time to allow hydroxide concentrations to build-up in the bulk electrolyte (fig 4.2).

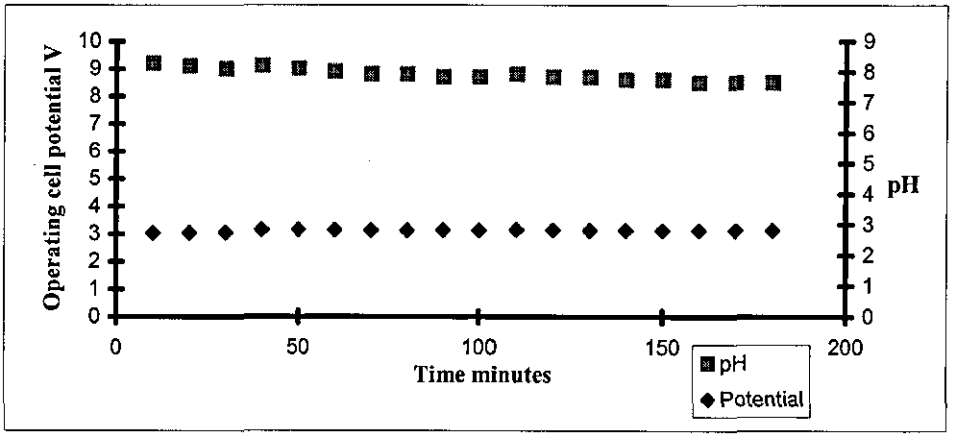


Figure 4.2 Operating cell potential ( no reference electrode ) and pH as a function of time for the rebalancing cell operating at 20 mA $cm^{-2}$ without initial pH modification of electrolyte

The potential remains very stable over the run time (180 minutes). In contrast, pH peaks at 9.2 at 10 minutes into the run and steadily decreases to pH 8.5. The drop in pH can be accounted for by the increase in water flux from anolyte to catholyte opposing back diffusion of sodium hydroxide. This is probably due to osmotic effects caused by the high concentration of sodium hydroxide at the interface and in the membrane. This view is supported by the apparent increase in volume of strongly alkaline fluid in the cathodic outlet

during the run. These observations are also consistent with the inhibition of tunnelling by the increased antisymmetrising Coulombic field effect of the cations and the anode. In addition, reactions (4.2) to (4.5) will also lower pH and will become more important with time as bromine concentrations rise.

## 4.8 Potential and pH variation with time of pH adjusted electrolytes

The bromide electrolyte of Regenesys can drop to around pH 1 or less. Therefore it is important to investigate the electrochemistry of the rebalancing cell at low pH values Adjustments of the electrolyte to pH 4 and 1 were made and the performance of the rebalancing cell was monitored. Operation of the electrolyser in this pH region is fortuitous because lower potential and power are required to effect hydrogen evolution to neutralise the acid electrolyte and to generate bromine.

## 4.9 Electrolyte adjusted to pH 1

The first run showed a rapid increase in potential within a minute of closing the circuit with pH remaining low for 2 minutes (figure 4.3). The potential was fast approaching 2 V within the first minute; indicating that basic conditions are established very quickly. In fact it was difficult to record the data. There was some oscillation around 2 V but stabilisation occurred after approximately 10 minutes.

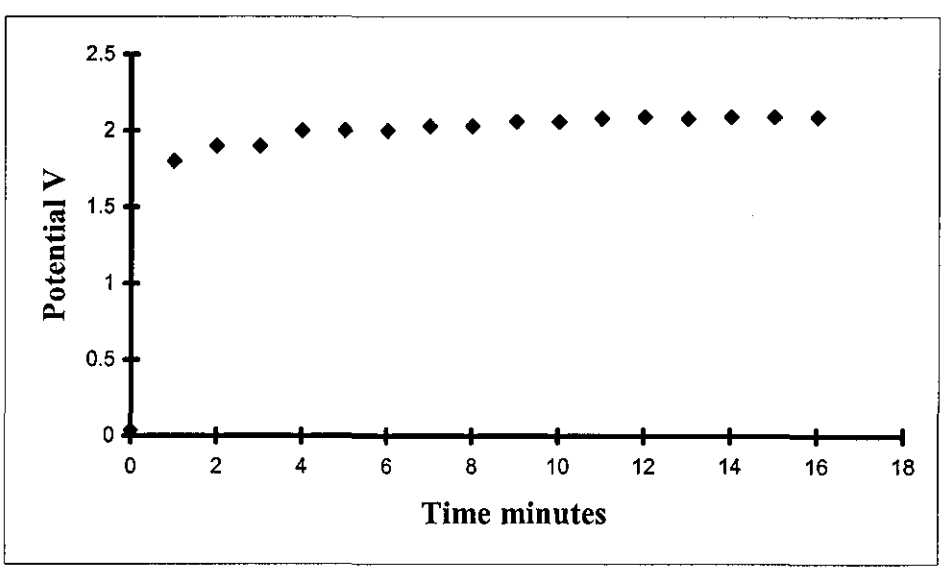


Figure 4.3 Operating cell potential (no reference electrode) as a function of time (first run) for the rebalancing cell operating at 20 mA $cm^{-2}$ with initial electrolyte pH 1

In contrast the second run with pH 1 gave a steady increase in potential which was recordable. This is probably due to the membrane being fully in the protonated form. An inflection was observed possibly reflecting the change in mechanism as protons are depleted. The resultant increased conductivity of the membrane being fully in the protonated form allows the acidic HER and membrane proton titration to be observed (figure 4.4) for the first 3 minutes of electrolysis. Following the plateau region (~1.3 V) a steady increase in potential was observed. The start of this incline corresponds to approximately pH 7 in the bulk electrolyte and change in mechanism. The potential finally levels out to a value corresponding to HER under basic conditions (2.2 V). This view is supported if the operating potentials are compared to the theoretical standard values for the cell reaction, i.e. pH < 7: 1.09 V and pH > 7: 1.92 V.

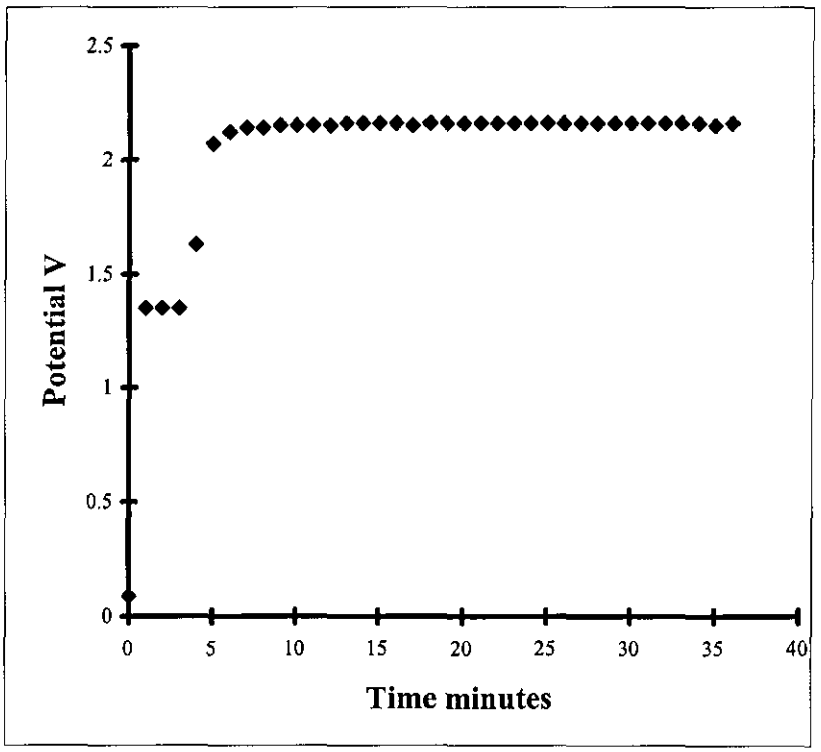


Figure 4.4 Operating cell potential (no reference electrode) as a function of time (second run) for the rebalancing cell operating at 20 mA $cm^{-2}$ with initial electrolyte pH 1

## 4.10 Electrolyte adjusted to pH 4

Runs with the electrolyte adjusted to pH 4 gave similar potential-time plots to the pH 1 electrolytes (figure 4.5). The membrane was sufficiently equilibrated with the electrolyte to correlate its behaviour directly to membrane proton concentration. The resultant conductivity

allows the transition in reduction mechanism to be seen; as was the case with the second run pH 1 experiment.

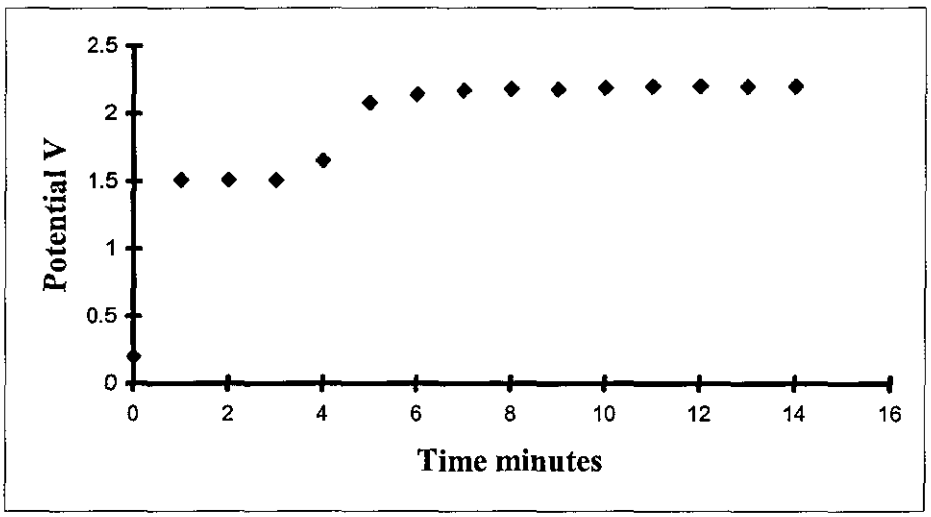


Figure 4.5 Operating cell potential (no reference electrode) as a function of time for the rebalancing cell operating at 20 mA $cm^{-2}$ with initial electrolyte pH 4

Extended runs of the pH 1 and pH 4 electrolyte systems tended to similar behaviour (figures 4.6 and 4.7).

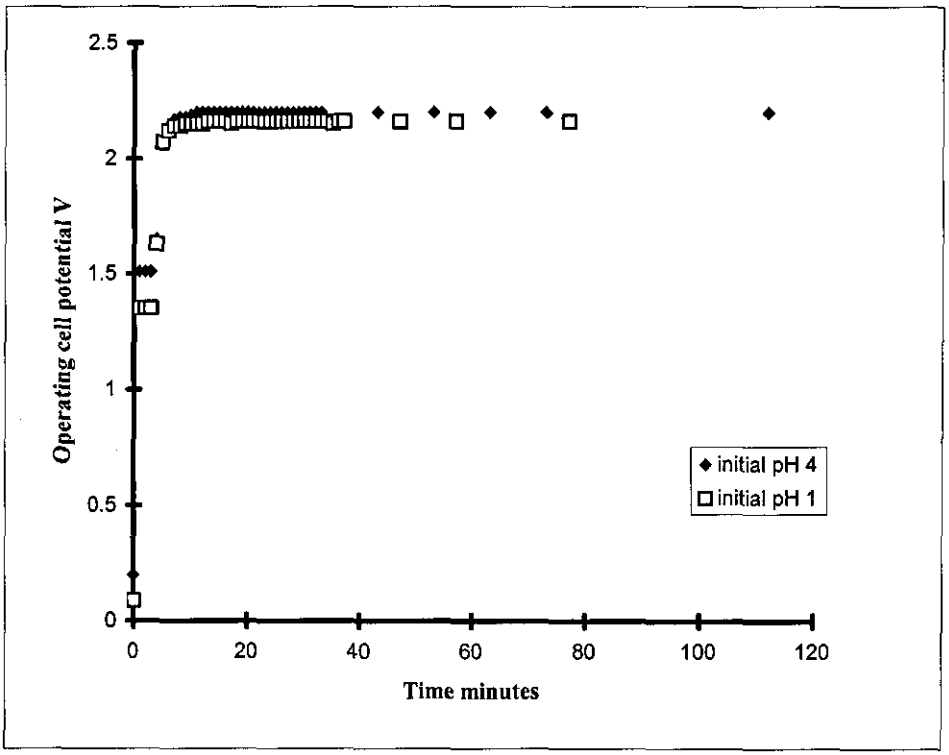


Figure 4.6 Operating cell potential (no reference electrode) as a function of time for the rebalancing cell operating at 20 mA $cm^{-2}$ with initial electrolyte pH 1 and 4

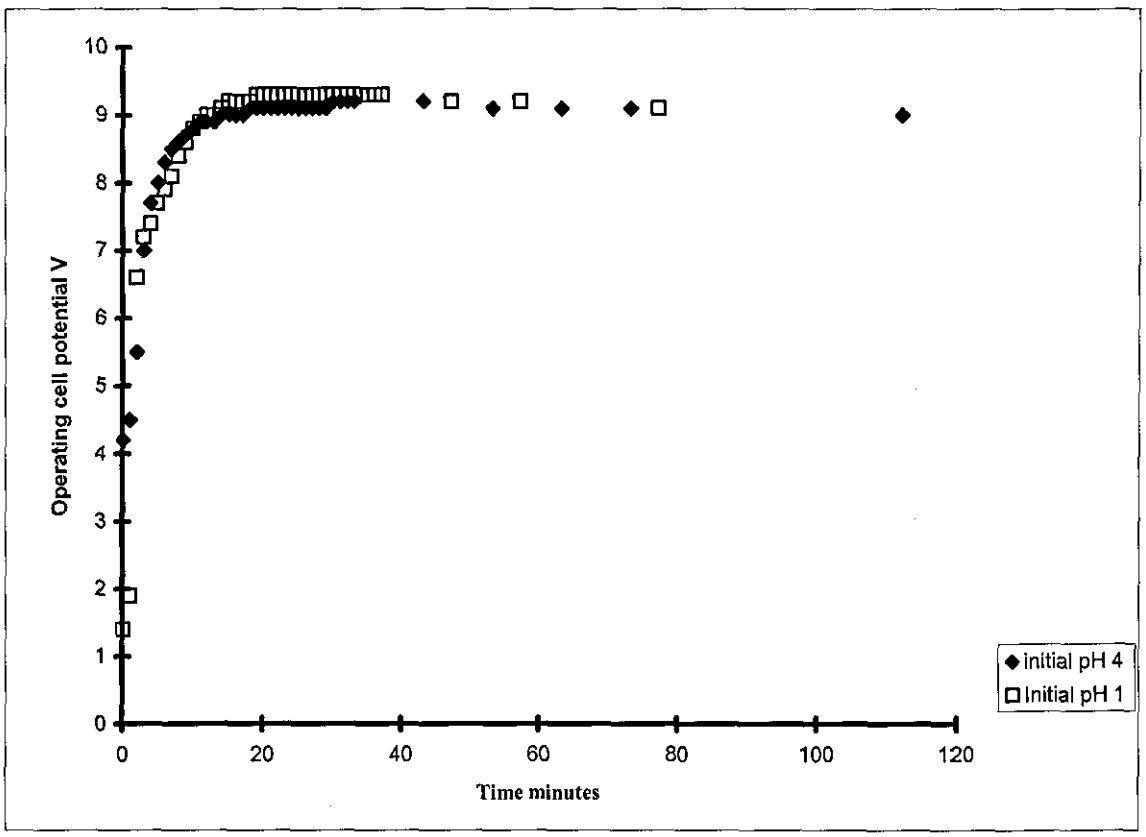


Figure 4.7 pH as a function of time for the rebalancing cell operating at 20 mA $cm^{-2}$ with initial electrolyte pH 1 and 4

The increase in potential for the two electrolytes ( pH 1 and 4) lasts for approximately 1 minute and reaches a plateaux region, lasting for two minutes, followed by a further increase in potential (figures 4.8 and 4.9). The bulk pH reflects this change. As the incoming flux of protons is neutralised proton concentration in the bulk electrolyte falls and pH rises. Proton discharge, being thermodynamically more favourable than the reduction of water and showing a high exchange current at this electrode, is the preferred cathodic reaction as long as protons are supplied to the cathode. Ultimately the proton flux is not sufficient to sustain the acid mechanism. The alkaline mechanism becomes more important and the potential starts to rise after 3 minutes corresponding to a bulk electrolyte pH of 7.

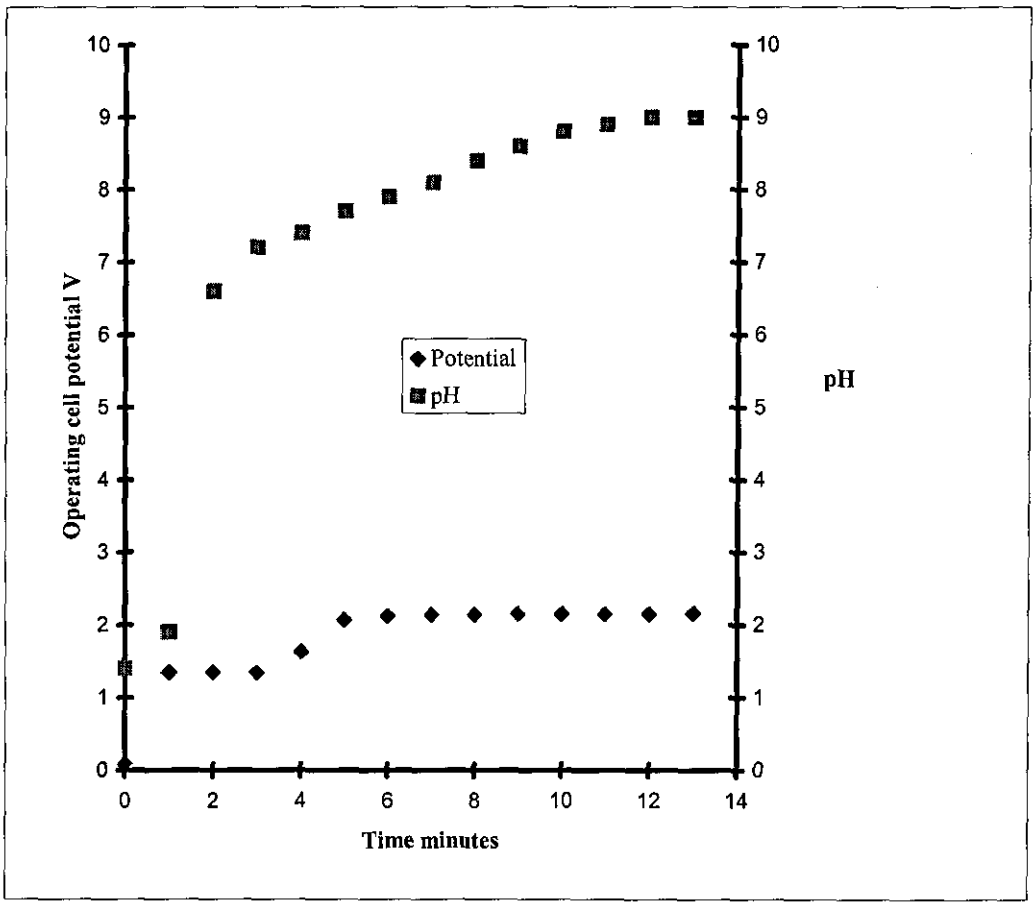


Figure 4.8 Operating cell potential (no reference electrode) and pH as a function of time for the rebalancing cell operating at 20 mA $cm^{-2}$ with initial electrolyte pH 1

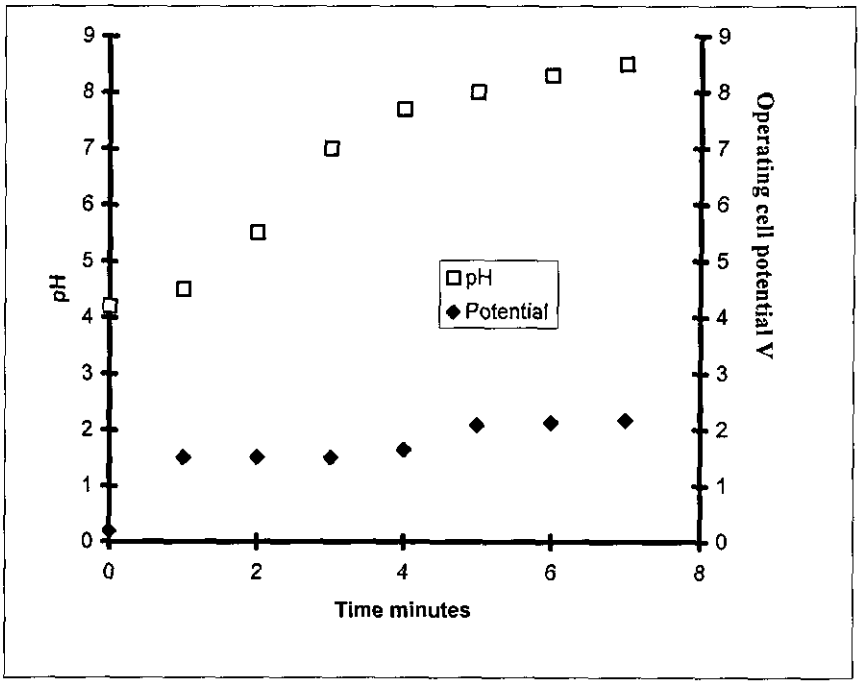


Figure 4.9 Operating cell potential (no reference electrode) and pH as a function of time for the rebalancing cell operating at 20 mA $cm^{-2}$ with initial electrolyte pH 4

## 4.11 Oxygen reduction as the cathode reaction

If air is fed to the cathode the cell potential drops from 2.2 V to 1.32 V with the cell running at 20 mA $cm^{-2}$. When oxygen is used a cell potential of 1.26V is observed, giving a saving of 900 mV. The cathode is now reducing oxygen. When the initial pH is depressed (pH 1 and 2) a further drop in operating potential is obtained. The operating potentials obtained, around 400 to 700 mV, clearly indicate that oxygen is being reduced under alkaline conditions close to the equilibrium value, i.e., at low overpotential where current is proportional to overpotential as described by the linear approximation of the Butler-Volmer equation (equation 4.6).

$$j = j_0 \frac{nF}{RT}\eta \quad (4.6)$$

The basic conditions are rapidly established even when the pH is initially set to one with the bulk electrolyte pH only remaining low during the early stages of operation. The highly reducing potential of the oxygen cathode consumes protons at a faster rate than can be supplied to the electrode and basic conditions are rapidly established. At an initial pH of 1 the electrolyte is neutralised at around 6 minutes (figure 4.10) while if the electrolyte is initially set to pH 2 neutralisation of the electrolyte is after 2 minutes. The incoming flux neutralises the hydroxyl ions preventing sodium hydroxide build-up and subsequent precipitation with voltage gain. Thus the cell operates at near theoretical value (figure 4.11). Furthermore, the intermediate peroxide undergoes reduction and catalytic decomposition to oxygen which will contribute to proton consumption. This contrasts with the HER experiments in which acid conditions remain established for part of the operation; reflecting the reducing power and stoichiometry of the oxygen reduction half cell reaction.

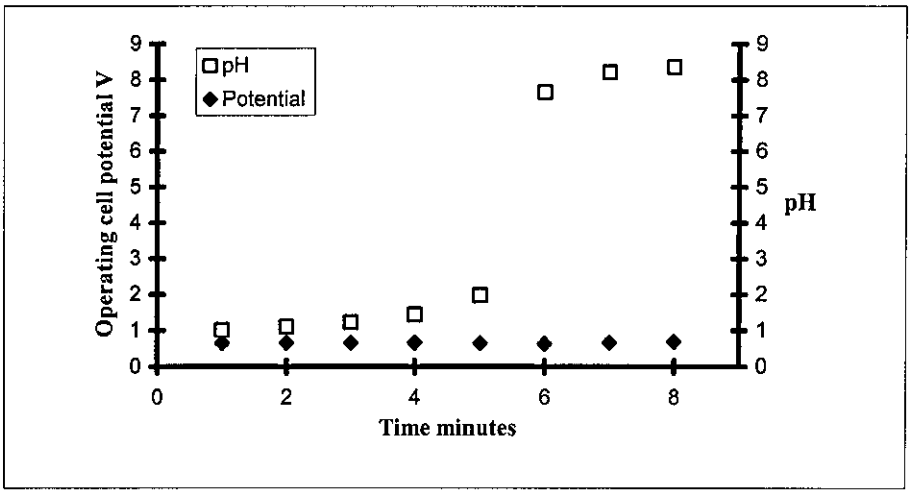


Figure 4.10 Operating cell potential (no reference electrode) and pH as a function of time for the rebalancing cell with the cathode reducing oxygen and operating at 20 mA $cm^{-2}$ with initial electrolyte pH 1

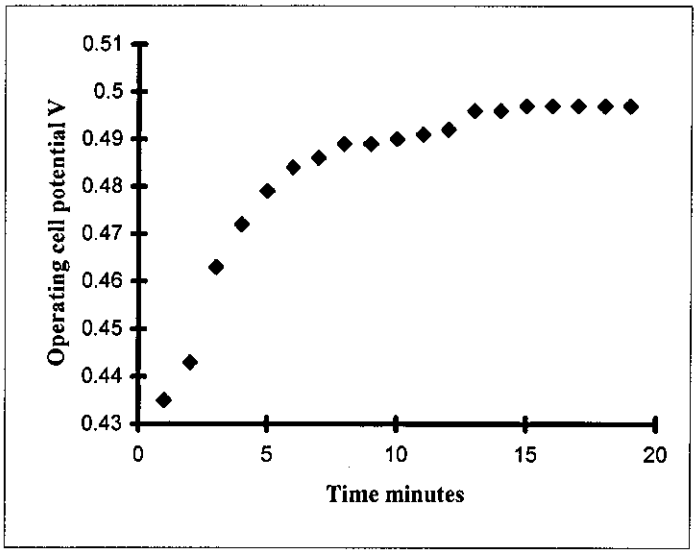


Figure 4.11 Operating cell potential (no reference electrode) as a function of time for the rebalancing cell with the cathode reducing oxygen and operating at 20 mA $cm^{-2}$ with initial electrolyte pH 2

When the electrolyte was depressed to pH 0 the near theoretical operating potentials were not repeated (figure 4.12). Operating potentials around 1.3 V were obtained immediately when electrolysis was initiated and the bulk pH remained low for a large part of the run; indicating poor mass transport. This result was attributed to delamination of the MEA. caused by the bonding limit of MEA and local dehydration and precipitation of solute.

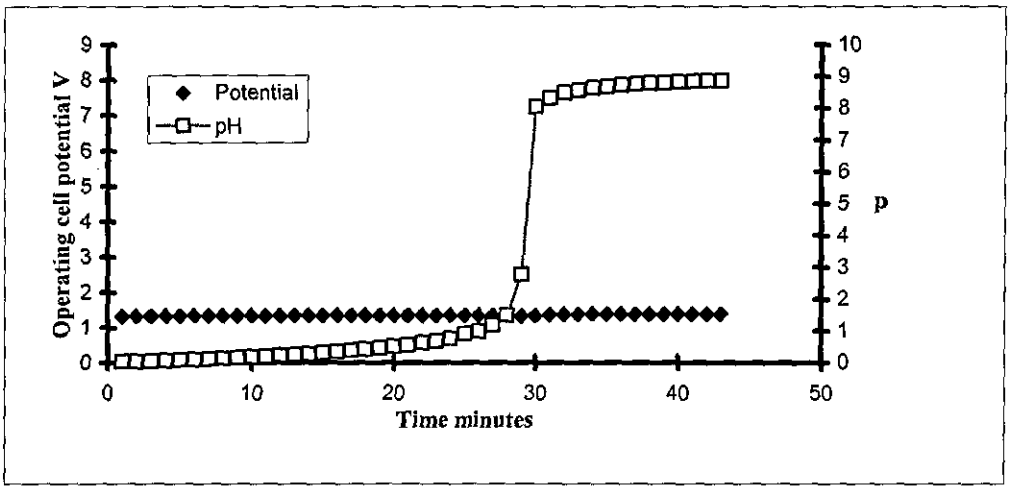


Figure 4.12 Operating cell potential (no reference electrode) and pH as a function of time for the rebalancing cell with the cathode reducing oxygen and operating at 20 mA $cm^{-2}$ with initial electrolyte pH 0

## 4.12 Conclusions

Hydroxide was easily generated and quickly neutralised acidic bulk sodium bromide electrolyte. Basic conditions were rapidly established at the cathode with HER and oxygen reduction at depressed pH. Alkaline conditions at the electrode were established much quicker with oxygen reduction as the cathodic reaction which reflected the reducing power and large exchange current density of this half cell reaction. The mechanism of neutralisation of the bulk electrolyte was by the influx of protons. This view was supported by the maintenance of the potential corresponding to proton reduction during the steady rise in bulk pH for the hydrogen evolution cathode reaction. The rate of proton influx is greater than or equal to the electrode reaction rate and local acid conditions are maintained. This condition is met until pH 7 of the bulk electrolyte was reached and the potential increases. In contrast with oxygen reduction as the cathode reaction the proton flux was unable to match the rate of the electrode reaction and alkaline conditions were established immediately. The rate of oxygen reduction may be enhanced initially by the coupling of the electrode reaction with that of the $Br_2$ / $Br^-$ system. To obtain the greatest efficiency the potentials of each redox system should be as close as possible. Under acid conditions the reversible potential of oxygen is 1.23 V whilst that of the $Br_2$ / $Br^-$ system is 1.09 V. The proton flux appears to match the generation of hydroxyl ions as a low potential was maintained, i.e., local pH is neutral. Excessively high cell voltage is associated with sodium hydroxide precipitation but a reasonably low potential was maintained even when the bulk pH became basic. This can be rationalised by the increased water content at the electrode generated initially by the oxygen

reduction under acid conditions. The increased water content would be expected to drain sodium hydroxide ion away from the electrode-nafion interface and indeed a strongly alkaline clear liquid , as indicated by a Litmus test, was observed to drain from the cathodic outlet. This process would be encouraged by the movement of air through the cathodic chamber. This view was supported by the decreased rate of acid neutralisation in the bulk electrolyte compared to that for the hydrogen evolution cathodic reaction. In addition increased water content of the membrane will increase its capacity for the hydroxyl species and will act as a 'hydroxide reservoir'. Conversely decreased water content will increase hydroxide transport by the mechanism of tunneling due to the increased degree of polarisation of the O-H bond in water and eventual inhibition as proposed by Mauritz and co-worker[18].

Summary of conclusions:

- Bromine and hydroxide can be generated easily, quickly and in sufficient quantity to meet electrolyte management demands
- Facile bulk electrolyte neutralisation by influx of protons aided by the coulombic field
- Facile hydroxide back diffusion
- Sodium hydroxide can be delivered to either or both electrolyte circuits
- Operate rebalancing cell when pH is low during charge cycle of main cell; hydrogen evolution at a lower potential
- Oxygen reduction as the cathodic reaction lowers cell potential by 900 mV when operating at 20mA.cm$^{-2}$ under normal conditions
- Depression of pH effects near theoretical cell potential for oxygen reduction under basic conditions

# Chapter 5 Carbon materials for the cathode

Due to the success of the electrolyser it was decided to look at alternative cathode materials which could be used in the gas diffusion electrode. This entailed looking at a variety of carbon materials. Materials were selected which were likely to pass large currents. To pass large currents these candidate cathode materials need a high surface or active electrode area and have hydrodynamic properties which enhance mass transfer and thereby decrease the diffusion layer. The large overpotential to oxygen reduction of carbon will be compensated for by the addition of a catalyst and or increasing the surface area of the cathode before operation in the rebalancing cell. Increased surface area greatly improves mass transfer of oxygen to the reaction site, the efficiency of sodium hydroxide drainage and hydrogen venting. This was achieved by using activated carbon to increase the microscopic surface area. The macroscopic surface area of the electrode can be increased by using a packed bed flow-through configuration in the operational rebalancing cell but this complicates the operation by the need to monitor and control process fluids. To effectively assess the suitability of the materials the well-characterised hexacyanoferrate (II) and hexacyanoferrate (III) redox couple was selected to characterise the electrode. Thus avoiding the problems of mass transfer associated with a gaseous electroactive species.

This chapter will discuss the electrochemical behaviour of the well-characterised hexacyanoferrate KCl system at the 'as received' carbon materials using cyclic voltammetry and rotating disc electrode voltammetry. The voltammetric areas will be compared as this corresponds to the active electrode area. To ensure the experimental set-up behaves well the glassy carbon electrode was investigated first. This also provided a reference point for comparison to the various carbon materials. The electrochemical behaviour of carbon materials in the sodium bromide (5 M) electrolyte solution will also be discussed.

## 5.1 Hexacyanoferrate-potassium chloride system at the glassy carbon electrode using the three voltammetric techniques

The range of voltammetric techniques available can be placed into three general groups: sweep, hydrodynamic and pulse techniques. A technique from each of these groups was selected to confirm good experimental set up. The techniques selected were cyclic voltammetry, rotated disc voltammetry and chronoamperometry using the well characterised reversible hexacyanoferrate system. For the trinity of voltammetric techniques, the method of

transport to the electrode is always diffusion, that is, Fickian behaviour. The only difference is the manner the diffusion is initiated and maintained in a predictable way. The distance the analyte diffuses in a unit time is invariably related to $t^{-1/2}$. The $t^{-1/2}$ time dependence in chronoamperometry is obvious from the Cottrell equation. In cyclic voltammetry the $t^{-1/2}$ time dependence is reflected in the square root of the sweep rate in the Randles-Sevcik equation and for rotated disc voltammetry the Levich equation includes the square root of the rotation rate. All three techniques were used to determine that the experimental system behaved as predicted by the relative equations of the different techniques. This was achieved by plotting the relevent parameters and checking the linearity of the plot.

## 5.2 Results and discussion

### 5.2.1 Cyclic Voltammetry

Reproducible signature cyclic voltammetric behaviour was observed in the potential window 1 to 0 V vs. a silver/silver chloride reference electrode and a glassy carbon working electrode. The scan was initiated in the cathodic direction. Cyclic voltammograms (CVs) were obtained at the following scan rates: 5, 10, 20, 50 and 100 mV/s (figure 5.1).

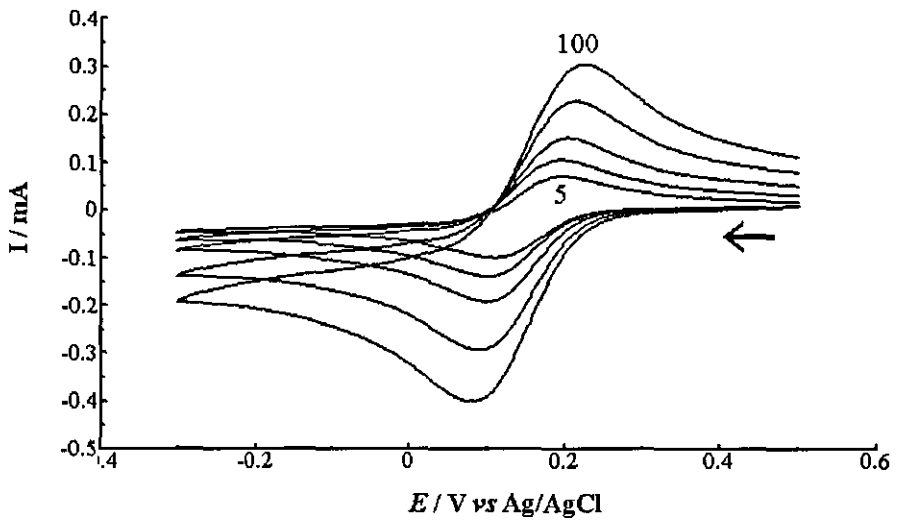


Figure 5.1 Peak current versus potential for 5, 10, 20, 50 and 100 mV $s^{-1}$ scan rates for hexacyanoferrate system at glassy carbon

The electrolyte is still, i.e., under simple diffusion, to check linearity of the variation of peak current with the square root of voltage scan rate as predicted by the Randles-Sevcik equation. A system under diffusion control must show this response. Figure 5.1 shows the current response to the working electrode potential being swept back and forth across the formal potential of the analyte. Repeated reduction and oxidation of the analyte gives an alternating

asymmetric cathodic and anodic current response at the electrode. The asymmetry of the current response is due to the depletion of the analyte which gives the characteristic decay in current flow. Experimental results are usually plotted as a current versus potential graph as is shown in figure 5.1.

### 5.2.2 Rotated Disc Voltammetry

Current-voltage plots were obtained to characterise the system with convection in addition to diffusional transport, termed convective-diffusion (figure 5.2). This involved measuring scans at 5 mV/s with rotation of the electrode at 5, 10, 15 and 20 Hz. The mass transport-limited current or Levich current must vary linearly with the square root of rotation rate, as predicted by the Levich equation, to indicate the current is entirely mass transport controlled. This was shown to be the case and the experimental system can be considered well behaved.

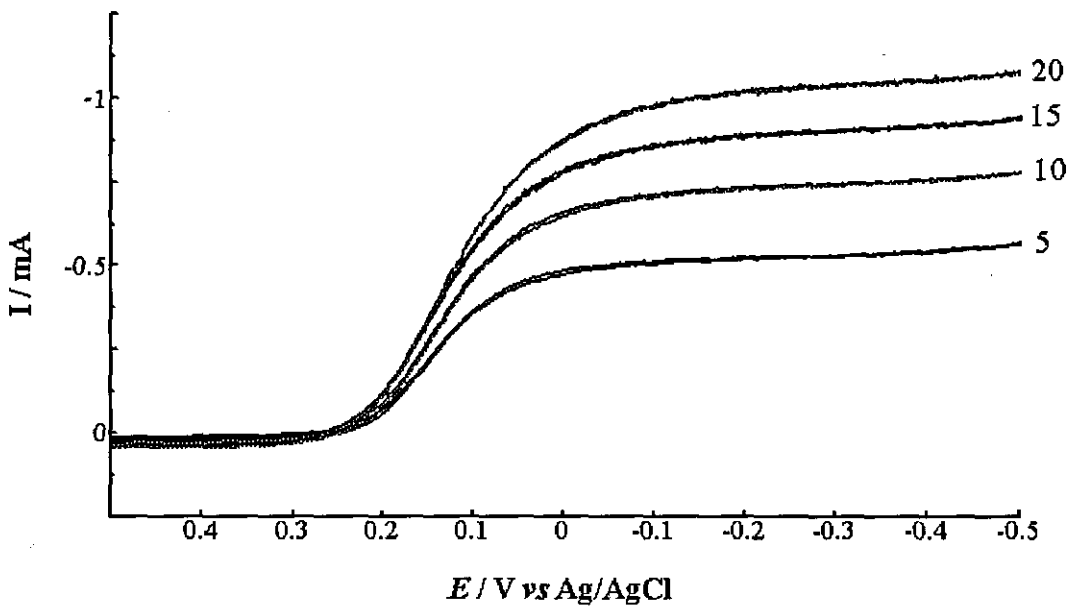


Figure 5.2 Limiting current versus voltage for hexacyanoferrate system at glassy carbon measured at 5, 10, 20, 15 and 20 Hz rotation. Scans measured at 5 mV $s^{-1}$.

### 5.2.3 Chronoamperometry

The plot of the current versus the reciprocal of the square root of time was linear as expected from the Cottrell equation and had a correlation coefficient of 1.000 (figure 5.3).

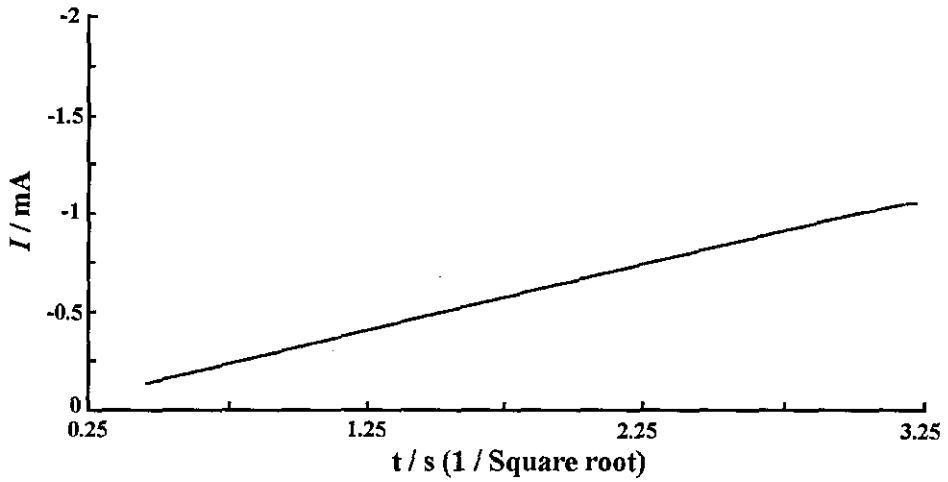


Figure 5.3 Current versus the reciprocal of the square root of time for hexacyanoferrate system at glassy carbon

The plots obtained from the voltammetric techniques can be used to determine the diffusion coefficient of the analyte by measuring the slope of the plot by linear regression, using the relevant equations and taking care with the units involved. It was decided to measure the diffusion coefficient of hexacyanoferrate using chronoamperometry. This technique gives a very direct measure of the diffusion coefficient and the only uncertainties are the electrode area and the concentration of the analyte.

To calculate the diffusion coefficient the Cottrell equation was rearranged to obtain an expression for the slope of the Cottrell plot,

$$I = nFAC(D/\pi)^{1/2} t^{-1/2} \qquad (1.34)$$

where the slope is $I/t^{-1/2}$ and rearrangement gives the following equation:

$$\text{slope} = nFAC(D/\pi)^{1/2} \qquad (5.1)$$

Using this expression, the values of the terms in the equation and unit analysis the diffusion coefficient was found to be $9.12 \times 10^{-6}$ cm$^2$ s$^{-1}$.

A selection of literature values are shown in table 5.1 for comparison.[42]

| Concentration (mM) | Electrolyte medium | $Dx10^{-6}cm^2 s^{-1}$ |
|---|---|---|
| 5 | 0.5 M KCl | 9.12[a] |
| 4 | 0.1 M KCl | 6.50 |
| 4 | 1 M KCl | 7.63 |
| 4 | 1 M KCl | 6.32 |
| 4 | 0.1 M KCl | 7.62 |

Table 5.1 Determined value of diffusion coefficient[a] for hexacyanoferrate in water compared to a selection of literature values

The value from this study is a little high. As stated previously, the only uncertainties are the electrode area and the concentration of the analyte. It is reasonable to assume that the electrode area is probably the source of greatest uncertainty and is consistent with the view that extra electrode surface may be exposed by the ingression of the electrolyte between the electrode and insulating sheath rather than a rough surface microstructure.

## 5.3 Hexacyanoferrate-potassium chloride system at graphitic electrodes

Having characterised the standard hexacyanoferrate system its electrochemistry can be studied at a variety of graphitic materials and compared to its behaviour at glassy carbon. Cyclic voltammetry and rotating disc voltammetry were performed on activated and unactivated carbon materials in an aqueous potassium chloride (0.5 M) supporting electrolyte with a hexacyanoferrate analyte (5 mM). These voltammetric techniques are highly dependant on the surface condition of the electrodes. The surface area of the electrode is directly proportional to the current signal. Unlike glassy carbon, porous carbon materials have a significantly larger real surface area than the geometric or measured surface areas. In addition, the micro-rough surface may have dimensions of a similar order to that of the diffusion layer and will have consequences to the hydrodynamic regime of the electrolyte; either under simple diffusion or convection. The nature of the PVDF-carbon composite electrode material will also have consequences to the mass transfer. This material can be thought of as an array of nano-electrodes in an inert matrix, each with its own diffusion zone.

The differences in electrochemical behaviour between the various materials and glassy carbon can therefore be attributed to their structural differences and chemical treatment histories.

## 5.4 Results and discussion

### 5.4.1 Cyclic Voltammetry

The RVC electrode is of particular interest because it is a high surface area and high void volume analogue of the bulk glassy carbon electrode. Redox peaks were present at all scan rates and an R-S plot showed a high degree of linearity with an intercept close to zero. There was some deviation from linearity at higher scan rates (>20 mV $s^{-1}$) with the current lower than expected. The system is clearly not under diffusion control. Furthermore, as can be seen by the family of plots at the various scan rates, peak separation as increased compared to that of the bulk glassy carbon electrode (figure 5.4). In fact peak separation is considerably greater than 59 mV and the oxidation and reduction peaks are of unequal height. This indicates that the redox system is less reversible at this RVC electrode. A reversible system should show a peak separation of around 60 mV, anodic and cathodic peak currents must be equivalent and the peak potential independent of scan rate. At 100 mV $s^{-1}$ there was some recovery of the positions of the peaks, i.e., an increase in reversibility, but insufficient to match the potentials obtained at the bulk glassy carbon electrode. The increased consumption of the analyte at RVC compared to that at the bulk glassy carbon material was indicated by the measured current of -0.2 mA and -0.1 mA at 5 mV $s^{-1}$ respectively and can be attributed to its high surface area. During the convective-diffusion experiment, with the extra mass transfer by forced convection of the rotating electrode, RVCs unique hydrodynamic properties comes into action. Mass transfer is greatly enhanced, even at relatively low rotation rates the limiting current was not reached within the potential window, i.e., a slight rotation greatly decreases the diffusion layer and as predicted from the equation of Fick's first law the limiting current tends to the maximum value with the decrease in the diffusion layer thickness and hence rotation rate. This manifests its self in the current voltage plots where the current continues to increase, giving rise to the usual exponential current-overpotential relationship (figure 5.5). The current response only approached the Levich or limiting current at a low rotation rate of 1 Hz. At rotation rates of 2.5 Hz the current continues to increase with potential and is not reproducible. This result is consistent with the view that the mass transfer is chaotic at this scan rate.

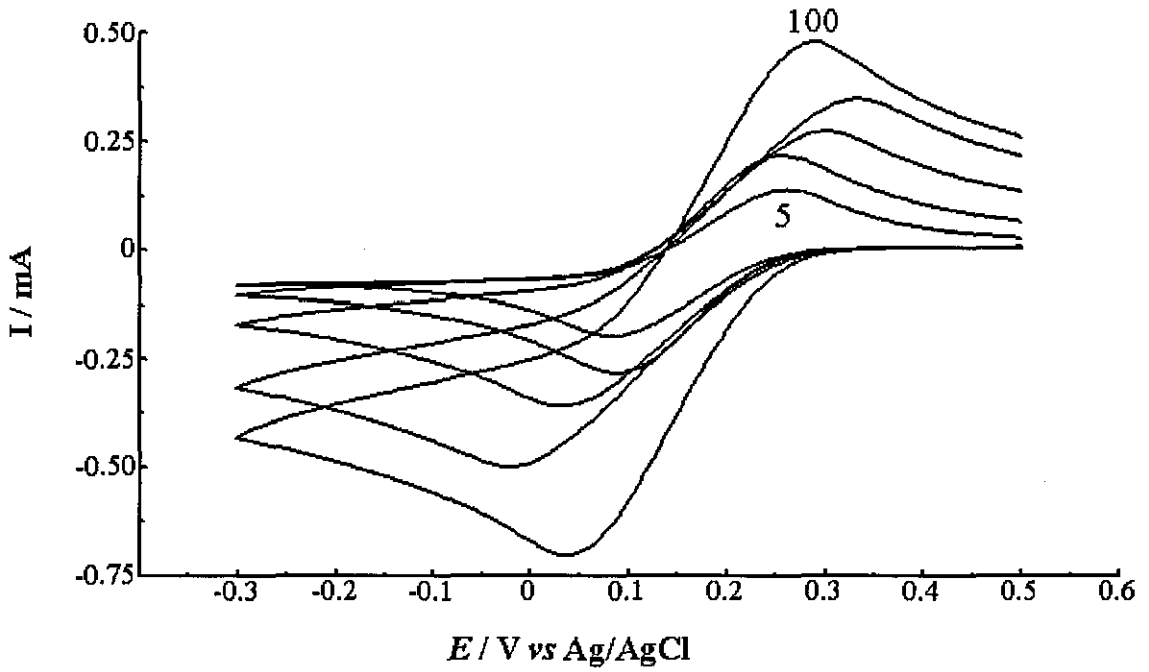


Figure 5.4 Peak current versus potential for 5, 10, 20, 50 and 100 mV $s^{-1}$ scan rate for the hexacyanoferrate system at RVC

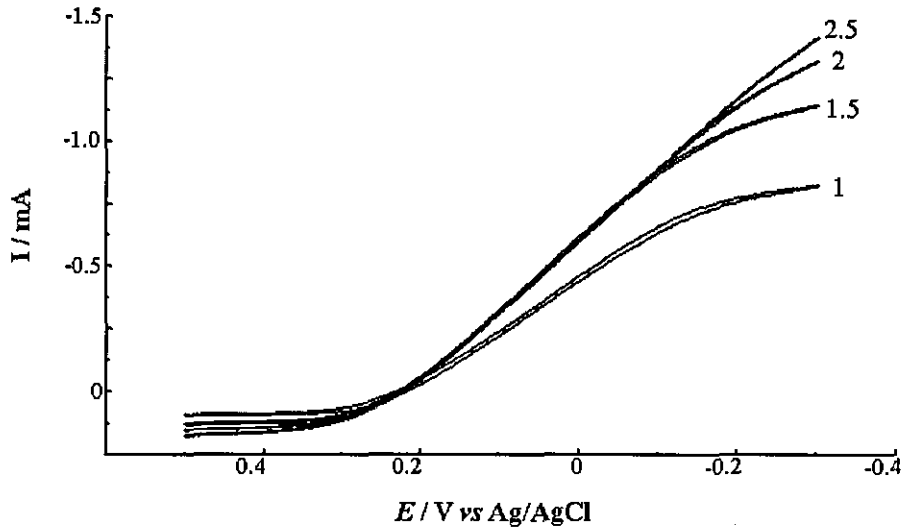


figure 5.5 Limiting current versus potential for hexacyanoferrate system at RVC with 1, 1.5, 2 and 2.5 Hz rotation. Scans measured at 5 mV $s^{-1}$.

### 5.4.2 PVDF:EG10 50:50

The R-S plot was well behaved but a higher Faradaic current for the microscopic area or amount of carbon present was observed, over 60% of the current for the bulk glassy carbon electrode. It was expected that the current would be around 50% of the value for glassy carbon because of the 50% carbon present. The capacitance current of composite materials is inherently low due to the relatively small fraction of the surface which is active electrode. The capacitance current is determined by the area of the active electrode, while the Faradaic current is proportional to the whole electrode area. Clearly some other effect was responsible for this greater than expected observed current. This extra current maybe due to a surface excess of carbon particles giving a higher current than normal. This excess current is more significant if the non-Faradaic or background current of glassy carbon is taken into account, giving a composite electrode current representing around 80% of the glassy carbon electrode faradaic current. It is unlikely this 30% extra current is due solely to carbon distribution. In fact, it is more probable that there is a deficit of carbon due to the polymer processing. A skin of polymer forms during the extrusion process and must be abraded away to expose the active carbon material before electrochemical use. This anomalous behaviour can be explained if the carbon particles in the composite electrode are considered as an array of carbon nanoelectrodes embedded in an electrochemically inert matrix. This is a reasonable assumption if the spacing of these particles is of sufficient distance so as each carbon particle electrode will have its own diffusional field. This will result in a radial diffusion layer which enhances the mass transfer and the consequential current.

### 5.4.3 Unactivated coconut shell (UCNS)

The behaviour of the UCNS electrode will be discussed before that of the activated materials. This will provide baseline behaviour to compare the effects of activation and activation affected by different chemical agents. No peaks were observed only the hysteresis of the scans which may have obscured the redox response (figure 5.6 and 5.7). A major component of the observed current probably originated from capacitance. This observed capacitance originates partly from the charging at the electrode-electrolyte interface, i.e., the charging of the double layer, which is the true capacitance. The other contribution to the observed capacitance is from surface redox reactions that originate from vestigial chemical groups including surface oxides. These surface oxides may also inhibit electron transfer to hexacyanoferrate(III). If a proportion of the observed current was due to solution species a further increase in current would be expected on increasing the flux of the reactant. If this was the case then a rotating disc electrode experiment would give a larger current response

due to enhanced mass transfer by convective-diffusion than the still experiment which relied purely on simple diffusion. Only a slight increase in reduction current was found compared to the current response of the simple diffusion experiment. The current obtained from the simple diffusion and the convective-diffusion experiment were -0.9 mA and -1.2 mA. respectively. The scan rate for both experiments was 5 mV $s^{-1}$. This result was consistent with an observed restricted redox response due to the high capacitance of the system.

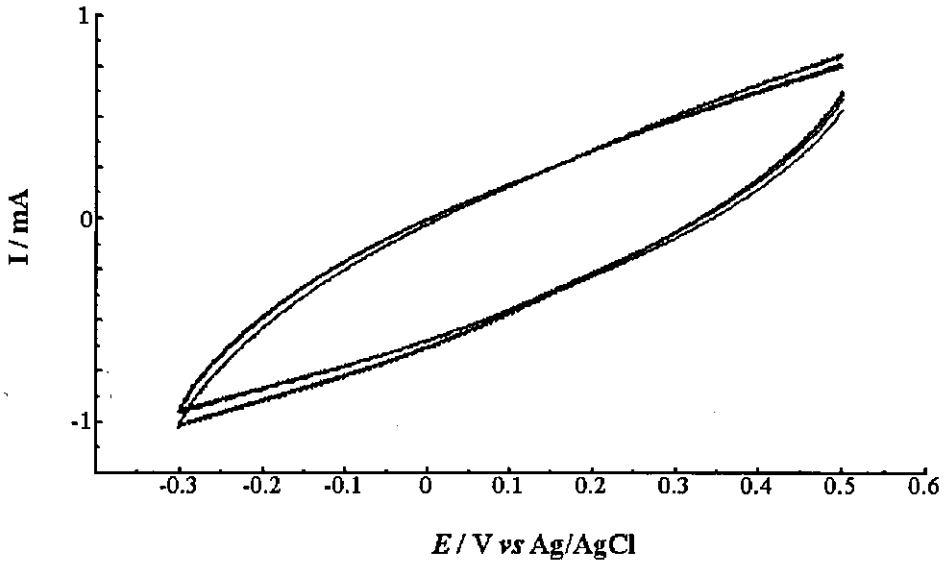


Figure 5.6 Limiting current versus voltage for the hexacyanoferrate system at UCNS with rotation rates of 1, 1.5, 2 and 2.5 Hz. Series of scans measured at 5 mV $s^{-1}$.

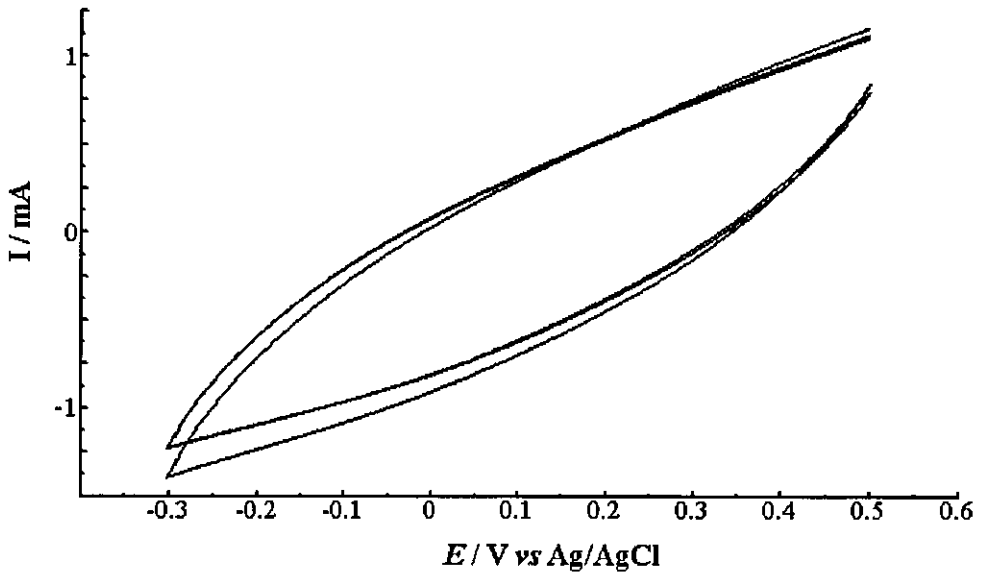


Figure 5.7 Limiting current versus voltage for the hexacyanoferrate system at UCNS with rotation rates of 5, 10, 15 and 20 Hz. Series of scans measured at 5 $mVs^{-1}$.

### 5.4.4 Activated coconut shell carbon

No peaks were observed during the cyclic voltammetry experiment. Hysteresis of the plots similar to the unactivated material were present. The voltammetric charge density greatly increased on activation. This is indicated by the area enclosed by the plot and corresponds to the electrochemically active surface area. A reproducible cathodic current of 4.6 mA ( cf. UCNS with a cathodic current around 1 mA) at the extreme range of the potential window was obtained after 10 runs at 5 mV $s^{-1}$. Currents obtained ranged from 4 to 4.6 mA (SR = 5 mV $s^{-1}$) as the system settled down. The wetting of the electrode was a problem initially with air bubble adhesion and the gradual ingression of the electrolyte into the porous matrix before acceptably reproducible voltammograms could be obtained. The increase in cathodic current from the rotating disc experiments at 15 Hz rotation were modest. Values stabilised at around 5.36 mA and started from 4.22 mA as the electrode wetted and electrolyte permeated its structure. The voltammetric area was large indicating a corresponding large active electrode area. The voltammetric behaviour of this material will provide a benchmark performance to compare the effect of chemical treatment on activation of the electrode.

### 5.4.5 Chemically activated carbons

Chemical treatment appeared to have an overall adverse effect on the voltammetric area. An insignificant improvement was obtained with the air treated sample as compared to the straight activated coconut shell material. The hydrogen treated sample had a slightly lower voltammetric area than the air treated material. The nitric acid treated carbon performed similar to the unactivated material. In contrast the sulphuric acid treated material had a considerably larger voltammetric area than that of the nitric acid treated material but considerably smaller than the chemically untreated activated and air treated samples. For clarity the order of increasing voltammetric area is shown: UCNS = $HNO_3$ < $H_2SO_4$ < $H_2$ < activated CNS = Air treated. With the exception of the nitric acid treated sample the order of the increase in the voltammetric area matches the increase in surface area of the carbons. No correlation between the porosimetry data and the electrochemical behaviour of the nitric acid treated sample was apparent (table 5.2).

| Surface treatment | UCNS | $HNO_3$ | $H_2SO_4$ | $H_2$ | CNS | Air |
|---|---|---|---|---|---|---|
| Surface area $m^2 g^{-1}$ | 652 | 1042 | 987 | 1004 | 1041 | 1043 |
| Micropore vol. $cm^3 g^{-1}$ | 0.29 | 0.45 | 0.44 | 0.43 | 0.45 | 0.45 |
| Narrow MPV $cm^3 g^{-1}$ | 0.26 | 0.37 | 0.36 | 0.36 | 0.37 | 0.38 |
| Broad MPV $cm^3 g^{-1}$ | 0.03 | 0.08 | 0.08 | 0.07 | 0.08 | 0.07 |

Table 5.2 Table showing surface area and micropore data in order of increasing voltammetric area. Micropore volume (MPV) = pores width >0, <2.0 nm. 'Narrow' MPV = pores width >0, <0.6 nm. 'Broad' MPV = pores width >0.6,<2.0

The anomalous behaviour of the nitric acid treated sample was made evident by examining the SEM image of the sample and comparing it with the other materials. Photographs of these images are shown below in figures 5.8. The nitric acid sample showed bulk loss of material in addition to the expected nanopore structure. In contrast the other samples, which showed very similar morphology, exhibited only the desired 'controlled' erosion of the material which increases the nanoporosity and hence the activity of the carbon.

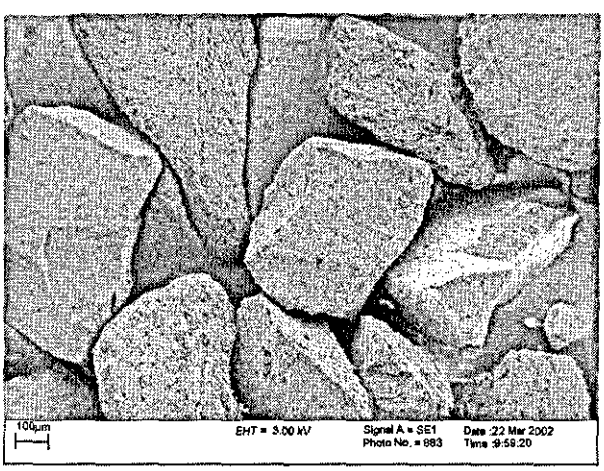


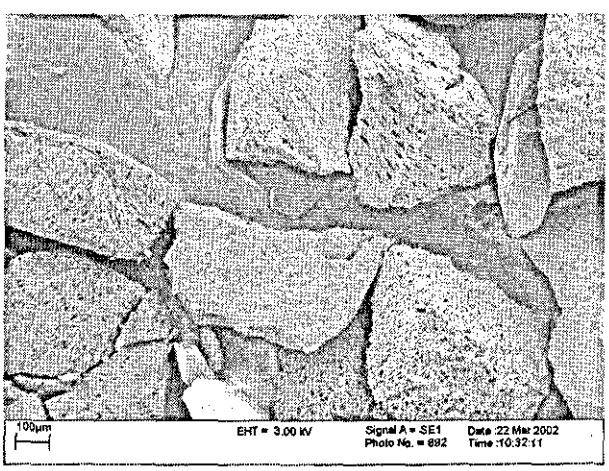


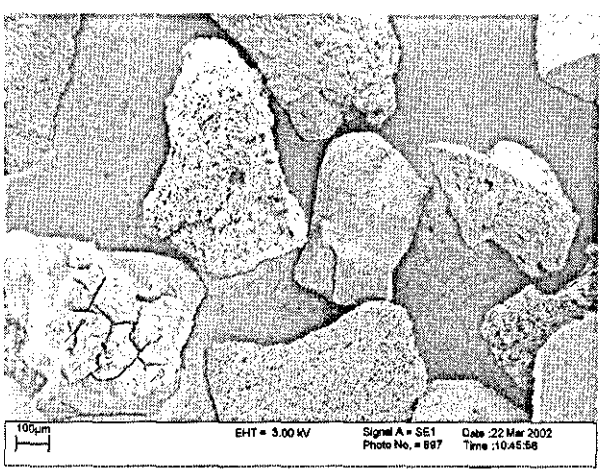


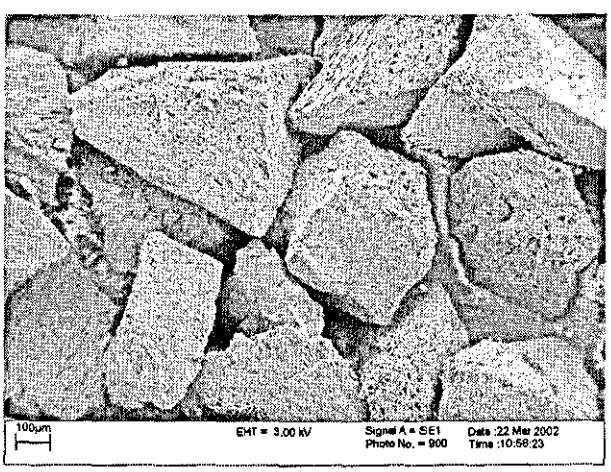

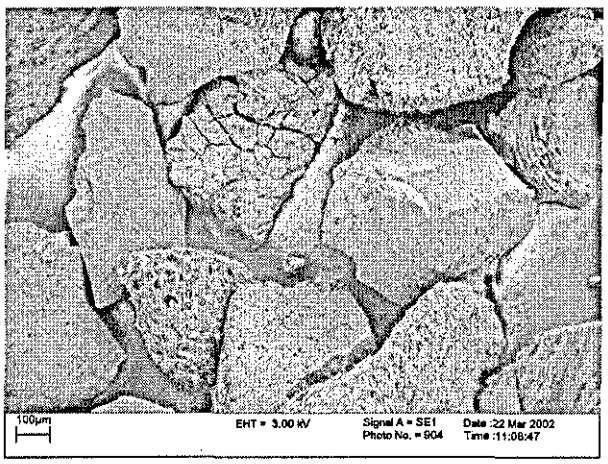


Figure 5.8 SEM images ( 100 µm scale) of the activated and chemically treated activated carbons. Top to bottom rows, left to right, activated carbon, sulphuric acid, nitric acid, air and hydrogen treated samples

## 5.5 Carbon materials in aqueous NaBr electrolyte

Oxygen electrochemistry is of great importance to industry from its electrogeneration and energy applications to its role in the corrosion of metals in air. Oxygen reduction electrodes are beginning to replace the hydrogen evolution cathodes in chloralkali cells affording a saving in energy. It is in this application in which we are interested. The oxygen cathodes performance, as discussed in chapter 4, gave a considerable drop in cell voltage of the electrolyser. A saving of nearly one volt was obtained in the unoptimised rebalancing cell. The performance was made even more remarkable considering the novel application of solid polymer with aqueous electrolyte technologies and in spite of electrolyte precipitation with consequent delamination of the GDE. Therefore it was decided to study the oxygen reduction reaction on various electrode materials and apply this information to the rational design of cathodes for the rebalancing cell.

Oxygen or water reduction sustains the anodic reaction of bromine evolution and generates hydroxyl species to neutralise hydroxonium ions in an aqueous sodium bromide electrolyte. Therefore it was important to study the electrochemical behaviour of the carbons in 5 M sodium bromide electrolyte in alkaline electrolyte conditions, avoiding bromine generation. It is energetically advantageous for the reduction to occur at the least negative potential possible. A potential window of 0.2 to -0.2 V was selected to observe any reduction processes. It was expected that the low rate of reduction in that potential range would be compensated for by the high surface area carbons and catalysis. The electrochemistry

observed here is mainly due to double layer charging and surface faradaic processes. The high porosity of these materials increases these processes. It has been reported that voltammograms of high porosity materials are difficult to interpretate due to poor mass transfer and the associated distributed IR drop within the pores.[21] This can be overcome if the pores are blocked to present a smooth electrode surface for the voltammetric experiment. This is obviously unacceptable in this present work because the performance of the electrode is determined by the level of porosity and hence surface area. The electrochemical behaviour of glassy carbon in the sodium bromide electrolyte will be discussed before that of the other materials as this carbon material has none of the aforementioned problems of the other materials. The comparative electrochemistry of oxygen reduction was studied at glassy carbon electrode in sodium bromide and sodium chloride electrolytes and compared to a literature study of oxygen reduction in sodium chloride electrolyte.

## 5.6 Results and discussion

### 5.6.1 Electrochemical behaviour of glassy carbon in 5 M NaBr and NaCl

The electrochemical behaviour of glassy carbon in 5 M NaBr, 5 M NaCl was studied using cyclic voltammetry. Bromine generation was avoided by working in a potential window of 0.2 to -0.2 V. In this region oxygen was reduced to the peroxide and oxidised back to oxygen. The currents were relatively low due to mass transfer limitations of the dissolved oxygen in the electrolyte. To overcome the low current the potential window was extended anodically and held for several seconds to generate oxygen at the electrode. Its greatly enhanced reduction was observed in the cathodic direction of the scan at 130 mV vs. SHE. ( Figure 5.9) The generation of bromine was shown to occur beyond the working potential range and therefore not interfere with the experiment. On extending the potential window further in the cathodic direction the reduction of the peroxide, at least in part, was observed at -180 mV vs. SHE. To make sure the observed waves could be attributed to oxygen reduction alone and not bromine reduction, the experiment was repeated in a sodium chloride electrolyte. The sodium chloride system (figure 5.10) gave similar shaped cyclic voltammograms as the sodium bromide electrolyte experiment but with the two step reduction starting at more negative potentials, that is at a greater overpotential. The two step reduction of oxygen in the sodium chloride electrolyte occurs at 40 mV vs. SHE for the reduction to peroxide and the reduction to the hydroxide at -470 mV vs. SHE. This agrees extremely well with the oxygen reduction results at a graphite paste and a RVC electrode obtained by Davison et al.[43]

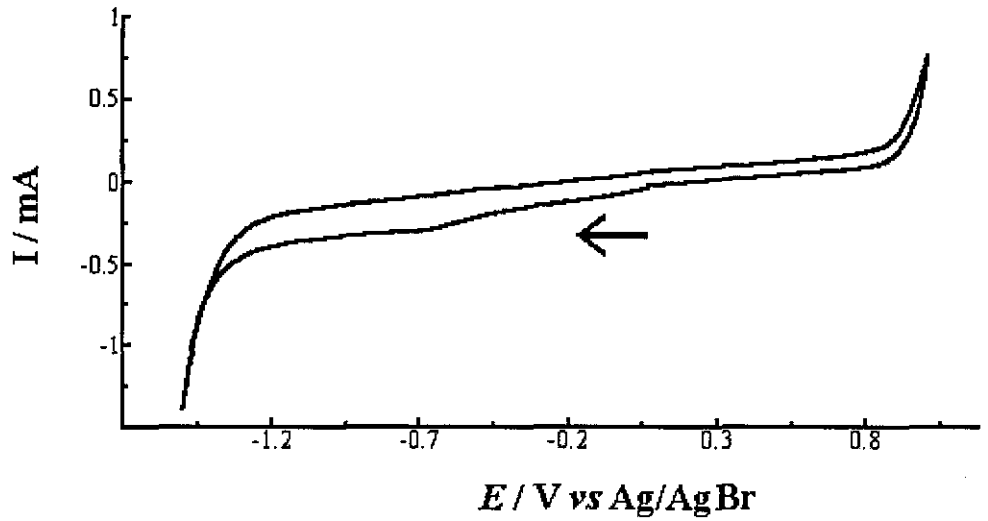


Figure 5.9 CV of 5 M NaBr at glassy carbon vs. Ag/AgBr reference electrode. Scan rate = 200 mV $s^{-1}$

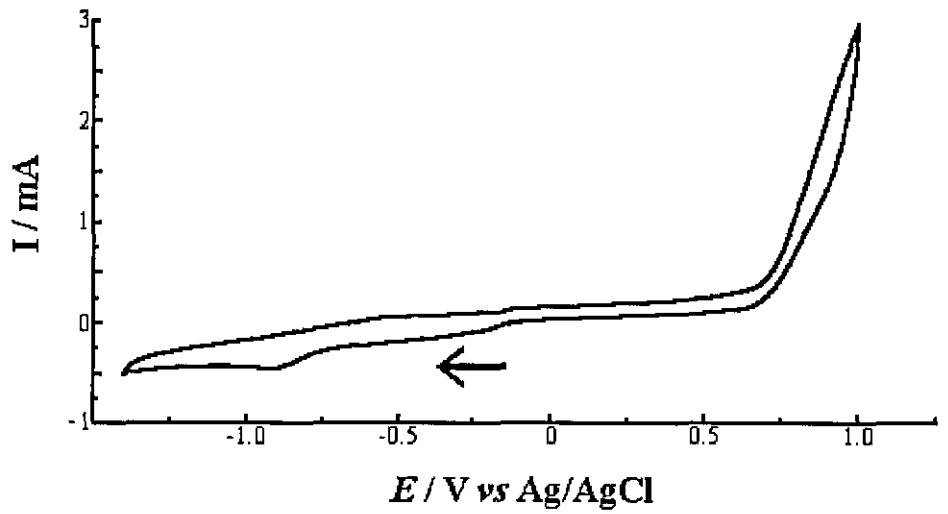


Figure 5.10 CV of 5 M NaCl at glassy carbon vs. Ag/AgCl reference electrode. Scan rate = 200 mV $s^{-1}$

Davison et al found the reduction of oxygen starts at 40 mV and the reduction of the peroxide at -470 mV both vs. SHE. The two step reduction of oxygen in sodium bromide occurs at 130 and 180 mV vs. SHE, 90 and 290 mV more positive than the reduction in the sodium chloride electrolyte. The lower overpotential, compared to oxygen reduction in the sodium chloride electrolyte, may be attributed to the catalytic decomposition of the peroxide by the bromide in addition to an increase in exchange current density. This was supported by the greatest

decrease in the overpotential for the second step; the reduction of peroxide. It is widely known that ions of variable valency are effective decomposition catalysts. If an element has two accessable oxidation states having a suitable redox potential, so that the lower oxidation state can be oxidised by the peroxide and the higher state can be reduced by it, at an appreciable rate, this element will act as a catalyst for hydrogen peroxide decomposition. The bromide ion is one of the most commonly encountered hydrogen peroxide decomposition catalysts.

During the 0.2 to -0.2 V potential range experiments, when double layer and surface faradaic processes dominate, a transient current response was evident. This reduction wave was observed immediately on the onset of the scan and quickly decays as the scan sweeps in the cathodic direction. It is unlikely that the source of this response was due to slow capacitance, caused by double layer charging or a slow faradaic process within a crack or pore, because the potentiostat imposes the initial potential very quickly. This response has been attributed to oxygen adsorbed onto the electrode which is quickly consumed on initiation of the scan. This was supported by the absence of this wave at the start of the second and subsequent scans. Furthermore, if the electrode is not allowed to fully recover the open cell voltage becomes less positive, as predicted by the Nernst equation, as the concentration of oxygen decreases and that of peroxide increases, and the initial reduction wave decreases on subsequent scans. Eventually, the initial reduction disappeared and was replaced by an initial anodic wave attributed to the oxidation of the peroxide. The electrode recovered and the reduction wave returns once the peroxide has diffused away from the electrode or decomposed into oxygen by a local cell mechanism. Initial anodic transients can be present after 24 hours with the sodium chloride electrolyte. In contrast, recovery can occur much quicker with the sodium bromide system due to the homogeneous catalysis by bromide.

Another feature of the CV is a quasi reversible couple that has been attributed to surface orthoquinones[28], although the details have been considerably debated. Nevertheless it has been generally agreed that the peaks are related to surface oxides. Nagaoka[28] proposed that these redox peaks originate from a pH dependent reaction not on the surface but deep in a pore or crack.

The transport of protons and the reaction may be slow thus giving rise to the observed slow current response or pseudocapacitance. This present study offered evidence to support this mechanism.

$$[>C=O] + H^+ + e^- = [>COH] \qquad (5.2)$$

During cyclic voltammetry the quasi-reversible couple was often detected with the peaks varying in size. The anodic peaks were generally much larger than the cathodic peaks and in the extreme case the cathodic peak was absent. The peak size tended to be more equal with shorter cathodic excursions, i.e., -0.25 V, where oxygen reduction is limited to the first 2 electron step. These peaks frequently show a degree of symmetry, indicating a partially surface controlled or dominated reaction. Occasionally, a shoulder was observed on the anodic peak and may be attributed to quinones on the carbon surface in a region of different electrode activity which changes with time. On subsequent scans the peaks decrease in size and eventually disappear. Therefore it was not possible to show that the current was proportional to scan rate, which is indicative of a surface-bound redox couple.

The predominance of the anodic peak and the gradual disappearance of the redox couple can be explained by the changing electrolyte composition during the reduction of oxygen and the effect on the hydrogen peroxide-perhydroxyl equilibrium. This in turn provided indirect evidence for Nagaoka's pore mechanism.

The electroreduction of oxygen produces one mole of hydroxyl ions for every mole perhydroxyl giving a highly alkaline solution of peroxide. These species can aid the proton transfer or transport involved in Nagaoka's pore mechanism and may involve the following reactions.

$$[>COH] + HO_2^- = [>C=O] + H_2O_2 + e^- \qquad (5.3)$$

$$[>COH] + OH^- = [>C=O] + H_2O + e^- \qquad (5.4)$$

When the potential was increased to more negative potentials and on increasing scan number more peroxide was reduced to the hydroxide. Thus more hydrogen peroxide will dissociate to the perhydroxyl as the equilibrium will be pushed further to the left, as the concentration of hydroxide in the pores and cracks increases, thus further suppressing proton transport to and from the surface oxides.

$$H_2O + HO_2^- = HO^- + H_2O_2 \qquad (5.5)$$

To summarise this process manifests itself in the initial enhancement of the anodic peak with an accompanying decrease in the cathodic peak after potential excursions of around 1V and their eventual disappearance after potential cycling. To complicate the situation further the electrode surface continually changed as active and less active areas exchanged along with the associated diffusional coupling and decoupling of these areas.

### 5.6.2 Electrochemistry of the activated carbon materials in sodium bromide electrolyte

Having characterised oxygen reduction at the glassy carbon electrode; where electrochemistry is relatively uncomplicated, the behaviour of the porous activated carbon materials was investigated and compared to unactivated materials. The aim of this section is to discuss the behaviour of these materials in the sodium bromide electrolyte and identify the most suitable carbon for the cathode. The materials that performed well in the ferrocyanate work were selected for further investigation were the activated carbons; air treated and coconut shell carbons. In addition, numerous activated and unactivated carbon materials were screened, but this discussion will be confined to the best performers as identified by the ferrocyanate study.

The potential was scanned from +0.2 to -0.2 V vs. Ag/AgBr, until reproducible CVs were obtained. On initiation of the scan the transient currents were again evident. The polarity and the magnitude of the current appeared to be dependent on the initial relative concentrations of peroxide and oxygen as reflected in the open cell voltage shifting to less noble values, that is less positive potentials, in agreement with the Nernst equation. In the working potential window both oxygen reduction and peroxide oxidation occur. The cathodic transient can start upto around -16 mA (oxygen reduction) and the anodic current at around 16 mA (peroxyl oxidation). Reproducible results were obtained after around 20 runs comprising 40 scans for the system to stabilize (figure 5.11).

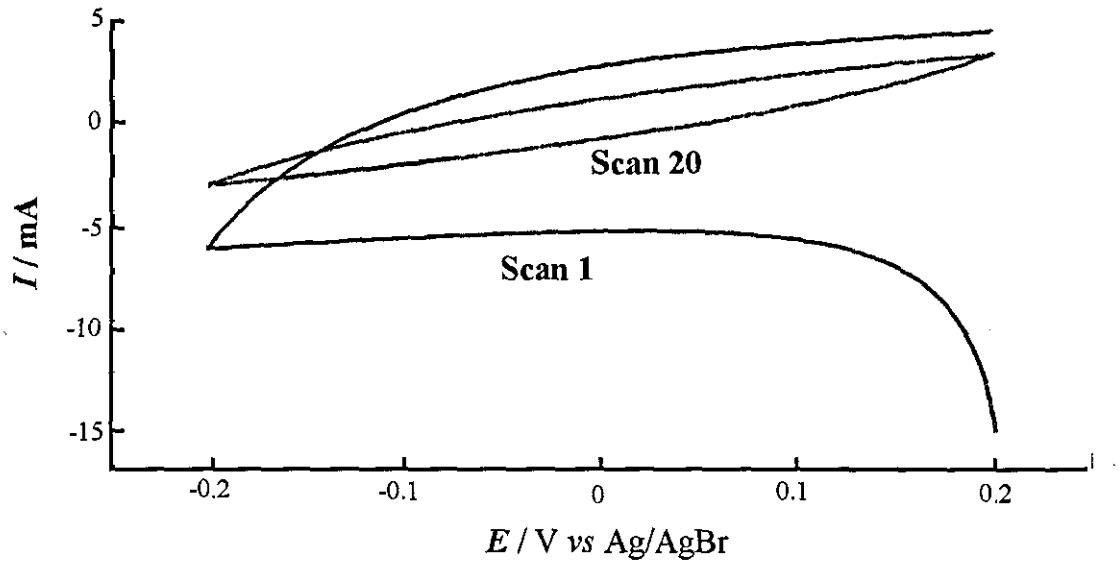


Figure 5.11 CV of 5 M NaBr at a porous activated carbon electrode with a 5 mV $s^{-1}$ scan rate

Polarisation characteristics changed on each scan due to distributed IR drop within the pores, ingression of electrolyte and the build-up of peroxide. Eventually, reproducible data was obtained indicated by the superimposition of the plots. The CVs were rather featureless; no peaks were usually present apart from the rare appearance of the so called quinone couple, but showed hysteresis giving the familiar large voltammetric areas similar to the hexacyanoferrate work. RDE experiments showed that the current often stabilises at lower values when convective mass transfer was employed. This was probably due to loss of peroxide to the bulk electrolyte.

The best performing materials, as indicated by the steady state current at the cathodic limit of the working potential window, were the porous carbon composites and the air activated composites. The respective currents obtained for these materials at steady state were -5 and -8 mA (scan rate = 5 $mVs^{-1}$). To put these results in context the UCNS materials gave steady state currents of around -1 mA.

## 5.7 Conclusions

This section will discuss the conclusions of the electrochemical studies of the various supplied carbon materials. To effectively assess the suitability of the materials the well-characterised hexacyanoferrate (III) and hexacyanoferrate (II) redox couple was selected to characterise the electrode. Thus avoiding the problems of mass transfer associated with a gaseous electroactive species. In addition, a survey of the three voltammetric methods was

undertaken. The electrochemical behaviour of these materials in sodium bromide electrolyte was investigated with focus on the best materials identified from the hexacyanoferrate - potassium chloride system studies.

### 5.7.1 Hexacyanoferrate-potassium chloride system at the glassy carbon electrode using the three voltammetric techniques

The three voltammetric techniques confirmed good experimental set-up by showing the predicted $t^{-1/2}$ time dependence and hence Fickian diffusion behaviour. The diffusion coefficient was found to be 9.12 x $10^{-6}$ $cm^2$ $s^{-1}$ using chronoamperometry. This result was a little high but can be explained by a larger real electrode area compared to the measured geometric area caused by electrolyte ingression between the electrode edge and insulating PTFE collar.

### 5.7.2 Hexacyanoferrate-potassium chloride system at graphitic electrodes

The activated coconut shell carbons gave the highest currents but with a large background or capacitance current. Chemical treatment had an adverse effect on the performance of the activated carbons except for the air activated material. These gave at best a slight improvement to the activated carbon. The RVC and the carbon composite materials gave relatively small currents but showed low capacitance. RVC's hydrodynamic properties are a clear advantage for an oxygen reduction electrode as flooding is prevented and consequently allowing efficient mass transfer of oxygen.

The carbon composites have the additional advantage of behaving as a collection of nanoelectrodes. In this type of system, if the mean distance between the active electrode particles is sufficiently large, reactant depletion due to slow mass transfer can be avoided. This appeared to be the case with the hexacyanoferrate system and would be expected to be more important and advantageous with the problematic mass transport of oxygen. The advantages of these separate materials can be utilised by incorporating their properties into one material, namely a porous activated carbon composite. The electrochemistry of these materials in the sodium bromide electrolyte, along with the unactivated coconut shell materials and the glassy carbon, was investigated. The conclusions of this study are discussed in the next section.

### 5.7.3 Carbon materials in NaBr and NaCl electrolytes

The two step reduction of oxygen in the sodium chloride electrolyte at glassy carbon occurred at 40 mV for the reduction to peroxide and at -470 mV vs. SHE for the reduction to the hydroxide This result is in agreement with the oxygen reduction results at a graphite paste and a RVC electrode obtained by Davison et al[43]. They found the reduction of oxygen starts at 40 mV and the reduction of the peroxide at -470 mV both vs. SHE. The two step reduction of oxygen in sodium bromide occurs at 90 and 290 mV more positive than the reduction in the sodium chloride electrolyte 130 and 180 mV vs. Ag /AgBr. The lower overpotential for the reduction of hydrogen peroxide, compared to that in the sodium chloride electrolyte, may be attributed to the catalytic decomposition of the peroxide by the bromide. This was supported by the greatest decrease in the overpotential for the second step; the reduction of peroxide.

The activated porous carbon composite materials offer the best route to efficient oxygen reduction cathodes. It is necessary to use these materials in high surface area configured electrodes with a catalyst to achieve acceptable geometric current densities and complete reduction to hydroxide.

# Chapter 6

# General conclusions, summary and future work

This chapter will state the conclusions and summarise the work on electrolyte management and the study of carbon materials. Future work will also be discussed. This will include applications of this technology. First, the need for rebalancing the pH of the electrolyte will be outlined and how it can be achieved.

## 6.1 Electrolyte management

Regenesys® relies on process control to ensure operation is optimal. An important aspect of process control is electrolyte pH management. The bromide electrolyte pH can drop to around pH 1 or less. This is symptomatic of the chemical imbalance within the system during normal operation. It has been shown that $HS^-$ is transported across the membrane where it is oxidised by the bromine to ultimately yield sulphuric acid. If low pH is maintained back diffusion of protons will occur inhibiting the hydroxyl dependent discharge process. The resultant decrease in the discharge capacity of the system is due to both direct loss of charged species ($HS^-$) by diffusion and neutralisation of the charged species ($HS^-$ and $OH^-$). Chemical loss of the charged species can be prevented by neutralisation of the acid. As we are in an electrochemical system it is convenient and efficient to use electrochemistry for this purpose.

Three rebalancing strategies can be employed by electrolysis; sodium hydroxide can be delivered into the polysulphide electrolyte to recover some of the lost capacity, directly into the bromide electrolyte to neutralise the protons at source or simultaneously to both electrolytes. Bromine evolution was advantageously selected as the anodic reaction, also enabling bromine losses to be countered.

The aim of this work was to evaluate electrochemical electrolyte pH management using a variable configuration electrolyser. This was achieved by looking at a porous cylinder carbon cathode which can be incorporated into the process stream in a flow by configuration and a separate flow cell electrolyser to generate hydroxide.

### 6.1.1 The porous cathode

The porous carbon cathode will achieve this by direct delivery of hydroxide into the bromide process stream along with the bromine anode generating electrode in a flow by configuration. The cathode will be coated in ion exchange resin or membrane for proton transport and as a barrier for neutral species such as bromine and hydrogen.

The aim of this work was to electrolyse a sulphuric acid solution to generate hydrogen and to see if the hydrogen is retained in the porous structure.

A preliminary investigation into a porous carbon open cathode was carried out. Hydrogen generation at the cathode was signalled by the onset of oxygen evolution at the counter electrode and soon after hydrogen bubbles were observed, initially on the bottom edge of the cylindrical carbon electrode, the site of greatest current density, and then the side surface.

Characterisation of the uncoated electrode proved to be impossible due to the constant change and uncertainty of active electrode area. Build-up of hydrogen in the carbon matrix continually blinds off electrode area. Therefore working current densities were very uncertain. Electrical resistance was also a problem due to the thickness of electrode material enhancing resistivity. This is especially important with the hydrogen evolution reaction because the current is carried through the thickness of the electrode to the surface where proton discharge occurs.

In addition, pore resistance caused preferential proton discharge on electrode surface, rather than internally. Surface bubble formation was probably increased by the hydrodynamic resistance of the electrolyte. Electrolyte flooding of the body of the electrode impedes hydrogen transport from the reactive sites on the surface to the internal structure prior to venting. This was probably more prominent at the bottom of the electrode due to the high hydrostatic pressure of electrolyte in the porous matrix. Bubble formation remained a problem even when the electrode was coated in Nafion® ionomer resin. The macroscopic roughness of the surface and porosity prevented the ion exchange material coating the electrode evenly. Penetration of the film, known as holidays, provided areas of low electrical resistance and high current density which favoured surface reduction and bubble formation. Efficient coating of the material may entail several applications of the resin. Alternatively, it is possible to coat the electrode with melt processable precursor forms of the ion exchange material and subsequently hydrolyse the material to form an ionomeric coating.

**Summary of porous cathode conclusions**

The porous carbon cathode will be a viable method for rebalancing electrolyte when the following modifications are made

- The cathode needs to be enveloped in an ion exchange material to prevent hydrogen permeation into the electrolyte
- Electrode needs to be hollowed to facilitate hydrogen removal or oxygen feed
- Dual porosity to prevent flooding and aid gas venting or supply

### 6.1.2 The flow cell electrolyser

The flow cell electrolyser, utilising a MEA in a novel manner, provided a viable and efficient method for electrolyte management. Hydroxide and bromine can be generated easily, quickly and in sufficient quantity to meet electrolyte management demands. Hydroxide was generated by both the cathodic evolution of hydrogen and the reduction of oxygen. Oxygen reduction gave a drop in cell voltage of around 1 V compared to the cathodic hydrogen evolution. Delamination of the membrane occurred when the electrolyser was excessively ran beyond neutrality. The delamination of the MEA was not envisaged to be a problem if hydroxide generation matches proton production or influx. The cell potentials (400 to 700 mV) obtained for the depressed pH experiments clearly show oxygen was reduced under basic conditions close to theoretical values. This was probably primarily due to the non build-up of caustic effected by efficient proton transport and neutralisation.

The use of the MEA in the electrolyser for pH rebalancing was not envisaged to be problem if hydroxide generation matches the incoming proton flux or only runs sufficiently to rebalance the electrolyte. If caustic is required on a synthetic scale a trickle bed cathode configuration[44] may be preferable to minimises caustic build-up. This may be achieved by using a particulate bed cathode of activated porous carbon composite chips or carbon composite foam. The composite chips are granular pieces of graphite coated with activated carbon and a fluorocarbon binder which can absorb oxygen bubbles into its pores. The carbon composite foam would have the benefits of dual porosity. The large pores would be equivalent to the high voidage or open RVC structure and would aid drainage. While on the microscopic level a large reaction surface would be presented along with the inert matrix encouraging oxygen absorption prior to reaction. Reaction can be further enhanced by the

loading of a catalyst. A highly porous carbonised polyacrylonitrile foam with a very low platinum loading (~13 μg $cm^{-2}$) has been reported in the literature.[45] Its excellent electrocatalytic activity, comparable to bulk platinum, has been attributed mainly to the suitable mean distance between the platinum particles on the catalyticaly inert foam. The system acted as a collection of nanoelectrodes with ideal spacing between catalyst particles. In this type of system, if the mean distance between the active electrode particles is sufficiently large, reactant depletion due to slow mass transfer can be avoided. This appeared to be the case with the activated carbon composites in this study. Therefore, considerable further enhancement of the composites performance would be expected with a very low catalyst loading of the electrochemically active sites.

**Summary of flow cell electrolyser conclusions**

- Bromine and hydroxide can be generated easily, quickly and in sufficient quantity to meet electrolyte management demands

- Facile bulk electrolyte neutralisation by influx of protons aided by the Coulombic field

- Facile hydroxide back diffusion

- Sodium hydroxide can be delivered to either or both electrolyte circuits

- Only need to operate rebalancing cell when pH is low during charge cycle of main cell; hydrogen evolution at a lower potential

- Oxygen reduction as the cathodic reaction lowers cell potential by 900 mV when operating at 20 mA $cm^{-2}$ under normal conditions

- Depression of pH effects near theoretical cell potential for oxygen reduction under basic conditions

## 6.2 Carbon materials

This section will state the main conclusions of chapter 4: carbon materials for the cathode. The well-characterised hexacyanoferrate(III/II) redox couple was selected to characterise the electrode to avoid the problems of mass transfer associated with a gaseous electroactive species such as oxygen. In addition, a survey of the three voltammetric methods was undertaken. The electrochemical behaviour of these materials in sodium bromide electrolyte was then investigated with the focus on the best materials identified from the hexacyanoferrate-potassium chloride system studies.

### 6.2.1 Hexacyanoferrate-potassium chloride system at the glassy carbon electrode using the three voltammetric techniques

The three voltammetric techniques confirmed good experimental set-up by showing the predicted $t^{-1/2}$ time dependence and hence Fickian diffusion behaviour. The diffusion coefficient was found to be 9.12 x $10^{-6}$ $cm^2$ $s^{-1}$ using the most direct method of chronoamperometry. The obtained value was a little high but can be explained by the difference between real electrode area compared to the measured geometric area. Electrolyte ingression between the electrode edge and insulating PTFE collar was proposed as possible explanation of the high value obtained.

### 6.2.2 Hexacyanoferrate-potassium chloride system at graphitic electrodes and physical characterisation of activated carbons

The activated coconut shell carbons gave the highest currents but with a large background or capacitance current. Chemical treatment had a detrimental effect on the performance of the activated carbons except for the air activated material. These gave at best a slight improvement to the activated carbon justifying further investigation. The increase in voltammetric area of the background current was in the following order: UCNS = $HNO_3$ < $H_2SO_4$ < $H_2$ < activated CNS = Air treated. With the exception of the nitric acid treated sample the order of the increase in the voltammetric area matched the increase in surface area of the carbons. The anomalous behavior of the nitric acid treated sample was not apparent from the porosimitry data but made evident by examining the SEM image of the sample and comparing it with the other materials. The nitric acid sample displayed bulk loss of material at the 100 lm scale but showed similar pore morphology to the other carbons at the 10 lm scale. The RVC and the carbon composite materials gave lower currents than the other materials but showed a lower capacitance due to the active area being relatively small

compared to the whole electrode. RVC's hydrodynamic properties are clearly evident from signature Randle-Sevcik and Levich voltammetric behavior. The hydrodynamic advantage of this material will benefit the oxygen electrode aiding efficient mass transfer and drainage of caustic. The carbon composites have, in addition to low capacitance, the advantage of behaving as a collection of nanoelectrodes. In this type of system, if the mean distance between the active electrode particles is sufficiently large, reactant depletion due to slow mass transfer can be avoided, resulting in an enhancement of current. This appeared to be the case with the hexacyanoferrate system and would be expected to be more important and advantageous with the problematic mass transport of oxygen. The advantages of these separate materials can be utilised by incorporating their properties into one material, namely a porous activated carbon composite. The electrochemistry of these materials in the sodium bromide electrolyte, along with the unactivated coconut shell materials and the glassy carbon for comparison, was investigated. The general conclusions of this study follows.

### 6.2.3 Carbon materials in NaBr and NaCl electrolytes

The two step reduction of oxygen in the sodium chloride electrolyte at glassy carbon occurred at 40 mV for the reduction to peroxide and at -470 mV vs. SHE for the reduction to the hydroxide This result is in agreement with the oxygen reduction results at a graphite paste and a RVC electrode obtained by Davison et al. Davison et al found the reduction of oxygen starts at 40 mV and the reduction of the peroxide at -470 mV both vs. SHE. The two step reduction of oxygen in sodium bromide occurred at 130 and 180 mV vs. SHE, 90 and 290 mV more positive than the reductions in the sodium chloride electrolyte. The lower overpotential, compared to oxygen reduction in the sodium chloride electrolyte, may be attributed to the catalytic decomposition of the peroxide by bromide. This was supported by the greatest decrease in the overpotential for the second step; the reduction of peroxide.

The activated porous carbon composite materials offer the best route to efficient oxygen reduction cathodes. The mass transfer was enhanced giving larger currents. This was probably due to each active area of the electrode having its own diffusional field because of isolation by the inert matrix. In addition, the inert binder is able to absorb oxygen bubbles and will therefore increase current and minimise the need for excess oxygen. It is necessary to use these materials in high surface area configured electrodes with a catalyst to achieve acceptable geometric current densities and complete reduction to the hydroxide. Electrocatalytic enhancement can be achieved by the introduction of the appropriate metal

salt by diffusion into the electrode structure followed by either chemical or electrochemical reduction to give the metal particulate catalyst.

## 6.3 Further work

### 6.3.1 Porous cathode

Further work required on the porous carbon cathode will include the following:

- Coat electrode in an ion exchange material to prevent hydrogen permeation into the electrolyte

- Electrode needs to be hollowed to facilitate hydrogen removal or oxygen feed

- Dual porosity to prevent flooding and aid gas venting or supply

### 6.3.2 The flow cell electrolyser

- Study performance of cell with hydroxyl repelling membrane and flushing of cathodic gas chamber to prevent sodium hydroxide build-up

- Investigate alternative configurations of electrolyser such as trickle bed electrolyser

- Revisit oxygen reduction at very low pH

### 6.3.3 Electrode materials

- Study activated porous carbon composite materials

- Investigate catalytic enhancement of carbon composite materials for the cathodic reduction of oxygen

- Investigate the highly porous materials such as carbonised polyacrylonitrile foam for the oxygen reduction cathode

# References


1 R. Zito, U.S. Patent 5439757

2. A. Price, S. Bartly, S. Male, G. Cooley, Power Engineering Journal, IEE, **13**, 122 1999

3 P.D Bennet, K.R. Bullock, M.E. Fiorino, The Electrochemical Society, Interface, Winter, **4**, 26, 1995

4 S. Megahed, B. Scrosati, ibid, **4**, 34, 1995

5 P. Bro, ibid, **4**, 42, 1995

6 K. Prater, J. Power Sources, **29**, 239, 1990

7 A. Hamnett, P. Christensen, in The New Chemistry, Editor-in-chief N. Hall Cambridge University Press, Cambridge, 407, 2000

8 National Power PLC, An Introduction to the Regenesys®, Energy Storage System, 1998

9 J. O'M. Bockris, D.M. Drazic, Electro-chemical Science, Taylor & Francis Ltd, New York, 228, 1972

10 D. Peramunage, R. Dillon, S. Licht, J. Power Sources, **45**, 311, 1993

11 R.S Yeo, D-T. Chin, J. Electrochem. Soc, **127**, 3, 1980

12 T. A. Davis, J.D. Genders, D. Pletcher, A First Course in Ion Membranes, The Electrochemical Consultancy, 2000

13 P.D. Naylor, R.T. Barton, P.J. Mitchell, Internal Report Loughborough University, August 1995

14 J. Wang, Electrochim. Acta, **26**, 1721, 1981

15 S.R. Lowry, K.A. Mauritz, J. Am. Chem. Soc., **102**, 4665, 1980

16 R.A. Komoroski, K.A. Mauritz, J. Am. Chem. Soc., **100**, 7487, 1978

17 W. Y. Hsu, T. D. Gierke, J. of Membrane Science, **13**, 307, 1983

18 K. A. Mauritz, C. L. Gray, Macromolecules, **16**, 1279, 1983

19 H. L. Yeager, B. O'Dell, Z. Twardowski, J. Electrochem. Soc., **129**, 85, 1982

20 H.G. Hertz, B.M. Braun, K.J. Muller, R. Maurer, J. Chem. Ed., **64**, 9, 1987

21 J. P. Hoare, The Electrochemistry of Oxygen, Interscience, New York, 122, 1968

22 J. A. McIntyre, The Electrochemical Society, Interface, Spring, **4**, 29, 1995

23 B. Bertsch-Frank, A. Dorfer, G. Goor, H.U. Suss in Industrial Inorganic Chemicals: Production and Uses. Ed. R. Thompson, The Royal Society of Chemistry, Cambridge, 175, 1995

24 M. Ardon, Oxygen, W.A. Benjamin, 87, 1965

25 D. J. Williams, Biochemistry, an Illustrated Outline, Gower Medical Publishing, London, 64, 1988

26 D. E. Fenton, Biocoordination Chemistry, OCP, Oxford Science Publications, Oxford, 48, 1997

27 P.C. Foller, R.T. Bombard, J. App. Electrochem. **25**, 613, 1995

28 R.L. McCreery in Electroanalytical Chemistry, Vol. 17, Marcel Dekker inc. New York, Ed A.J. Bard, 221, 1991

29 W. J. Blaedel, J. Wang, Anal. Chem., **52**, 76, 1980

30 Anon., Educator's Guide for Electrochemistry, Pine Instruments, Pennsylvania, 2000

31 A.C. Fisher, Electrode Dynamics, OCP, Oxford Science Publications, Oxford, 1996.

32 A.J. Bard, L.R. Faulkner, Electrochemical Methods Fundamentals and Applications, Wiley and Sons, Inc., Chichester, 280, 1980

33 D.H. Evans, K.M. O'Connell, R.A. Petersen, M.J. Kelly, J. Chem. Ed., **60**, 290, 1983

34 F.C. Anson, R.A. Osteryoung, ibid, **60**, 293, 1983

35 J. Osteryoung, ibid, **60**, 296, 1983

36 H.G. Petrow, R.J. Allen, U. S. Patent 3,992,512, 1976

37 H.G. Petrow, R. J. Allen, U. S. Patent 3,992,331, 1976

38 H.G. Petrow, R.J. Allen, U. S. Patent 4,044,193, 1977

39 H. G. Petrow, R. J. Allen, U. S. Patent 4,082,699 1978

40 T. Doherty, J.G. Sunderland, E.P.L. Roberts, D. J. Pickett, Electrochim. Acta., **41**, 293, 1996

41 A.T. Kuhn, Ed., Industrial Electrochemical Processes, Elsevier, Amsterdam, 121, 1971

42 D.T. Sawyer, J.L. Roberts Jr., Experimental Electrochemistry for Chemists, J. Wiley and Sons, London, 77, 1974

43 J.B. Davison, J.M. Kacsir, P.J. Peerce-Landers, R. Jasinski, J. Electrohem. Soc., **130**, 1497, 1983

44 C. Oloman, A. Waktinson, J. Electrochem. Soc., **126**, 1885, 1979

45 S. Ye, A.K. Vijh, L.H. Dao, J. Electrochem. Soc., **143**,L7, 1996

# Appendix

**PhD Research Training**

MSc by research programme at UEA Norwich with Prof A McKillop and Dr GR Stephenson (supervisor): Organoiron Dications. UEA studentship.

Research visit at Instituto Superior Technico, Lisboa Dr MFNN Carvalho (supervisor).

Postgraduate courses included problems in synthetic organic chemistry, advanced organometallics and nuclear magnetic resonance.

Presentations including sector talks and EU molecular electronics group.

Papers to date:

Electrochemical behavior and reactivity of cyclohexadienyl iron complexes, Carvalho MFNN, Pombeiro AJL, Shropshire IM, Stephenson GR, Inorganica Chimica Acta, **248**, 45, 1996.